IJVST

Number 1
Volume 16
Year 2024
ijvst.um.ac.ir

Iranian Journal of Veterinary Science and Technology

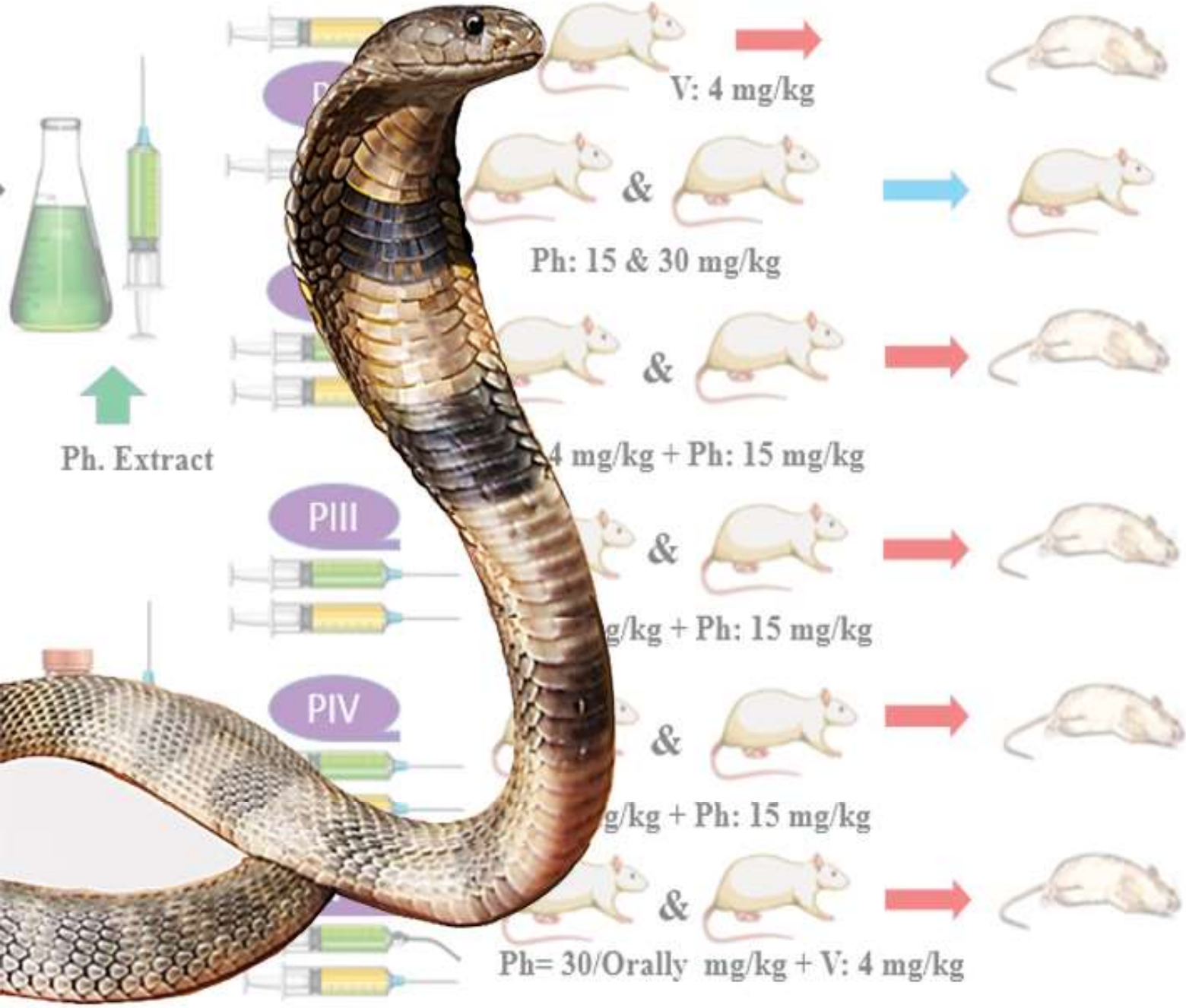

Ferdowsi Univerity of Mashhad

ISSN (Print): 2008-465X
ISSN (Online): 2423-6306
Serial number: 35

In the Name of God, the Compassionate, the Merciful

Iranian Journal *of* Veterinary Science and Technology

Editorial Office:
Faculty of Veterinary Medicine,
Ferdowsi University of Mashhad,
Azadi Square, Mashhad, IRAN
P.O. Box: 1793; Postal Code: 9177948974

Tel: +98 51 3880 3742 ***Fax:*** +98 51 3876 3852
Web: ijvst.um.ac.ir ***Email:*** ijvst@um.ac.ir

FERDOWSI UNIVERSITY OF MASHHAD PRESS

GENERAL INFORMATION

ISSN Print Edition: 2008-465X
ISSN Online Edition: 2423-6306

Journal Homepage:
ijvst.um.ac.ir

Abstracting and Indexing:
Scopus, ISI Master Journal List, Zoological Record; EMBASE, EBSCO, MIAR, Scientific Information Database (SID); Islamic World Science Citation Database (ISC); Magiran; Google Scholar; Centre for Agriculture and Biosciences International (CABI), DOAJ.

This journal has achieved the rating of:
- "Scientific-Research", by Commission of Evaluation of Iranian Scientific Journals, the Ministry of Science, Research and Technology, from Vol.7, No. 1, July 2015 onward.
- "International", by Commission of Evaluation of Iranian Scientific Journals, the Ministry of Science, Research and Technology, from Vol.13, No. 2, 2021 onward.

Publication Date:
Iranian Journal of Veterinary Science and Technology (IJVST) is published 4 times a year. Volume 14 with 4 issues appear in 2022.

SCOPE

Iranian Journal of Veterinary Science and Technology (IJVST) publishes important research advances in veterinary medicine and subject areas relevant to veterinary medicine including anatomy, physiology, pharmacology, bacteriology, biochemistry, biotechnology, food hygiene, public health, immunology, molecular biology, parasitology, pathology, virology, large and small animal medicine, poultry diseases, diseases of equine species, and aquaculture. Articles can comprise research findings in basic sciences, as well as applied veterinary findings and experimental studies and their impact on diagnosis, treatment, and prevention of diseases. IJVST publishes four kinds of manuscripts: Research Article, Review Article, Short Communication, and Case Report.

ON THE COVER

The Caspian cobra, Naja naja oxiana, is a highly venomous species of cobra. Its potent venom, with an LD50 value of 0.1 mg per kg, makes it one of the deadliest cobras. When threatened, it exhibits defensive behaviors, hood spreading and emitting hissing sound and strike repeatedly. The Caspian cobra's envenomation can cause severe neurotoxic symptoms, intense pain, and pronounced swelling at the bite site. Its bites mortality rate is 70 to 75%, the highest among all species of cobras. In Central Asia, the Caspian cobra is responsible for a significant number of snake bite-related deaths (Photo & drawing by B. Fathi-see page 52).

Editorial Office:
Faculty of Veterinary Medicine,
Ferdowsi University of Mashhad,
Azadi Square, Mashhad, IRAN
P.O. Box: 1793; Postal Code: 9177948974

Tel: +98 51 3880 3742 ***Fax:*** +98 51 3876 3852
Web: ijvst.um.ac.ir ***Email:*** ijvst@um.ac.ir

FERDOWSI UNIVERSITY OF MASHHAD PRESS

TABLE OF CONTENTS

IRANIAN JOURNAL OF VETERINARY SCIENCE AND TECHNOLOGY

Editorial Office:
Faculty of Veterinary Medicine, Ferdowsi University of Mashhad,
Azadi Square, Mashhad, IRAN
P.O. Box: 1793; Postal Code: 9177948974

Tel: +98 51 3880 3742 ***Fax:*** +98 51 3876 3852
Web: ijvst.um.ac.ir ***Email:*** ijvst@um.ac.ir

TABLE OF CONTENTS

IRANIAN JOURNAL OF VETERINARY SCIENCE AND TECHNOLOGY

Editorial Office:
Faculty of Veterinary Medicine, Ferdowsi University of Mashhad,
Azadi Square, Mashhad, IRAN
P.O. Box: 1793; Postal Code: 9177948974

Tel: +98 51 3880 3742 ***Fax:*** +98 51 3876 3852
Web: ijvst.um.ac.ir ***Email:*** ijvst@um.ac.ir

Iranian Journal of Veterinary Science and Technology

Received: 2023- Jun-10
Accepted after revision: 2024- Jan-10
Published online: 2024-Feb-01

RESEARCH ARTICLE

DOI: 10.22067/ijvst.2024.82675.1260

Causes for Carcass Condemnations of Slaughtered Poultry in the Industrial Slaughterhouse of Namin, Ardabil Province, Iran

Aidin Azizpour[a], Zahra Amirajam[b]

[a] Department of Medicinal Plants, Meshginshahr Faculty of Agriculture, University of Mohaghegh Ardabili, Ardabil, Iran.
[b] Department of Cardiology, Ardabil University of Medical Sciences, Ardabil, Iran.

ABSTRACT

Poultry meat production worldwide has continued to expand over the last two decades. In this regard, hygienic meat inspection and monitoring of diseases at slaughter lines have been recognized as essential for assessing flocks' status. This study aimed to determine the condemnation rate of slaughtered poultry and calculate the economic losses due to condemnations in the Namin industrial slaughterhouse, Ardabil Province of Iran. The data were collected by a veterinarian inspector in the slaughterhouse. The number of poultry slaughtered, their weight, the number and weight of condemned carcasses, and the reasons for condemnation were recorded. In this study, 3,488,916 poultry were slaughtered, and 42,310 carcasses (1.202 %) were condemned, weighing 66,385 kg. The highest percentage of condemned poultry was observed in autumn (1.61%), and the lowest in spring (0.93%). The direct financial loss incurred due to condemnations was estimated to be as high as 153,067 USD. Septicemia and dead on arrival (DOA) were the most common reasons for the rejection of carcasses, accounting for 47.85% and 0.580 of the total condemnations and total slaughtered poultry, respectively. The highest frequency percentage of the condemnation due to diseases occurred during autumn.In contrast, summer had the highest condemnation rate in association with DOA. The current survey showed that diseases caused the most condemnations compared to other causes. Therefore, improving disease control programs on flocks and increasing the welfare of birds before slaughter is recommended.

Keywords

Condemned carcasses, Septicemia, Dead on arrival, Slaughterhouse, Namin

Number of Figures: 1
Number of Tables: 4
Number of References:: 25
Number of Pages: 9

Abbreviations

DOA: Dead on arrival
USD: United States Dollar
DEL: Direct economic loss
NC: number of condemned poultry carcasses
P: average price of poultry carcasses (USD/Kg)
W: average poultry carcasses weight (Kg).
RLCL = ratio of condemnation losses to total condemnation economic losses

Corresponding author: Aidin Azizppour
Email: Aidin_azizpour@uma.ac.ir
Tel: +98(453)25425-4621

Introduction

Regarding the importance of poultry production in providing the protein needed by human societies and the dramatical development of the poultry industry in recent decades, attention to hygienic carcass inspection in abattoirs has been increased to monitor production levels and assurance of meat quality [1]. Because of this issue, the need to establish and develop industrial slaughterhouses and hygienic inspection of slaughtered poultry has gained special importance, on the one hand, to prevent the transfer of live poultry to the consumption market as well as the spread of contamination caused by them, and on the other hand, to remove contaminated and unusable carcasses from the slaughter line by strict sanitary monitoring on the slaughter line. Finally, meat in completely hygienic conditions free from contamination and disease can be available to consumers [1-3].

Therefore, attention has shifted to the evaluation of the causes of carcass condemnation at slaughterhouses in many countries during recent decades. In a survey conducted from 2019 to 2020 in broiler slaughtered in Germany, the most common reasons for rejected carcasses were deep dermatitis (mean 0.63%) and ascites (mean 0.53%) [3]. Studies conducted over 6 years in the district of Olsztyn, Poland, showed that in the slaughterhouse inspection process, Mark's disease (MD) was seen in the internal and external organs of 2265 chickens (0.095%) [4]. According to the research by Santana et al. [5] from January to April 2007 in Brazil, the most common cause for condemnation in slaughterhouse A was related to cellulitis (4.25%). Various factors such as infectious diseases, ascite /peritonitis, mechanical factors (impact), cachexia, dead on arrival (DOA), poisoning, and tumors have been reported, which caused the condemnation of carcasses during the inspection process in abattoirs [1, 3, 4, 6-12].

In addition, the increase in condemnation rate due to diseases and other abnormalities will finally lead to great economic losses in the poultry industry [13-15]. Therefore, this study aimed to determine the rate and the causes of condemned carcasses and estimate economic losses due to condemnations in industrial slaughterhouse in Namin, Ardabil province, for one year.

Abbreviations-Cont'd

CL: condemnation economic losses due to a specific cause (USD)
TL: total condemnation economic losses (USD)
RLSI= ratio of condemnation losses to total slaughter financial income
CL: condemnation economic losses due to a specific cause (USD)
TI: total slaughter financial income (USD)

Results

The total number of slaughtered poultry in the industrial slaughterhouse of Nemin was 3,488,916, which included a total slaughter weight of 10,392,234 kg. During this study, 42,310 carcasses were condemned, accounting for 1.202% of the total slaughter and weighing 66,385 kg (Tables 1 and 2).

Statistical analysis shows a significant difference ($p < 0.001$) among the total number of condemnation carcasses in different seasons. Despite the high slaughter rate in summer compared to other seasons, autumn had the highest rate of condemnations while the least of it was observed in spring (Table 1).

There is a significant difference among different seasons regarding the weight of condemned poultry carcasses ($p < 0.001$). Thus, the lowest and highest weights of condemnations were in the spring and autumn seasons, respectively (Table 2).

The average annual direct economic loss due to condemnations is estimated at 4,089,058,000 Rial, equivalent to 153,067 USD. The highest economic loss was in autumn compared to other seasons (Table 3).

In this study, a total of nine reasons for the condemnation of carcasses were identified. The total number of condemnations and their percentage compared to the total number of condemned carcasses and slaughter are shown in Table 4. Of all condemned carcasses, the most condemnations, with 13,810 carcasses, were related to septicemia, which includes 32.64% of all condemnations and 0.396% of total slaughter. With 6,437 carcasses, 15.21% of total condemnations, and 0.184% of the total slaughter, DOA is in the second rank. The lowest condemned carcasses were due to contusion/fracture/ bruising, with 0.20% of the total condemnations and 0.002 % of the total slaughter. According to the findings from Table 4, from all condemned carcasses, the highest weight of condemnations, with a weight of 22,460 kg, was related to septicemia, which was included 33.83% and 0.216% of the total weight of the condemned carcasses and the total slaughter, respectively. The resulting losses were estimated at 49,511 USD. In the second rank was the DOA with a weight of 15,231 kg, which constituted 22.94 % of the total weight of condemnations and 0.146 % of the total slaughter weight, and economic losses caused by it were estimated at 37,069 USD. The lowest weight of condemned carcasses was due to contusion/fracture/ bruising, with 0.21% of the total condemnations and 0.001 % of the total slaughter. The economic loss related to it was calculated at 329 USD.

Frequency percentages of septicemia, ascites/ peritonitis, poisoning, arthritis/synovitis, cachexia, cellulite, contusion/fracture/ bruising, and CRD in autumn were higher than in other seasons. Whereas

Table 1.
Comparison of the total number of slaughtered and healthy carcasses and the total number of condemned carcasses in the industrial slaughterhouse of Namin during different seasons.

Seasons	Number of slaughter	Number of healthy carcasses	Number of condemnations (%)
April–June	797,819	790,388	7,431 (0.93)
July–September	984,560	971,656	12,904(1.31)
October–December	906,207	892,107	14,100 (1.61)
January–March	800,330	792,455	7,875 (1.01)
Total	3,488,916	3,446,606	42,310 (1.20)

$\chi 2(3)=1532$, $p =< 0.001$

Table 2.
Comparison of net weight of slaughter and healthy carcasses and weight of condemned carcasses in the industrial slaughterhouse of Namin during different seasons.

Seasons	Weight of slaughter	Weightof healthy carcasses	Weight of condemnations (%)
April–June	2,473,930	2,462,270	11,660 (0.47)
July–September	2,905,204	2,884,665	20,539(0.70)
October–December	2,797,645	2,774,396	23,249 (0.83)
January–March	2,215,455	2,204,518	10,937 (0.49)
Total	10,392,234	10,325,849	66,385 (0.63)

$\chi 2(3)=3696$, $p =< 0.001$

Table 3.
Comparison of economic income of slaughter and healthy carcasses and economic losses of condemnations in the industrial slaughterhouse of Namin during different seasons.

Seasons	Economic income from slaughter	Economic income of healthy carcasses	Economic losses of condemnations (%)
April–June	6,461,581	6,431,127	30,454 (0.47)
July–September	7,020,145	6,970,514	49,631(0.70)
October–December	5,777,622	5,729,609	48,013 (0.83)
January–March	5,057,841	5,032,872	24,969 (0.49)
Total	24,317,189	24,164,122	153,067 (0.63)

$\chi 2(3)=5325$, $p =< 0.001$

summer had the highest frequency percentages of condemnations related to dead on arrival (Fig 1).

Table 4.
Number, weight and financial losses of condemned carcasses according to their causes in the slaughterhouse of Namin.

Cause of condemnations	No.	CTC (%)	CTS (%)	WC Kg	RWCW (%)	RWSW (%)	ELC	RLCL	RLSI
Septicemia	13,810	32.64	0.396	22,460	33.83	0.216	49,511.47	32.35	0.203
DOA	6,437	15.21	0.184	15,231	22.94	0.146	37,069.05	24.22	0.152
Ascite /peritonit	5,439	12.85	0.155	8,203	12.35	0.078	17,446.90	11.40	0.071
Cachexia	4,725	11.16	0.135	2,610	3.93	0.025	6,287.71	4.11	0.025
CRD	4,591	10.85	0.131	6,799	10.24	0.065	16,254.70	10.62	0.066
Poisoning	3,481	8.22	0.099	5,335	8.03	0.051	12,774.13	8.34	0.052
Cellulite	3,343	7.90	0.095	5,004	7.53	0.048	12,033.07	7.86	0.049
Arthritis /synovitis	397	0.94	0.011	603	0.90	0.005	1,360.13	0.89	0.005
Contusion/fracture/ bruising	87	0.20	0.002	140	0.21	0.001	329.93	0.21	0.001
Total condemnations	**42,310**	**100**	**1.202**						
Total weight of condemnations				**66,385**	**100**	**0.638**			
Total direct economic losses							**153,067**	**100**	**0.629**

No: Number. CTC: Ratio of condemnation number to total condemnations. CTS: Ratio of condemnation number to total slaughter. WC :Weight of condemnations. RWCW: Ratio of condemnation weight to total condemnation weight. RWSW:Ratio of condemnation weight to total slaughter weight. ELC: Economic losses of condemnations. RLCL :Ratio of condemnation economic losses to total condemnation economic losses. RLSI :Ratio of condemnation economic losses to total slaughter financial income. DOA: dead-on arrival.

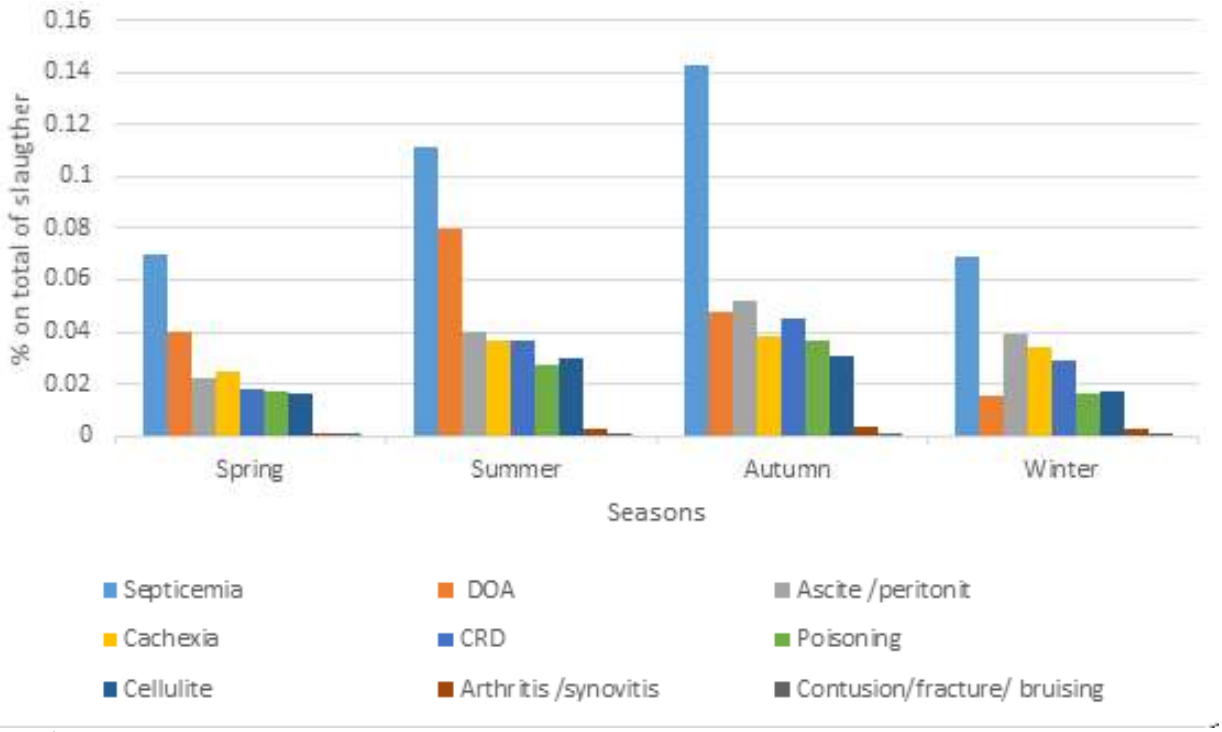

Figure 1.
Seasonal frequency of condemnation causes in the industrial slaughterhouse of Namin.

Discussion

Every year, in different parts of the world, extensive research is conducted on the causes of condemnation carcasses, which is very important to identify and determine the distribution of diseases to prevent carcass condemnation and ultimately reduce financial losses [5, 7, 13-14]. Researchers have shown that the proportion of total carcass condemnation to slaughtered birds and the reasons for condemnations differ in countries [4, 6]. This difference is related to ecologic conditions, epidemiology of diseases, age and type of slaughtered poultry, and management practice of poultry in every country [4, 6].

According to Bremner [2] studies in England and Wales from 1992 to 1993, 1.3% of all slaughtered broilers were condemned for various causes, and septicemia /toxemia/fever were the most common causes of condemnation (65.6%). Herenda and Jakel [8] investigated causes for carcass condemnations in Ontario, Canada, between 1991 and 1992. Out of 9,829,296 slaughtered broilers, 100,369 (1.02%) were rejected; ascites and cellulitis were the most frequent reasons for condemned carcasses (0.52%). A survey conducted in Olsztyn, Poland, during 1986-1991 showed that 1.66% was condemned from 37,779,959 slaughtered poultry, and the most common reason for the condemned chicken carcasses was related to Marek's disease [4]. The research carried out by Petracci et al. (2006) on 1266 million broilers in thirty-three slaughterhouses from 2001 to 2005 in Italy shows that the average percentage of DOA was 0.35 and its rate significantly increased during summer. Mukaratirwa et al. [10] showed that from 1999 to 2005, out of 55,957 ostriches slaughtered in Norton, Zimbabwe, 0.05% of the carcasses were rejected due to septicemia. In another study conducted by Dzoma et al. [7] between 2001 and 2005 in Botswana, 3,814 ostriches were referred to the slaughterhouse; during an inspection, 949 organs were rejected for various reasons, and the highest condemnations were due to lungs. Santana et al. [5] studied two slaughterhouses in Goias State, Brazil, from January to April 2007. Of 40,732,773 and 6,457,166 slaughtered poultry in slaughterhouses A and B, 3,384,861 (8.3%) and 235,014 (3.6%) carcasses were rejected, respectively. The most common causes of condemnations in slaughterhouse A, with 51.20% of all condemned carcasses and 4.25% of all slaughter, were observed due to cellulite. In contrast, in slaughterhouse B, fracture and bruising, with 28.90% of all condemnations and 1.04% of all slaughter, were the most common causes of condemnations.

A survey conducted on 404 broiler flocks referred to 15 industrial slaughterhouses in western France during 2008 reported 0.87% of condemned carcasses, and the highest condemnations were related to cachexia 0.30% and hyperemia (0.22%) [16]. In a study accomplished by Haslam et al. [17] in England, the mean percentage of rejection was 1.23%, and the main reason for cause condemnation was reported to be acute internal pathology (0.22%) and Cachexia (0.20%). Alloui et al. [18] studied the condemnation rate in the poultry slaughterhouse of Batna City (Algeria), where 8.4 % of carcasses were rejected, and the major causes of condemnations were congestion, skin lesions, cachexia. In the report of Mwimali et al. [19], 405,778 (1.88%) birds were condemned from 21,549,233 slaughtered broilers in Kenya, which Ascites and DOA were the most frequent causes of rejection (92.74%).

In 2017, Salines et al. [12] investigated the reasons for the condemnation of broilers at 10 slaughterhouses in France which the most common reason for condemnations was cachexia (41.8 %), generalised congestion (29.3%) and non-purulent cutaneous lesions (14.2%). Abdelrahman et al. [13] reported that 49,638 (0.95%) and 16,382 (0.32%) of total slaughtered poultry (5,181,189) in at Damietta poultry abattoir, Damietta governorate, Egypt, were condemned for DOA and condemned broilers, respectively. Cellulitis (11.2%), ascites (10.5%), and septicemia (9.7%) were the most important causes of condemnation, and the annual total economic loss was 2668600.2 EC/P. In another study, 33,54,747 slaughtered broilers were surveyed in England slaughterhouses from 2017–2018, and ascites and abnormal colour were the main reason for condemnations [20]. According to a study by Törmä et al. [21] from approximately 370 million broilers slaughtered in four Finnish slaughterhouses from 2015–2019, the condemnation rate varied between 2.6% and 4.8%, and Cellulitis (0.3–1.0%), ascites (0.3–0.4%), and body cavity disorders (0.2–0.3%) were the most common condemnation causes. A survey by Alfifi et al. [22] in a main slaughterhouse in Denmark from 2020 to 2021 showed that from 17,331,511 slaughtered chickens, 205,879 (1.2%) carcasses were condemned. The main causes of condemnations were due to scratches (23.6%), cellulitis (19.2%), and hepatitis (8.3%).

The studies carried out in Iran have reported that the rate and reasons for condemnations vary in different regions. Research conducted by Ansari-Lari and Rezagholi [6] on eleven industrial slaughterhouses in Fars province from 2002 to 2006 shows that out of the total 130,967,021 slaughtered poultry, 959,416 (0.73%) carcasses were condemned; 62% (595,287) of all condemnations were related to cachexia and septicemia. A study of Jalilnia and Movassagh [23] in the industrial slaughterhouse of East Azarbaijan Province in 2011 revealed that from the total of 14,788,995 slaughtered poultry, 55,325 (0.37%) carcasses were

condemned, and the most causes for condemnation was due to cachexia (30.46%). Hosseini Aliabad et al. [9] reported that 380140 poultry were slaughtered in the Nowshahr slaughterhouse between 2005 and 2006, where 2,548 carcasses (0.67%) were condemned; the DOA was the highest condemned carcasses (0.172%).

In a study conducted by Gholami et al. [15] in 28 slaughterhouses of Tehran province from 2009 to 2011, out of a total of 214,997,429 slaughtered poultry, 705,046 (0.33%) carcasses were rejected; cachexia was the most cause for condemnations (46.57%). Also, they estimated the average annual economic loss due to the condemnations of 14,594,452,200 rials. In the Khodaei-Motlagha et al. [24] study, the most common causes for condemnations of slaughtered broilers in Shanzand slaughterhouse were due to excessive atrophy, trauma, and septicemia during 6 months in 2009. According to reports by Ghaniei et al. [14] at 11 abattoirs in West Azerbaijan province from 2008 to 2015, 171,297,886 poultry were slaughtered, and 1,580,570 (0.92 %) poultry carcasses were condemned for different reasons: septicemia and cachexia were the most common reasons for the condemnation (60.3%) and financial loss due to condemnation was estimated to be as high as 3,731,905 USD.

The present study condemned 42,310 carcasses (1.202%) for various reasons. The 1.202% rate for condemnation in our study is similar to those of Bremner [2], Abdelrahman et al. [13], Haslam et al. [17], and Alfifi et al. [22], who reported 1.30%, 1.27%, 1.23%, and 1.20%, respectively. However, it varied substantially with other studies. The condemnation rate of our study is higher than those reported by Gholami et al. [15] (0.33%), Jalilnia and Movassagh [23] (0.37%), Hosseini Aliabad et al. [9] (0.67%), Ansari-Lari and Rezagholi [6] (0.73%), Ghaniei et al. [14] (0.92%) and Herenda & Jakel [8] (1.02%) and Salines et al. [12] (1.04%). While it is lower than rates reported by Alloui et al. [18] 8.4% in Algeria, Santana et al. [5] 8.3% and 3.6% for two different slaughterhouses in South America, Törmä et al. [21] between 2.6% and 4.8% in Finnish, Radkowski et al. [4] 1.66% in Poland, Junghans et al. [3] 1.48% in Germany and Kittelsen et al. [25] mean 1.4% in Norway.

As shown above, the overall rate of condemnation was different compared with other studies; the reasons for the condemnation were also different. In this survey, of all the condemnations, the most frequent causes of condemned carcasses belonged to septicemia and DOA (20,247 carcasses). So it can be said that the rate of condemnation related to these two factors is very significant compared to other causes, including 47.85% and 0.580% of the condemnations and the total of slaughtered poultry, respectively. The highest financial losses in the present study were observed due to septicemia and DOA; the estimated economic losses related to these two reasons (86,580 USD) are much higher than other causes and constitute 56.52% of the total economic losses.

The highest incidence rate of septicemia was observed in autumn during this study. Septicemia is an almost non-specific term and indicates an infectious disease whose clinical diagnosis is based on carcass congestion, muscle darkening, kidney inflammation, and inflammatory lesions such as airsacculitis and perihepatitis [1]. Various microbial causes cause septicemia, the most important of which are E.coli, influenza, Salmonella enteridis, and Pasteurella multicida, important pathogens of human relevance [6]. In this work, bacteriologic examination on septicemic carcasses was not done. However, identifying the microorganisms causing septicemia is highly recommended in future works, which might have important public health implications.

Mortalities due to DOA have welfare and great economic implications in the poultry industry [13]. This study revealed an increased frequency of DOA in summer, similar to the report provided by Salines et al. [12] Incidence of high mortality of DOA in the hot months of the year may reflect the effects of hot stress during the time of broiler harvest and transport and also increased transit times [12]. DOA are carcasses that have perished between the farm and the slaughter or before slaughter. The main reason is the failure to comply with management issues in transporting poultry from farms to the slaughterhouse, which other things can mention for heat stress and humidity in early summer, especially in July, feed and water withdrawal, long transit times, physical injury, environmental condition, high ambient temperature, and overcrowding [13, 18, 25]. This study showed that most reasons for condemnations are due to diseases, accounting for 84.59%. The estimated annual economic losses during this survey were 115,669 USD for diseases and 37,069 USD for DOA. The high rate of condemnations for diseases in colder months was logical.

Conclusion

The meat inspection records in the present survey are a useful tool to help monitor the status of diseases on the flocks and the welfare of birds, which can be used as prevention measures. Therefore, improving disease control programs on flocks and increasing the welfare of birds from flocks to slaughter is necessary. The present results can act as baseline data for the future monitoring of condemnations in poultry slaughterhouses.

Materials & Methods

Study Design and Data Collection

This study was carried out using a cross-sectional method from April 2019 to March 2020. Data were obtained with the help of an experienced team of veterinarians. In this survey, DOA and condemned carcasses in the Parkan slaughterhouse of Namin, located in Ardabil province, were investigated. Under the supervision of the responsible veterinarian on the slaughter chain, the total number of slaughtered poultry (broiler, broiler breeder, turkey) and their weight were recorded daily, and in the second stage, after isolating and weighing unusable carcasses, the number of condemnations were recorded and then causes of condemnations were identified based on their morphological characteristics and symptoms, as well as necropsy lesions [6].

Finally, data were collected separately in tables. The prevalence rate was sorted monthly to determine the difference between the distribution of condemned carcasses and the season. The overall rate of condemnations for the one year was also determined. The proportions (%) of condemnations were calculated considering the number and weight of rejected carcasses due to a specific cause against the total number and weight of condemned carcasses and slaughtered poultry.

Inspection of Poultry

Veterinarians carried out routine meat inspection, and condemnation was dependent on the inspector's experience. In Brief, hygienic carcass inspections were performed in two stages in the abattoir: before slaughter (stage I) and post-slaughter (stage II) [1]. In the first stage of the inspection (before weighing), were taken a sanitary license from the veterinary organization and records of the poultry, including age, average weight, ration type, and diseases involved during the breeding period; then all the poultry were transferred to the slaughter line and inspected before blood sampling. At this stage, acute infectious diseases, cachexia, DOA, general contamination, common infections, and abnormal smells were diagnosed.

The post-slaughter inspection was carried out in three stages, in which the surface parts of the body, intestines, and visceral and internal cavities of the body were inspected, and in this process, inedible carcasses were rejected from the cycle of slaughter; after ending the inspection and unloading of intestines and viscera to obtain the net weight of slaughter, carcasses were weighed. In this study, the net weight of slaughter was 72.4 to 72.6% of the slaughter.

Assessment of the Financial Loss

The direct economic losses due to condemnation were calculated by this formula:

$DEL = NC \times P \times W$

The Average sell price of carcasses (p) was calculated based on the prices of slaughtered poultry (Rials/kg) for Ardabil province, which is announced on the website of Iran Poultry Industry Information and Communication Technologies Institute (www.itpnews.com) daily, monthly, and annual. Then, the monthly average sell price of condemned carcasses was estimated in Rial. Later, the calculated Rial was converted into Dollars by checking the reliable currency sell markets such as the Bank Melli Iran (www.bmi.ir) in Tehran province during different months. The average annual sell prices for each kilogram of carcasses were 61,596 Rial or 2.3 USD.

The Average poultry carcass weights (W) were determined by weighting 100 carcasses of different ages. The average weights were calculated as 0.5 kg, 1.6 kg, and 2.3kg for cachexia, diseases, and DOA in this region, respectively.

The proportions (%) of condemnation economic loss were calculated by these formulas:

$RLCL = CL \div TL \times 100$

$RLSI = CL \div TI \times 100$

In this study, SPSS software was used for statistical data analysis. Seasonal patterns of variables were investigated with the chi-square ($\chi 2$) test. The P-value less than 0.05 is considered statistically significant.

Authors' Contributions

Aidin Azizpour: Supervision, Planning, Conceptualization, Visualization, Writing- Reviewing and Editing Manuscript. Zahra Amirajam: Supervision, Investigation, Data Analysis, Resources and Validation.

Acknowledgements

The authors would like to thank University of Mohaghegh Ardabili for financial support and everyone who helped us in performing this study.

Conflict of interest

The authors declare that there is no conflict of the interest

References

1.Gracey JF, Collins DS, Huey RJ. Poultry production, slaughter and inspection. In: Meat Hygiene. 10th Ed. W.B, Saunders Company: LTD; 2008.

2.Bremner AS. Post mortem condemnation return from poultry slaughter houses in England and Wales. Pre Vet Med. 1994; 135: 622-623. PMID: 7716871.

3.Junghans A, Deseniß L, Louton H. Data evaluation of broiler chicken rearing and slaughter—An exploratory study. Front Vet Sci. 2022; 9: 957786. DOI: 10.3389/fvets.2022.957786.

4.Radkowski M, Uradzinsk J, Szteyn J. The occurrence of infections and parasitic diseases in poultry slaughtered in the district of Olsztyn, Poland 1986–1991. Avian Dis. 1996; 40: 285–289. DOI: 10.2307/1592222.

5.Santana AP, Murata LS, de Freitas CG, Delphino MK, Pimentel CM. Causes of condemnation of carcasses from poultry in slaughterhouses located in State of Goiás, Brazil. Cien Rural. 2008; 38: 2587-2592. DOI:10.1590/S0103-84782008005000002.

6.Ansari-Lari M, Rezagholi M. Poultry abattoir survey of carcass condemnations in Fars province, southern Iran. Pre Vet Med. 2007; 79: 287-293. DOI:10.1016/j.prevetmed.2006.12.004.

7.Dzoma BM, Pansiri E, Segwagwe BE.A retrospective study on the prevalence of ostrich carcass and organ condemnations in Botswana. Tropical Anim Heal Prod. 2009; 41: 443–448. DOI:10.1007/s11250-008-9206-6.

8.Herenda D, Jakel O. Poultry Abattoir survey of carcass condemnation for standard, vegetarian, and free range chickens. Canadian Vet J. 1994; 35: 293–296. PMCID: PMC1686657.

9.Hosseini Aliabad SA, Mortazavi P, Khoshbakht R, Mousavi AS. Causes of Broiler Carcasses Condemnation in Nowshahr Poultry Slaughters (North of Iran) with Histopathologic Study of Cases Suspected to Marek's Disease. J Agri Sci Tech A. 2011; 1: 1069-1073. DOI: 10.17265/2161-6256/2011.11A.017

10.Mukaratirwa S, Dzoma BM, Matongo C, Nyahuma N. Some Causes of Organ and Carcass Condemnations in Ostriches Slaughtered at the Only Ostrich Abattoir in Zimbabwe from 1999-2005. Inter J Poult Sci. 2009; 8: 1096 -1099. DOI: 10.3923/ijps.2009.1096.1099.

11.Petracci M, Bianchi M, Cavani C, Gaspari P, Lavazza A. Preslaughter mortality in Broiler chicken,Turkey and spent hens under commercial slaughter. Poul Sci. 2006; 85:1660-1665. DOI: 10.1093/ps/85.9.1660.

12.Salines M, Allain V, Roul H, Magras CS, Le Bouquin S. Rates of and reasons for condemnation of poultry carcasses: harmonized methodology at the slaughterhouse. Vet Rec. 180 (21): 506524. DOI: 10.1136/vr.104000.

13.Abdelrahman HB, Shimaa Sabry ME, Heba Mohamed AS. Evaluation of Chicken Broiler Carcasses Condemnation in Damietta Province Abattoir- Egypt. Suez Canal Vet Med J. 2022; 27(1): 59-69. DOI: 10.21608/scvmj.2022.123484.1070.

14.Ghaniei A, Mojaverrostami S, Sepehrnia P. Survey of Poultry Carcass Condemnations in Abattoirs of West Azerbaijan Province (North West of Iran). J Hellenic Vet Med Soc. 2016; 67(3): 183–188. DOI: 10.12681/jhvms.15637.

15.Gholami F, Bokaie S, Khanjari A, Esameili, H, Mirzapour A. A retrospective survey of poultry carcass condemnation in abattoirs of Tehran province, Capital of Iran, Iran (2009-2011). Inte J Bioflux Soci. 2013; 5(4): 114-116.

16.Lupo C, Chauvin C, Balaine L, Petetin I, Peraste J. Postmortem condemnations of processed broiler chickens in western France. Vet Rec. 2008; 162(22): 709-713. DOI: 10.1136/vr.162.22.709.

17.Haslam SM, Knowles TG, Brow S.N,Wilkins LJ, Kestin SC. Prevalence and factors associated with it, of birds dead on arrival at the slaughterhouse and other rejection conditions in broiler chickens. British Poul Sci. 2008; 49: 685–696. DOI: 10.1080/00071660802433719.

18.Alloui N, Guettaf L, Djeghouri F, Lombarkia O. Quality of broilers carcases and condemnation rate during the veterinary control in the Batna slaughterhouse. J Vet Advan. 2012; 2: 70-7.3.

19.Mwimali MI, Kitaa JMA, Osoro LN. An Analysis of the Causes of Poultry Condemnations at A Nairobi Slaughter House, Kenya (2011-2014). Inter J Vet Sci. 2018; 102 7(3): 121-126. PMCID: 201924676.

20.Buzdugan SN, Chang YM, Huntington B, Rushton J, Guitian J, Alarcon P. Identification of production chain risk factors for slaughterhouse condemnation of broiler chickens. Pre Vet Med. 2020; 181: 105036. DOI: 10.1016/j.prevetmed.2020.105036.

21.Törmä, K, Kaukonen E, Lundén J, Fredriksson-Ahomaa M, Laukkanen-Ninios R. Acomparative analysis of meat inspection data as an information source of the health and welfare of broiler chickens based on Finnish data. Food Cont. 2022; 138: 109017. DOI: 10.1016/j.foodcont.2022.109017.

22.Alfifi A, Christensen JP, Gildas Hounmanou YM, Sandberg M, Dalsgaard A.Characterization of Escherichia coli and other bacteria isolated from condemned broilers at a Danish abattoir. Food Microb. 2022; 13: 10. DOI:10.3389/fmicb.2022.1020586.

23.Jalilnia M, Movassagh MH. A study on causes of poultry carcasses condemnation in East Azerbaijan province (North West of Iran) poultry slaughter house. Annal Biol Res. 2011; 2 (4): 343-347. PMCID: 55319022.

24.Khodaei-Motlagha M, Yahyaib M, Rezaeic M, Eidid A, Moazami-godarzid MR, Hajkhodadadia I. Determination carcass condemnation causes of broiler chickens (Gallus Domesticus) at industrial slaughter house of Shazand, Markazi province of Iran.

25.Kittelsen KE, Moe RO, Hoel K, Kolbjørnsen Ø, Nafstad O, Granquist E G. Comparison of flock characteristics, journey duration and pathology between flocks with a normal and a high percentage of broilers 'dead-on-arrival' at abattoirs. Anim. 2017; 11(12): 2301-2308. DOI:10.1017/S1751731117001161.

How to cite this article
Azizpour A, Amirajam Z Causes for Carcass Condemnations of Slaughtered Poultry in the Industrial Slaughterhouse of Namin, Ardabil Province, Iran . Iran J Vet Sci Technol.2024; 16(1): 1-9.
DOI: https://doi.org/10.22067/ijvst.2022.77084.1153
URL: https://ijvst.um.ac.ir/article_44779.html

Iranian Journal of Veterinary Science and Technology

Received: 2023- Oct- 01
Accepted after revision: 2023- Dec-06
Published online: 2024- Feb-01

RESEARCH ARTICLE

DOI: 10.22067/ijvst.2023.84439.1301

Alterations in the Clinical Manifestations of Cutaneous Leishmaniasis in Various Total Antioxidant Capacities: An Animal Study Using BALB/c Mice

Mojtaba Yousefi[a], Seyed Masoud Zolhavarieh[b], Alireza Nourian[a], Hossein Rezvan[a], Ali Sadeghi-nasab[b]

[a] Department of Pathobiology, Faculty of Veterinary Medicine, Bu-Ali Sina University, Hamedan, Iran.
[b] Department of Clinical Sciences, Faculty of Veterinary Medicine, Bu-Ali Sina University, Hamedan, Iran.

ABSTRACT

The severity of the clinical manifestations of cutaneous leishmaniasis can vary depending on various factors, such as the *Leishmania* species involved as well as hosts and their immune response. This study aimed to investigate the relationship between the severity of different clinical signs, histopathological changes, and genetic indicators with TAC in mice experimentally infected with *Leishmania major*.A total of 105 eight-week-old BALB/c mice of both sexes were assigned to seven experimental groups (15 in each) as follows: 1) healthy mice, 2) *Leishmania*-infected mice treated with 100 mg/kg/day of SC glucantime until complete healing, 3) mice which received 20 IU/kg/day of vitamin E (SC for 10 days) to increase TAC prior to infection and further treatment with glucantime, 4) *Leishmania*-infected mice which received both vitamin E and glucantime daily until complete healing, 5) mice which received 20 IU/kg/day of vitamin E (SC for 10 days) before infection, and 6) *Leishmania*-infected mice which received 20 IU/kg/day of SC vitamin E up to the end of the trial, and 7) mice which received daily vitamin E until the end of the experiment. Wound size, expression of pro-inflammatory cytokines (IFN-γ and TNF-α) and healing genes (KGF and EGF), histopathological findings, and mortality rate were assessed three times on days 31, 38, and 72 post-infection. Approximately, 31 days after the parasite inoculation, dermal lesions were developed in all infected mice. In group 3, the clinical manifestations, healing time, and histopathological changes were significantly more favorable, while group 4 showed the worst situation in terms of the evaluated indicators. A high level of TAC before the onset of the disease has an effective role in the recovery indicators. However, its simultaneous elevation at the beginning of infection will decrease the body's ability to effectively clear the parasite, heal the tissue, and improve the clinical manifestations of the disease.

Keywords

Antioxidant capacity, Clinical manifestations, Cutaneous leishmaniasis, Leishmania, IFN-γ, TNF-α

Number of Figures: 7
Number of Tables: 3
Number of References:: 27
Number of Pages: 9

Abbreviations

EGF: Epidermal growth factor

OH˙: Hydroxyl radical

Corresponding author:
Seyed Masoud Zolhavarieh
Email: mzolhavarieh@basu.ac.ir
Tel: +98(81)3140-6022

Introduction

Various species of *Leishmania* are obligate intracellular protozoa that replicate within macrophages after being phagocytized by these cells. This parasite has an extracellular promastigote form in its arthropod vector, sandfly, and an intracellular form inside the mammalian macrophages known as amastigote. Upon the sandfly bite, the parasites transfer into the dermis and are subsequently phagocytized by neutrophils, which are immediately called to the site. Within 2 days after the arrival of monocytes/macrophages, as the second wave of inflammatory cells infiltration, the parasites are engulfed mainly by these mononuclear phagocytes, lose their flagella, and differentiate into amastigotes [1, 2].

Macrophages are equipped with microbicidal mechanisms, from which, the intracellular microorganisms must escape to survive [3]. During leishmaniasis, the germicidal processes may occur in two stages. First, during the initial phagocytosis of promastigotes, the macrophage can show a fast oxidative response stimulated by the phagocytic event. Second, once infection with amastigotes is established, the quiescent macrophages can slowly be activated to potentially destroy the intracellular *Leishmania* [4].

Efficient escape from microbicidal molecules produced at each stage of infection is important for *Leishmania* to initiate and maintain the host cell infection. Two important macrophage-derived oxidants are critical in controlling *Leishmania* infection. During the early stage of infection, the free radical superoxide anion ($O2^{\bullet-}$) is produced as a part of the macrophage respiratory burst in response to the phagocytized cell [5, 6]. Superoxide production is catalyzed by NADPH oxidase, a heme-containing cytochrome that comprises cytosolic and membrane-bound components. After assembly, the oxidase transfers an electron from NADPH to molecular oxygen and produces $O2^{\bullet-}$. Promastigotes are susceptible to being killed by exposure to $O2^{\bullet-}$ and hydroxyl radical ($OH^{\bullet}$) produced from H_2O_2 [7, 8].

The second anti-leishmanial oxidant produced by macrophages is $NO^{\bullet}$ [4]. Unlike $O2^{\bullet-}$, which is generated during parasite phagocytosis, $NO^{\bullet}$ is produced after macrophage activation by IFN-γ and TNF-α and is closely associated with the intracellular killing of amastigotes [9].

Neutrophils normally have a short lifespan (less than a day) and undergo spontaneous apoptosis. This period may be elongated when these cells are infected with microorganisms [10]. *L. major* can suspend neutrophil apoptosis for up to two days by inducing the secretion of anti-apoptotic cytokines, such as granulocyte-macrophage colony-stimulating factor and IL-8 [11]. It has also been reported that infected neutrophils undergoing apoptosis release more macrophage inflammatory protein 1 beta to attract macrophages to the site of infection and prepare a safe and silent entry to these cells [12]. In other words, the prevention of neutrophil apoptosis is an important mechanism used by *Leishmania* to subvert its death [12, 13]. This silent entry into macrophages is reminiscent of the Trojan Horse scenario [2, 14] as promastigotes suspend the neutrophils' apoptosis process until macrophages arrive at the site of infection, and also suppress $O2^{\bullet-}$ and $NO^{\bullet}$-mediated microbicidal responses [11, 12]. Infected neutrophils are engulfed by macrophages and allow promastigotes to multiply and transform into amastigotes in macrophage phagosomes.

Many studies emphasize the key role of parasite proliferation and host inflammatory responses in leishmaniasis and the impact on the clinical course of the disease [9, 15, 16]. It has been shown that skin wounds and tissue destruction are necessary for effective parasite clearance [3]. Therefore, the clinical manifestations of leishmaniasis, which range from skin lesions to potentially fatal visceral disease [17], are caused by parasite replication and the host's inflammatory responses [9, 18]. In a clinical study, it was shown that the TAC level in leishmaniasis patients suffering from unhealed chronic wounds is significantly higher than in healed patients [19]. *Leishmania* causes inflammation by stimulating the connective tissue mast cells and the resultant production of reactive oxygen species (ROS) pro-inflammatory mediators. The production of ROS and $NO^{\bullet}$ during an inflammatory response leads to oxidative damage to cells. On the other hand, similar to the lipophosphoglycan of the promastigote membrane, the intracellular amastigotes disrupt IFN-γ signaling and therefore, significantly inhibit the activity of superoxide dismutase and catalase (CAT) [20]. In other words, during *leishmania* infection, on one hand, free radicals are created during an inflammatory response, and on the other hand, the TAC level decreases simultaneously with the healing of skin wounds and improvement of other clinical manifestations [21]. The present study was conducted to investigate the relationship between the severity of leishmanial lesions with different levels of TAC to better understand the course of the disease and improve the treatment process.

Abbreviations-Cont'd

IL-1α: Interleukin-1 alpha
IFN-γ : Interferon-gamma
KGF: Keratinocyte growth factor
NADPH: Nicotinamide adenine dinucleotide phosphate
ROS : Reactive oxygen species
$O2^{\bullet-}$: Superoxide
TAC: Total antioxidant capacity

Results

Leishmaniasis lesions in different groups

On average, after 31 ± 2 days, a *Leishmania* wound was observed in the parasite inoculation area (Figure 1). In this study, it was observed that the wounds in all groups except for group 2 (LT) became wider until the second sampling time (day 38) and then, their size gradually decreased. The smallest size of the wounds was in group 3 ($(20.2^{mm2} \pm 23.5)$), while the largest was in group 2 ($p < 0$) (Figure 2). Moreover, in the last sampling time, the wounds of group 3 had the highest percentage of healed area (83.9%), and the lowest percentage was observed in group 4 (47.5%) ($p < 0$) (Figure 3). In the groups administered with glucantime with or without vitamin E, after approximately 72 days, the cutaneous wounds were completely healed and no nodules or remnants were observed.

Figure 1.
Cutaneous wounds caused by the Leishmania major parasite.

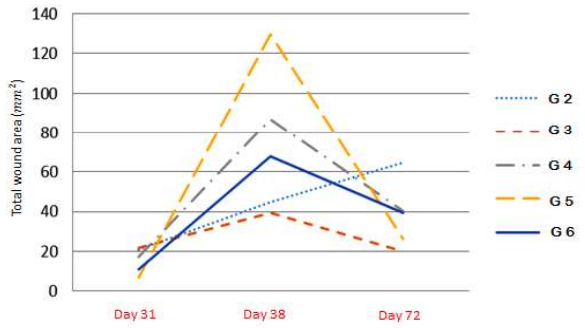

Figure 2.
Changes in total wound area in different groups (mm2). Groups 1 and 7 are not included in this diagram, because they had no wounds.

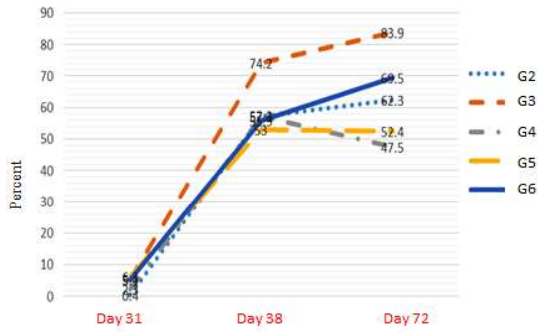

Figure 3.
Changes in the ratio of healed areas to the initial size of the wound in each group (percentage)..

TAC measurement

While group 3 (ALT) had the lowest amount of TAC compared to other groups (Figure 4), wound healing in this group showed a significant inverse relationship with the amount of TAC ($64.5^{mm2} \pm 45.1$) [Pearson correlation (P-value) respectively] (Table 1). Furthermore, in group 5 (AL), it was observed that the total area of the wound had an inverse relationship with the level of [-0.5 (0.001)] [Pearson correlation (P-value) respectively] (Table 1).

RT-PCR results

It was found that IL-1α and IFN-γ genes were not expressed simultaneously in groups infected with *Leishmania*, and as soon as glucantime was used in them, the concurrent expression of inflammatory genes was observed. In group 3, which showed the smallest size of cutaneous wound and the highest proportion of healed area, the inflammatory genes were expressed without any significant differences between sampling times, and the expression of healing genes

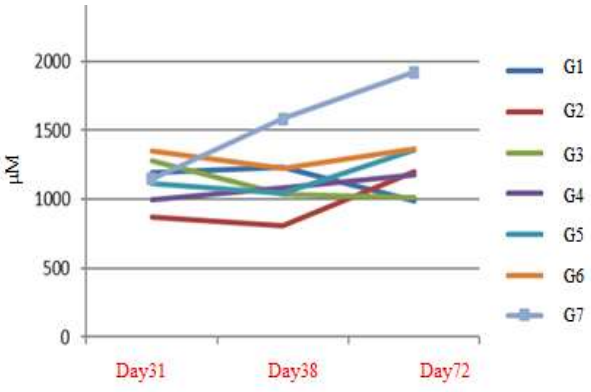

Figure 4.
Changes in the TAC levels (µM).

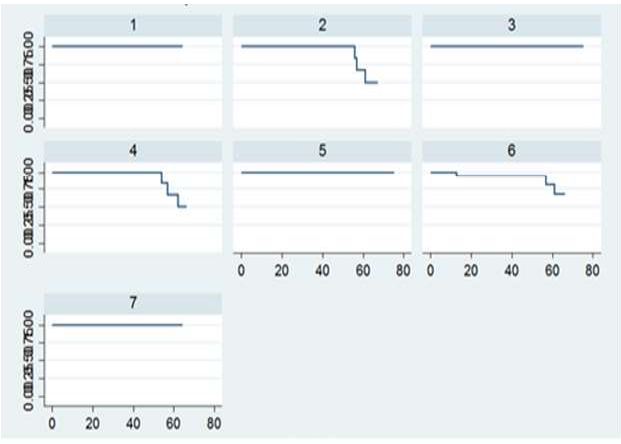

Figure 5.
The occurrence of death in healthy and test groups.

Table 1.
Changes in the expression pattern of the healing and pro-inflammatory genes in relation to changes in the TAC amount and the healed area of the wound

Healed		TAC		
IL or INF	**EGF or KGF**	**IL or INF**	**EGF or KGF**	**Group**
70.2 ± 19.5*	0	1.74 ± 0.34	1.79 ± 0.30	
31.3 ± 26.0**	44.2 ± 30.2	1.70 ± 0.31	1.68 ± 0.35	2
(0.000)	(0.000)	(0.647)	(0.195)	
72.6 ± 29.7	45.4 ± 38.4	1.52 ± 0.28	1.54 ± 0.17	
27.1 ± 31.9	81.5 ± 18.7	1.52 ± 0.21	1.51 ± 0.32	3
(0.000)	(0.001)	(0.987)	(0.569)	
49.4 ± 26.9	31.0 ± 36.4	1.58 ± 0.22	1.38 ± 0.21	
24.4 ± 22.1	51.2 ± 7.2	1.81 ± 0.10	1.65 ± 0.19	4
(0.009)	(0.033)	(0.019)	(0.001)	
56.5 ± 26.3	100 ± 0.00	1.71 ± 0.32	1.36 ± 0.03	
18.0 ± 16.3	38.4 ± 25.9	1.54 ± 0.31	1.71 ± 0.32	5
(0.000)	(0.000)	(0.076)	(0.000)	
51.4 ± 28.3	24.5 ± 35.5	1.90 ± 0.28	1.91 ± 0.20	
29.9 ± 0.00	60.0 ± 15.7	1.53 ± 0.00	1.88 ± 0.30	6
(0.000)	(0.006)	(0.000)	(0.664)	

The numbers in the first row: the mean ± standard deviation of the group in which none of the genes are expressed. The numbers in the second row: the mean ± standard deviation of the group in which at least one of the two genes is expressed. Numbers in parentheses are probability values (P-values). Groups 1 and 7 were not shown in this diagram because they had no wounds.

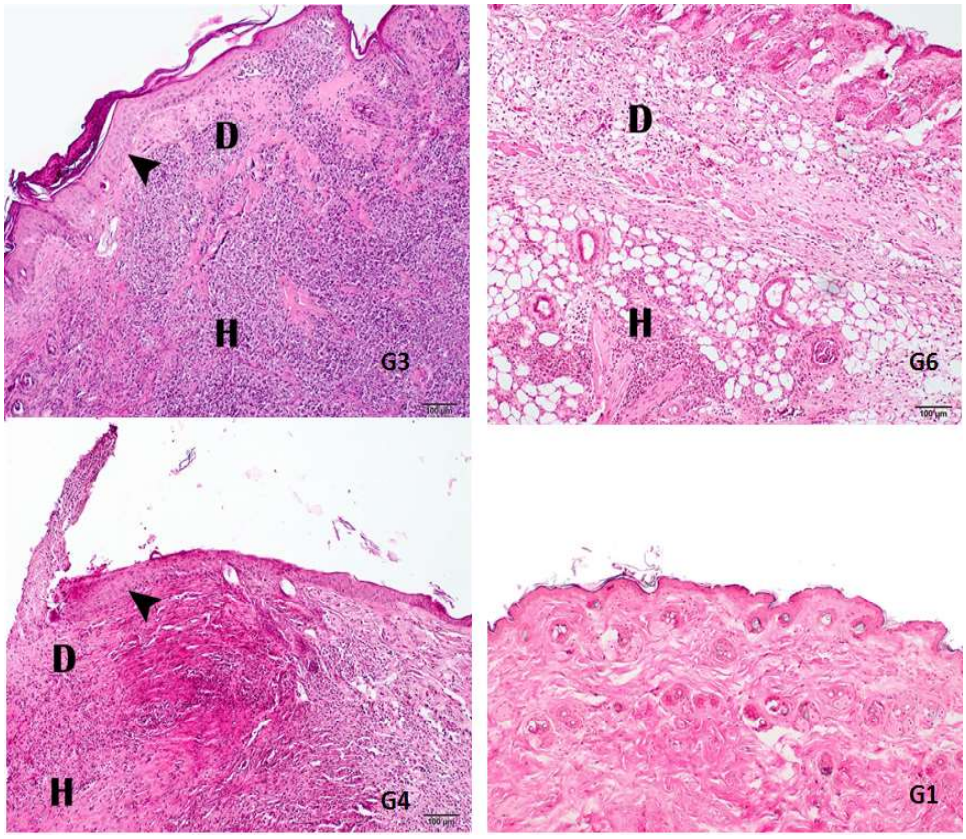

Figure 6.
Histopathological changes in the skin, G1: The normal microscopic structure of the skin, G3: Regeneration of the epidermis (arrowhead), G4: Partial regeneration of the epidermis (arrowhead) and the presence of edema and inflammation in the dermis (D) and hypodermis (H), G6: The presence of edema and severe inflammation in the dermis (D) and hypodermis (H) and the presence of a large number of amastigote forms of the parasite (arrow) in these parts (inset).

increased from the second sampling time (results not shown). In addition, in group 6 (LA), which showed the highest levels of TAC, although the expression of the KGF gene increased at the last sampling, the expression of pro-inflammatory genes was very low. Meanwhile, our results showed that the rise in the ratio of healed area to the total wound area was greatly related to the expression of pro-inflammatory genes rather than to the expression of healing genes (Table 2).

Mortality rate

Although the death that occurred in some groups was not statistically significant, there was no death in groups 3 and 5, and the deterioration of the lesions in these groups was less than in others (clinical observation) (Figure 5).

Histopathologic findings

Histopathological examination of the skin and spleen tissue samples showed the most promising results in group 3 (ALT) and the least in group 6 (LA). Although treated with glucantime, group 4 indicated impaired microscopic architecture in the spleen tissue (Figures 6 and 7). The absence of granulomatous lesions in all groups was a remarkable finding in this study.

Table 2.
Changes in the total wound area and its healed part in relation to the TAC

TAC		
Healed Percent	**Total Wound Area**	
1.7 ± 0.3*	1.7 ± 0.3§	
44.2 ± 30.2**	48.7 ± 0.3§§	G2
[-0.261 (0.142)] ***	[-0.322 (0.067)] §§§	
1.6 ± 0.3	1.6 ± 0.3	
62.1 ± 35.5	28.0 ± 27.2	G3
[-0.401 (0.011)]	[-0.231 (0.157)]	
1.6 ± 0.1	1.6 ± 0.1	
41.1 ± 27.8	46.1 ± 34.9	G4
[-0.112 (0.516)]	[-0.076 (0.659)]	
1.7 ± 0.3	1.7 ± 0.3	
42.8 ± 29.6	59.1 ± 60.8	G5
[-0.004 (0.98)]	[-0.5 (0.001)]	
1.9 ± 0.2	1.9 ± 0.2	
49.9 ± 27.9	43.5 ± 37.2	G6
[-0.03 (0.849)]	[-0.266 (0.088)]	

Group

* Mean ± standard deviation of TAC
** Mean ± standard deviation of the total wound area
§Mean ± standard deviation of TAC
§§ Mean ± standard deviation of the percentage of the healed part of the wound
***The Pearson correlation coefficient and the numbers in the parentheses are the P-value.
Groups 1 and 7 were not shown in this diagram because they had no wounds

Discussion

Considering the destructive effects of the oxidant systems and the interaction of these microbicidal mechanisms with the proliferation of the Leishmania parasite, this study aimed to evaluate the outcomes of *L. major* infection in association with different levels of TAC. Therefore, the most important criterion of this investigation was the clinical presentation of the disease. In all experimental groups, the wound size increased first, and then, gradually decreased. This phenomenon did not occur in group 2, and its reason has not yet been determined by the authors.

Leishmania down-regulates the pro-inflammatory genes [16, 19, 20], but once treatment with glucantime is started, the expression of main pro-inflammatory genes (IL-1α and IFN-γ), as important and influential factors in the immune response against *Leishmania*, is resumed [19]. Contrary to what was expected in group 4 (LTA), the expression of pro-inflammatory genes was not resumed, which might have been due to the use of glucantime. It was observed that in this group, the expression of pro-inflammatory (p = 0.019) and healing (p = 0.001) genes declined. In other words, raising the TAC level together with treatment with glucantime may delay the immune system to reach the threshold for the production of essential pro-inflammatory cytokines, such as IL-1α and IFN-γ [11, 21]. Therefore, it seems that parasite survival is facilitated by increasing exogenous TAC levels in the host.

Interleukin-1α and IFN-γ, as "warning cytokines", are the main pro-inflammatory cytokines secreted by macrophages. It has been reported that IL-1α induces the expression of adhesion molecules on the surface of endothelial cells and leukocytes, and initiates and propagates the host's inflammatory response [17, 23]. Several studies have emphasized the crucial role of IL-1α in the control of inflammatory and immune responses in leishmaniasis for changing the clinical course of this disease. This function is conferred by T-helper cell type-1 lymphocytes, which limit the

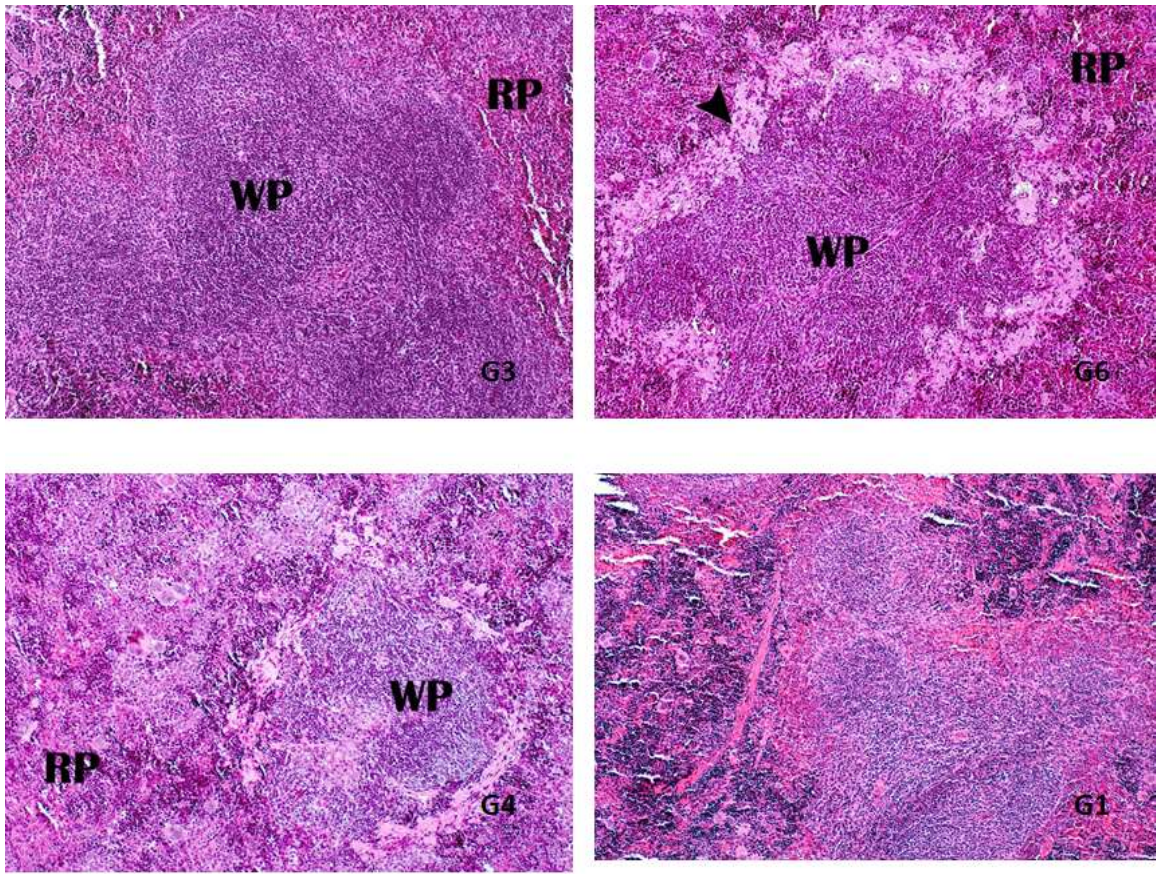

Figure 7.
Histopathological changes in the spleen, G1: Normal microscopic structure of the spleen with normal white (WP) and red (RP) pulps, G3: The structure of the organ is observed normally, G4: Disruption of the normal structure of the organ, reduction in the size of white pulp and severe necrosis in white and red pulps, G6: Severe necrosis (arrowhead) in white and red pulps.

spread of the parasite and lead to wound healing [17, 22, 23]. It seems that wound healing cannot be coordinated as long as the number of neutrophils in the wound exceeds the number of lymphocytes and macrophages. Therefore, the prolongation of the acute inflammatory phase and the delay in the replacement of acute inflammatory cells (granulocytes) by chronic cells (mononuclear) in this group can be due to the lack of (or very low) expression of IL-1α and IFN-γ genes [24]. In the third group, the presence of an inverse statistical relationship between TAC levels and wound healing (p = 0.011) strongly supports the fact that rising TAC levels in leishmaniasis worsen the clinical manifestations of the disease [25].

Granuloma formation is another feature of tissue pathology in wound healing as well as fibrous transformation due to excessive collagen deposition and resultant scar tissue. Not only granulomas can keep microorganisms alive, but also they prevent the spread of infection. The granulomatous reaction occurs in response to infection by some *Leishmania spp.* as fibroblasts migrate into the area and change the normal tissue structure. However, in the histopathological examination of the spleen and skin samples, no organized amastigotes containing granulomatous lesions were detected in any of the groups. According to other studies, the absence of granuloma formation is associated with the dissemination of cutaneous leishmaniasis. In other words, the severity of the disease depends on the ability of the host to develop a granulomatous reaction [24]. In the present study, there were no signs of disease spread and visceralization, and it is difficult to assess whether the non-spreading behaviour of the disease is the cause or the result of IL-1α and IFN-γ genes expression. Because the expression of other inflammatory genes was not investigated in this study, further evaluations and tracking of more pro-inflammatory cytokines might be helpful.

In groups 3 and 5, the mortality rate was zero (Figure 5). This result can probably be related to the protective role of vitamin E against the occurrence of some co-existing infections that otherwise may lead to the deterioration of the patient's condition and death. When administered systemically, vitamin E has been shown to increase the resistance of wounds to infections. However, no effects other than inhibiting collagen synthesis have been found for this vitamin when administered topically [26, 27].

Conclusion

In cutaneous leishmaniasis, a delicate balance between tissue pathology and infection control determines the clinical presentation of the disease. T-cells are the main infiltrating lymphocytes in the skin lesions of leishmaniasis to control the parasite proliferation as well as tissue destruction. Upon the inoculation of mice with *L. major,* the epidermis is damaged as a result of tissue destruction by neutrophils, macrophage necrosis, and keratinocyte apoptosis mediated by FasL/TRAIL [3]. Consequently, in the treatment of cutaneous leishmaniasis, it is necessary to control both parasite proliferation and tissue damage [3, 9, 16-18]. It was concluded from the results of this study that in the BALB/c mouse model, by increasing TAC levels before infection with *L. major*, the severity of the clinical manifestations of the disease will be reduced.

Materials & Methods

This study was approved by the Medical Ethics Committee of Bu-Ali Sina University, Iran (protocol number: 8-13/02/1399) based on international protocols for working with laboratory animals). A total of 105 BALB/c mice of both sexes at the age of 8 weeks old were randomly allocated into seven groups (n=15 in each group) as follows: 1) healthy mice (N), 2) *Leishmania*-infected mice treated with 100 mg/kg/day of SC glucantime (Sanofi Aventis, France) until complete healing (LT), 3) mice which received 20 IU/kg/day of SC vitamin E (Aburaihan, Iran) for 10 days to increase TAC prior to infection and further treatment with glucantime (ALT), 4) *Leishmania*-infected mice which received both vitamin E and glucantime daily until complete healing (LAT), 5) mice which received 20 IU/kg/day of vitamin E (SC) for 10 days before infection, 6) *Leishmania*-infected mice which received 20 IU/kg/day of vitamin E (SC) until the end of the experiment, and 7) mice which received daily vitamin E until the end of the experiment to increase TAC levels (A).

An inoculate of 10^6 *L. major* promastigotes MHOM/76/ER was injected intradermally (tail base) in each mouse [17]. The animals were housed in polycarbonate cages under standard conditions of cycles of 12 hours of light-dark and at a temperature of 25°C±1°C. Animals were fed ad libitum with a balanced diet and tap water. Mortality was checked daily.

Wounds were photographed by placing a one-centimeter marker next to the lesion. The lesion size was calculated using ImageJ with Java 1.8.0_172 after the calibration of photographs. At the first appearance of the ulcerative lesion (31 ± 2 days), 7 days later (day 38), and at the time of recovery, five mice from each group were euthanized and sampled (blood, skin, and spleen). Blood samples were collected immediately after euthanizing with chloroform, and skin and spleen tissue samples were surgically harvested. The tissue samples were cut in half for molecular and histopathological analyses.

All the collected blood and half of tissue samples (skin and spleen) were stored at -80°C for further molecular analysis of healing (KGF and EGF) and pro-inflammatory (IL-1α and IFN-γ) genes (Table 3). The remaining half of the skin and spleen tissue samples were placed immediately in 10% neutral buffered formalin and processed to obtain hematoxylin and eosin-stained tissue sections. The sections were then examined independently by a veterinary pathologist using a light microscope equipped with a digital camera (Olympus DP25, Germany).

Measurement of TAC

In this study, the TAC level in the sera was measured using a commercial enzyme-linked immunosorbent assay kit (Kiazist, Iran) according to the ferric-reducing antioxidant power method.

Statistical analysis

After testing the normality and homogeneity of variances at the level of groups and different stages of the experiment, repeated measures analysis of variance and Tukey's test as a follow-up test were performed by the SPSS statistical software (version 19). The significance level was considered less than 0.05.

Table 3.
The nucleotide sequence of PCR primers.

NO.	Genes	Sequence		Annealing temperature	Product size
1	β -actin	Forward	5/ ATGGTGGGTATGGGTCAGAAGG 3/		265
		Reverse	5/ TGGCTGGGGTGTTGAAGGTC 3/	58	
2	IL-1α	Forward	5/ TTGGTTAAATGACCTGCAACA 3/		122
		Reverse	5/ GAGCGCTCACGAACAGTTG 3/	56	
3	IFN-γ	Forward	5/ GCTCTGAGACAATGAACGCT 3/		227
		Reverse	5/ AAAGAGATAATCTGGCTCTGC 3/	56	
4	KGF	Forward	5/ GCAAACGGCTACGAGTGTGA 3/		182
		Reverse	5/ CCATGATGTTGTAGCTGTTCTTCA 3/	58	
5	EGF	Forward	5/ GCTCCGTCCGTCTTATCAGG 3/		232,984
		Reverse	5/ GGATCCTTAGCAGCGTCCTC 3/	58	

Authors' Contributions

All the authors had an essential role in all stages of the study.

Acknowledgements

The authors consider it their duty to appreciate the efforts of Mr. Khoshrouzi who provided technical assistance.

Conflict of interest

The authors declare that there is no conflict of the interest.

References

1. Laskay T, van Zandbergen G, Solbach W. Neutrophil granulocytes as host cells and transport vehicles for intracellular pathogens: apoptosis as infection-promoting factor. Immunobiology. 2008;213(3-4):183-91. DOI:10.1016/j.imbio.2007.11.010.

2. Peters NC, Egen JG, Secundino N, Debrabant A, Kimblin N, Kamhawi S, et al. In vivo imaging reveals an essential role for neutrophils in leishmaniasis transmitted by sand flies. Science. 2008;321(5891):970-4. DOI:10.1126/science.1159194.

3. Nylén S, Eidsmo L. Tissue damage and immunity in cutaneous leishmaniasis. Parasite Immunology. 2012;34(12):551-61. DOI:10.1111/pim.12007.

4. Gantt KR, Goldman TL, McCormick ML, Miller MA, Jeronimo SM, Nascimento ET, et al. Oxidative responses of human and murine macrophages during phagocytosis of Leishmania chagasi. The Journal of Immunology. 2001;167(2):893-901. DOI:10.4049/jimmunol.167.2.893.

5. Channon J, Roberts M, Blackwell J. A study of the differential respiratory burst activity elicited by promastigotes and amastigotes of Leishmania donovani in murine resident peritoneal macrophages. Immunology. 1984;53(2):345. PMID: 6490087 PMCID: PMC1454813.

6. Murray H. Cell-mediated immune response in experimental visceral leishmaniasis. II Oxygen-dependent killing of intracellular Leishmania donovani amastigotes. Journal of immunology. 1982;129(1):351-7.

7. Miller MA, McGowan SE, Gantt KR, Champion M, Novick SL, Andersen KA, et al. Inducible resistance to oxidant stress in the protozoan Leishmania chagasi. Journal of Biological Chemistry. 2000;275(43):33883-9. DOI:10.1074/jbc.M003671200.

8. Zarley JH, Britigan BE, Wilson ME. Hydrogen peroxide-mediated toxicity for Leishmania donovani chagasi promastigotes. Role of hydroxyl radical and protection by heat shock. The Journal of clinical investigation. 1991;88(5):1511-21. DOI:10.1172/JCI115461.

9. Panahi E, Stanisic DI, Peacock CS, Herrero LJ. Protective and Pathogenic Immune Responses to Cutaneous Leishmaniasis. 2021. DOI: 10.5772/intechopen.101160.

10. Rodriguez NE, Chang HK, Wilson ME. Novel program of macrophage gene expression induced by phagocytosis of Leishmania chagasi. Infection and immunity. 2004;72(4):2111-22. DOI:10.1128/iai.72.4.2111-2122.2004.

11. van Zandbergen G, Klinger M, Mueller A, Dannenberg S, Gebert A, Solbach W, et al. Cutting edge: neutrophil granulocyte serves as a vector for Leishmania entry into macrophages. The Journal of Immunology. 2004;173(11):6521-5. DOI:10.4049/jimmunol.173.11.6521.

12. Romano A, Carneiro MB, Doria NA, Roma EH, Ribeiro-Gomes FL, Inbar E, et al. Divergent roles for Ly6C+ CCR2+ CX3CR1+ inflammatory monocytes during primary or secondary infection of the skin with the intra-phagosomal pathogen Leishmania major. PLoS pathogens. 2017;13(6):e1006479. DOI:10.1371/journal.ppat.1006479.

13. Aga E, Katschinski DM, van Zandbergen G, Laufs H, Hansen B, Müller K, et al. Inhibition of the spontaneous apoptosis of neutrophil granulocytes by the intracellular parasite Leishmania major. The Journal of Immunology. 2002;169(2):898-905. DOI:10.4049/jimmunol.169.2.898.

14. Almayouf MA, El-Khadragy M, Awad MA, Alolayan EM. The effects of silver nanoparticles biosynthesized using fig and olive extracts on cutaneous leishmaniasis-induced inflammation in female balb/c mice. Bioscience Reports. 2020;40(12). DOI:10.1042/BSR20202672.

15. Almeida B, Narciso L, Melo L, Preve P, Bosco A, Lima VMFd, et al. Leishmaniasis causes oxidative stress and alteration of oxidative metabolism and viability of neutrophils in dogs. The Veterinary Journal. 2013;198(3):599-605. DOI:10.1016/j.tvjl.2013.08.024.

16. Vieira LQ, Goldschmidt M, Nashleanas M, Pfeffer K, Mak T, Scott P. Mice lacking the TNF receptor p55 fail to resolve lesions caused by infection with Leishmania major, but control parasite replication. The Journal of Immunology. 1996;157(2):827-35. DOI:10.4049/jimmunol.157.2.827.

17. Voronov E, Dotan S, Gayvoronsky L, White RM, Cohen I, Krelin Y, et al. IL-1-induced inflammation promotes development of leishmaniasis in susceptible BALB/c mice. International immunology. 2010;22(4):245-57. DOI:10.1093/intimm/dxq006.

18. Baldwin T, Sakthianandeswaren A, Curtis JM, Kumar B, Smyth GK, Foote SJ, et al. Wound healing response is a major contributor to the severity of cutaneous leishmaniasis in the ear model of infection. Parasite immunology. 2007;29(10):501-13. DOI:10.1111/j.1365-3024.2007.00969.x.

19. Akhzari S, Rezvan H, Zolhavarieh M. Expression of Pro-inflammatory Genes in Lesions and Neutrophils during Leishmania major Infection in BALB/c Mice. Iranian Journal of Parasitology. 2016;11(4):534. PMID: 28127365; PMCID:

PMC5251182.

20. Nashleanas M, Kanaly S, Scott P. Control of Leishmania major infection in mice lacking TNF receptors. The Journal of Immunology. 1998;160(11):5506-13. DOI:10.4049/jimmunol.160.11.5506.

21. Ribeiro-Romão RP, Moreira OC, Osorio EY, Cysne-Finkelstein L, Gomes-Silva A, Valverde JG, et al. Comparative evaluation of lesion development, tissue damage, and cytokine expression in golden hamsters (Mesocricetus auratus) infected by inocula with different Leishmania (Viannia) braziliensis concentrations. Infection and immunity. 2014;82(12):5203-13. DOI:10.1128/iai.02083-14.

22. Awasthi A, Mathur RK, Saha B. Immune response to Leishmania infection. Indian Journal of Medical Research. 2004; 119:238-58. PMID: 15243162.

23. Scapini P, Lapinet-Vera JA, Gasperini S, Calzetti F, Bazzoni F, Cassatella MA. The neutrophil as a cellular source of chemokines. Immunological reviews. 2000; 177:195-203. DOI: 10.1034/j.1600-065X.2000.17706.x.

24. Sakthianandeswaren A, Elso CM, Simpson K, Curtis JM, Kumar B, Speed TP, et al. The wound repair response controls outcome to cutaneous leishmaniasis. Proceedings of the National Academy of Sciences. 2005;102(43):15551-6. DOI:10.1073/pnas.0505630102.

25. Latifynia A, Khamesipour A, Bokaie S, Khansari N. Antioxidants and proinflamatory cytokines in the sera of patients with cutaneous leishmaniasis. Iranian Journal of Immunology. 2012;9(3):208-14. DOI: ijiv9i3a8.

26. MacKay DJ, Miller AL. Nutritional support for wound healing. Alternative medicine review. 2003;8(4). PMID: 14653765.

27. Taş A, Karasu A, Yener Z, Yıldırım S, Atasoy N, Düz E, et al. Histopathological and Immunohistochemical Study of the Effect of Sildenafil Citrate, Vitamin A, Vitamin C and Vitamin E on Wound Healing in Alloxan-induced Diabetic Rats. West Indian Medical Journal. 2021;69(5). DOI: 10.7727/wimj.2015.596.

How to cite this article
Yousefi M, Zolhavarieh SM, Nourian A, Rezvan H, Sadeghi-nasab A. Alterations in the Clinical Manifestations of Cutaneous Leishmaniasis in Various Total Antioxidant Capacities: An Animal Study Using BALB/c Mice. Iran J Vet Sci Technol.2024; 16(1): 10-18.
DOI: https://doi.org/10.22067/ijvst.2023.84439.1301
URL: https://ijvst.um.ac.ir/article_44564.html

Iranian Journal of Veterinary Science and Technology

Received: 2023- Apr-27
Accepted after revision: 2024- Jan-06
Published online: 2024- Feb-01

RESEARCH ARTICLE

DOI: 10.22067/ijvst.2024.81545.1237

Computational Evaluation of the B-Cell Epitope of 37-kDa Outer Membrane Protein H *Pasteurella multocida* Type B from Nusa Tenggara Timur, IndonesiaTenggara Timur, Indonesia

Firdausy Kurnia Maulana [a], Didik Handijatno [b]

[a] Airlangga Disease Prevention and Research Center, Universitas Airlangga, Indonesia.
[b] Laboratory of Bacteriology and Mycology, Department of Veterinary Microbiology, Faculty of Veterinary Medicine, Universitas Airlangga, Indonesia.

ABSTRACT

HS is still a frequently reported endemic disease, with outbreaks in Indonesia. HS vaccines distributed in Indonesia exhibit various limitations. This study computationally evaluated the B-cell epitope of the 37-kDa OmpH derived from the amino acid sequence of Pasteurella multocida from the NTT and Katha strains and compared the epitopes of the two strains. Amino acid sequences were obtained from NCBI and analyzed for multiple sequence alignment, and homology was analyzed using the BLASTp program at NCBI. Epitope prediction was performed using the IEDB B-cell epitope and ABCPred prediction tools. The VaxiJen v.2 online platform was used for antigenicity analysis, and IEDB was used for epitope conservancy analysis. The results of the homology analysis revealed that local NTT isolates had a high (>95%) identity with the Katha strain and isolates from China, India, Iran, Japan, and the USA. The epitope predictions from both methods were cross-checked, overlapping epitopes were shortlisted, and only five epitopes were predicted. Among the five, one epitope, ALEVGLN, appeared to be antigenic to both NTT and Katha strains. The antigenic sequence of 37 kDa OmpH can be used for peptide-based vaccine development and immunotherapeutic design.

Keywords

Haemorrhagic Septicemia, P. multocida, Outer membrane protein H (OmpH), Epitope, Antigenicity

Number of Figures: 2
Number of Tables: 6
Number of References:: 32
Number of Pages: 8

Abbreviations

HS: Haemorrhagic Septicemia
OmpH: Outer membrane protein H
kDa: Kilo Dalton
NCBI: National Center for Biotechnology Information
NTT: Nusa Tenggara Timur
IEDB: Immune Epitope Database
WOAH: World Organization for Animal Health

Corresponding author:
Firdausy Kurnia Maulana
Email: firdausykm@alumni.unair.ac.id
Tel: +62(81)7977-2700

Introduction

HS, also known as snoring disease in Indonesia, is caused by Pasteurella multocida, a gram-negative bacterium that commonly infects cattle and buffalo [1].

HS has a wide distribution, especially in tropical regions, such as Middle-East, Central Africa, North-East Africa, South Africa, South Asia, and South-East Asia [2]. In Indonesia, 12,058 cases of HS were reported between July 2007 and December 2019, with cases in buffaloes (4,047), cattle (5,809), pigs (2,108), goats/sheep (64), and Equidae (30) [3].

The disease causes huge losses due to livestock mortality, as well as losses in the meat- and dairy-related industries [4]. The economic loss of the livestock industry is estimated at 792 million USD per year [5], and the mortality rate of HS is up to 100% [6]. Considering its socioeconomic impact, HS is classified as one of 22 strategic infectious diseases in Indonesia, where control measures are coordinated at the central level [7].

The disease remains endemic in Indonesia, and several regions continue to report outbreaks [8, 9, 10] despite vaccination efforts. Currently, the disease is present in multiple areas of Indonesia, including Bali, Bengkulu, DKI Jakarta, Java, Aceh, West Nusa Tenggara, East Nusa Tenggara, North Sumatra, South Kalimantan, South Sumatra, Jambi, Riau, Central Sulawesi, West Sumatra, East Kalimantan, and Central Kalimantan [3].

The HS vaccines in Indonesia are administered once annually in the form of either an oil adjuvants vaccine or an aluminum precipitate vaccine, both of which are developed using the Katha strain from Burma [7]. The most effective option in the market is the oil adjuvant vaccine, which can provide immunity for up to one year. However, this vaccine has limitations, including the high viscosity of the solution, which makes injection challenging and can lead to swelling and abscesses at the injection site [2, 11]. Furthermore, this type of vaccine has a short storage time because it is susceptible to damage caused by temperature fluctuations [12].

The OmpH is a prominent protein in the purified envelope of P. multocida envelope and was identified as an immunodominant porin. Ongoing research has explored the feasibility of utilizing OmpH as a subunit vaccine in both native and recombinant forms to combat avian cholera, bovine respiratory illness, and HS [4, 13-16]. Vaccination with the recombinant form of OmpH, which has a molecular weight of 37 kDa, can induce both antibody- and cell-mediated immune responses in dairy calves and swamp buffaloes, protecting HS [4, 17]. Research conducted by Maulana et al. (2018) demonstrated that 37-kDa OmpH from a local strain of P. multocida isolated from NTT and Katha strains exhibit similar B-cell epitopes [18].

Immunoinformatics is a valuable technique for identifying new antigenic epitopes that can be used to design new vaccines against a variety of infectious diseases, including peptide-based vaccines. Given the advancement of immunoinformatics technologies, more accurate prediction of B-cell epitopes can now be made. Compared to strict laboratory studies, employing immunoinformatics methods to anticipate epitopes and develop peptide-based vaccines minimizes costs and saves time, whilst also elevating precision [19, 20].

This study was conducted to computationally evaluate the B-cell epitope of the 37-kDa OmpH derived from the amino acid sequence of P. multocida from NTT and Katha strains, and compare the epitopes of the two strains. The results can be used for further evaluation in the development of a peptide-based vaccine candidate.

Results

Multiple Sequence Alignment and Homology Analysis

Conserved and varied regions of the 37 kDa OmpH from NTT and other sources were evaluated through homology analysis and multiple sequence alignment as depicted in Figure 1. Specifically, Clustal W was employed to assess seven different sequences of the OmpH gene from NTT-Indonesia, China, Japan, India, Iran, the USA, and Katha strains. Most of the alterations were point mutations, whereas there were identified insertions at positions 66-71, and deletions at positions 60-61, 189, and 196-197. The Entropy (Hx) Plot in Figure 2 indicates high entropy, revealing a significant variation between each sequence. The highest entropy values of 0.95570 were was recorded at positions 6. The homology analysis results showed that the 37 kDa OmpH asam amino sequence in local NTT isolates was significantly similar (>95%) to the Katha strain and isolates from China, India, Iran, Japan, and the USA (Table 1).

Prediction of the B-Cell Epitope of the OmpH P. multocida isolates of NTT and Vaccines

Kolaskar and Tangoankar method was employed to predict both the NTT isolates and Katha strain, possessing 11 potential B-cell epitopes within the 37 kDa OmpH gene that met the specified threshold value. In addition, the ABCpred prediction server was utilized in this study for predicting linear B-cell epitope regions in an antigen sequence through an artificial neural network. The results of both methods

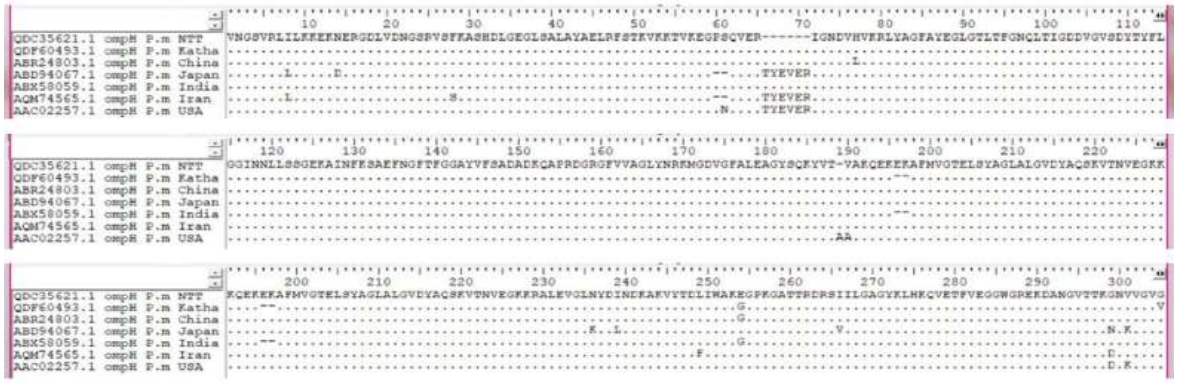

Figure 1.
Multiple alignment of amino acid sequences of 37 KDa gene OmpH P. multocida NTT isolates compared with and isolates from GenBank

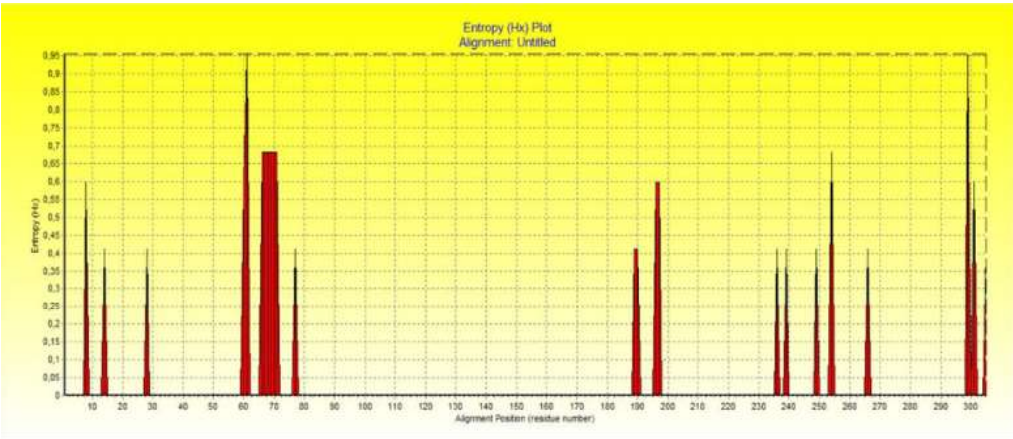

Figure 2.
Entropy (Hx) Plot graphic of multiple sequence alignment of all amino acid sequence of 37 KDa gene OmpH P. multocida NTT isolates with vaccines and isolates frim GenBank

Table 1.
Homological value of the nucleotide sequences of OmpH *P. multocida* NTT isolate and vaccine

Comparison isolate (Data GenBank)	NTT Isolate QDC35621 (%)	Katha Strain QDF60493.1
Outer membrane protein [Pasteurella multocida]. Accession Number ABR24803.1 - China	99.30%	98.95%
Adhesive protein, partial [Pasteurella multocida]. Accession Number ABX58059.1 - India	98.95%	100.00%
Outer membrane protein, partial [Pasteurella multocida]. Accession Number AAC02257.1 -USA	96.92%	95.24%
OmpH, partial [Pasteurella multocida]. Accession Number AQM74565.1 - Iran	96.54%	95.53%
Outer membrane protein [Pasteurella multocida]. Accession Number ABD94067.1 - Japan	95.85%	94.85%
Katha Strain Accession Number QDC35621	98.95%	100%

$\chi 2(3)=1532$, $p =< 0.001$

were cross-checked, and overlapped epitopes were shortlisted. Next, only five epitopes were ultimately selected and listed in Tables 2 and 3.

Antigenicity Analysis

Antigenicity analysis was conducted using the VaxiJen test with a threshold value of 0.5 (tables 4 and 5). Out of the five epitopes, one appeared to be antigenic in both NTT and Katha strains with the same peptide sequence ALEVGLN and a score of 1.3471.

Conservancy Analysis

Conservation analysis was performed on 100 sequences retrieved from the NCBI database via the BLASTp tool against the NTT isolate. Only ALEVGLN was deemed as a possible antigen when it came to antigenicity, while both GFVVAGL and ALEVGLN showed relatively high conservation levels (93%) (Table 6).

Table 2.
Potential shortlisted BCL epitopes of OmpH *P. multocida* NTT isolate using Kolaskar and Tongaonkar antigenicity method and ABCpred method

Kolaskar and Tongaonkar Antigenicity Method	Amino Acid Position	ABCpred Method	Start Position
DVGVSDYTYFLG	100-111	DVGVSDYTYFLGGINN	98
GAYVFSA	136-142	GFTFGGAYVFSADADK	131
GFVVAGL	154-160	RGFVVAGLYNRKMGDV	153
SQKYVTVA	177-184	AGYSQKYVTVAKQEKE	174
ALEVGLN	223-229	ALEVGLNYDINDKAKV	223

Table 3.
Potential shortlisted BCL epitopes of OmpH *P. multocida* Katha strain using Kolaskar and Tongaonkar antigenicity method and ABCpred method

Kolaskar and Tongaonkar Antigenicity Method	Amino Acid Position	ABCpred Method	Start Position
DVGVSDYTYFLG	100-111	DVGVSDYTYFLGGINN	100
GAYVFSA	138-144	GFTFGGAYVFSADADK	133
GFVVAGL	156-162	RGFVVAGLYNRKMGDV	155
SQKYVTVA	179-185	AGYSQKYVTVAKQEKA	179
ALEVGLN	223-229	ALEVGLNYDINDKAKV	223

Table 4.
Prediction of B-cell epitope antigenicity from outer membrane protein H (OmpH) amino acid sequences of *P. multocida* local isolates NTT

Antigenicity test by Vaxijen v 2.0		
Sequences	Score*	Probability
DVGVSDYTYFLG	0.2146	Probable Non-Antigen
GAYVFSA	-0.1360	Probable Non-Antigen
GFVVAGL	-0.1978	Probable Non-Antigen
SQKYVTVA	0.2844	Probable Non-Antigen
ALEVGLN	1.3471	Probable ANTIGEN

*threshold score 0.5

Table 5.
Prediction of B-cell epitope antigenicity from outer membrane protein H (OmpH) amino acid sequences of Katha vaccine strain

Antigenicity test by Vaxijen v 2.0		
Sequences	Score*	Probability
DVGVSDYTYFLG	0.2146	Probable Non -Antigen
GAYVFSA	-0.1360	Probable Non -Antigen
GFVVAGL	-0.1978	Probable Non -Antigen
SQKYVTVA	0.2844	Probable Non -Antigen
ALEVGLN	1.3471	Probable ANTIGEN

*threshold score 0.5

Table 6.
Conservation analysis of selected peptides from *P. multocida* NTT isolate and Katha strain through the IEDB epitope conservancy analysis website

Peptide Sequence	%Protein Sequence Identification
DVGVSDYTYFLG	84.00% (84/100)
GAYVFSA	74.00% (74/100)
GFVVAGL	93.00% (93/100)
SQKYVTVA	28.00% (28/100)
ALEVGLN	93.00% (93/100)

Discussion

The OmpH is an antigenic surface protein in the envelope of P. multocida. It has been identified in all bovine isolates and is being considered a vaccine candidate by some researchers [2]. Conserved and varied regions of the 37 kDa OmpH protein from NTT and other sources were assessed through multiple sequence alignment. The entropy (Hx) plot graphs were utilized to illustrate the variations between sequences. The entropy values had a range of 0-1. The more varied a sequence, the higher the entropy value. The positions with the highest entropy were 61 and 299. Sequences resulting in high entropy alignment are unlikely to make good vaccine candidates. An entropy value of 0 was observed in regions 1-7, 14-27, 29-59, 78-188 191-195, 198-235, 240-248, 254-265, and 267-298. In the low-entropy alignment, it is crucial to consider regions that correspond to very low entropy when designing peptide vaccines. This highly conserved region across antigens results in the formation of antibodies by the peptide, which protects against pathogens of different serotypes. Furthermore, this region demonstrates several critical functions due to its high level of conservation, making it resistant to mutation under positive selection pressure. In addition, the binding of antibodies to this region deactivates essential functions [21]. The 37 kDa amino acid sequence of OmpH local isolates in NTT showed high identity (>95%) with the Katha strain and isolates from China, India, Iran, Japan, and the USA, suggesting that the nucleotide sequences of NTT, vaccines, and other reference isolates may share a common ancestor [22].

A B-cell epitope refers to a defined region on the surface of an antigen that binds to an antibody. There are two categories of epitopes, comprising continuous (linear or sequential) and discontinuous (nonlinear or conformational) epitopes [23]. Linear B-cell epitopes are made up of peptides that can be readily used in immunization and antibody production as substitutes for antigens [24]. The Kolaskar and Tangoankar methods revealed that both the NTT isolates and Katha strain possess 11 potential B-cell epitopes in the 37 kDa OmpH gene that surpass the specified threshold value in this study. The Kolaskar and Tongaonkar antigenicity techniques evaluate the antigenicity dependent on the physiochemical properties of amino acids as well as the number of experimentally confirmed epitopes [25].

Another prediction method for B-cell epitopes utilized in this study was the ABCpred prediction server. This server implements an artificial neural network to predict the linear regions of B-cell epitopes in an antigen sequence. The methodology for this server is developed on a recurrent neural network (machine-based technique), which relies on fixed-length patterns. The accuracy of this prediction method is 65.93%.

ABCpred was utilized to identify potential B-cell epitopes from 37 kDa OmpH P. multocida NTT isolate and Katha strain. The results from both methods were cross-checked, narrowed down, shortlisted to overlapping epitopes, and only five were selected. The combination of both methods can enhance the results of the prediction accuracy of B-cell epitope [26].

The peptides in the epitope prediction were chosen using the Kolaskar and Tongaonkar antigenicity methods and subsequently verified with the ABCpred method. They were then tested for antigenicity using the VaxiJen test, with a minimum threshold value of 0.5. VaxiJen is a pioneering server for the alignment-independent prediction of protective antigens [27]. Out of the five epitopes, one appeared to be antigenic in both NTT and Katha strains with the same peptide sequence ALEVGLN, scoring 1.3471. The high antigenicity value of this peptide sequence indicates its potential as an ideal vaccine candidate. A higher antigenicity value translates to a greater ability to induce the production of specific antibodies by B-cells [28].

The 37 kDa OmpH peptides with fairly high conservation (93%) comprise GFVVAGL and ALEVGLN, although only ALEVGLN is considered a probable antigen. In a study conducted by Bui et al. [29], conservation refers to the part of a protein sequence that contains an epitope that is considered to be at or above a certain level of identity. Regions with lower variability in the parts of the protein sequence that contain epitopes indicate greater epitope uniqueness. This indicates the degree of variability or uniqueness of the epitope. Therefore, these regions often serve as good targets for the development of epitope-based vaccines since the targeted epitopes are present in various strains of specific pathogens.

Conclusion

According to the findings of our bioinformatics studies, there was only one epitope of 37 kDa OmpH P. multocida both from NTT isolate and Katha strain that met the selected criteria of antigenicity and conservancy analysis. The epitope "ALEVGLN" is hypothesized to be the most potential candidate for a seed epitope/peptide vaccine within the 37 kDa OmpH. Further studies are needed to investigate the conserved regions of OmpH and assess their efficacy as vaccines against P. multocida infection.

Materials & Methods

Data Retrieval

The amino acid sequences of the 37 kDa OmpH P. multocida isolate retrieved from NCBI with accession numbers QDC35621 and QDF60493, as well as other reference isolates with accession numbers ABR24803.1, ABX58059.1, AAC02257.1, AQM74565.1, and ABD94067.1 were analyzed [31].

Multiple Sequence Alignment

Amino acid sequences obtained from NCBI were analyzed for multiple sequence alignment by employing the CrustalW method in the BioEdit program. Amino acid sequences of seven different strains were included in this analysis to identify the conserved regions of 37 kDa OmpH [32].

Homology Analysis

Homology analysis was performed using the BLASTp program at NCBI [22]. Specifically, the amino acid sequence of the 37 kDa OmpH of the NTT local isolate was compared to the Katha strain and five other isolates from different countries retrieved from GenBank, NCBI.

Epitope Prediction

Epitope prediction was performed using the IEDB B-Cell epitope prediction tool (http://tools.iedb.org/bcell/) with default thresholds. The Kolaskar and Tongaonkar antigenicity method was employed, which can predict antigenic determinants with approximately 75% accuracy. Moreover, ABCpred (http://crdd.osdd.net/raghava/abcpred/) was utilized, which can achieve an accuracy of up to 65.93% using recurrent neural networks with a 0.5 threshold [24]. Predicted peptides were acquired and analyzed further for their antigenicity using the VaxiJen v 2.0 tools [27].

Antigenicity Analysis

The antigenicity analysis was completed using VaxiJen v.2 online platform (http://www.ddg-pharmfac.net/vaxijen/VaxiJen/VaxiJen.html). The targeted proteins in VaxiJen2.0 were predicted using the auto-cross covariance method with a threshold of 0.5 [30].

Conservancy Analysis

The epitope conservancy analysis tool used in this study was epitope conservancy analysis (http://tools.iedb.org/conservancy/) at the IEDB (Immune Epitope Database) webserver with sequence identity threshold set at 100%. Selected peptide sequences from the previous step were assessed for their conservation among 100 homologous sequences of P. multocida retrieved from the NCBI database where BLASTp was performed against the NTT isolate [29].

Authors' Contributions

F.K.M and D.H conceived and planned the experiments. F.K.M carried out the experiments. F.K.M and D.H. contributed to the interpretation of the results. F.K.M took the lead in writing the manuscript. All authors provided critical feedback and helped shape the research, analysis and manuscript.

Acknowledgements

We would like to thank the Balai Besar Veteriner Denpasar, Department of Microbiology and Mycology and Bacteriology and Mycology Laboratory of Veterinary Medicine Faculty of Airlangga University for the permission and support of the research.

Conflict of interest

The authors declare that there is no conflict of the interest

References

1. Prihandini SS, Noor SM, Kusumawati A. 2017. Deteksi serotipe, karakterisasi molekuler dan studi kekerabatan genetik isolat lokal Pasteurella multocide. JITV 22(2): 91-99. DOI: 10.14334/jitv.v22i2.1630.

2. Almoheer R, Abd Wahid ME, Zakaria HA, Jonet MAB, Al-shaibani MM, Al-Gheethi A, Addis SNK. 2022. Spatial, Temporal, and Demographic Patterns in the Prevalence of Hemorrhagic Septicemia in 41 Countries in 2005–2019: A Systematic Analysis with Special Focus on the Potential Development of a New-Generation Vaccine. Vaccines. 10(2): 315. DOI: 10.3390/vaccines10020315

3. [WOAH] World Organization of Animal Health. 2022. World Animal Health Information System (Surveillance and control measures: Hemorrhagic Septicemia). Available online: https://wahis.woah.org/#/dashboards/control-measure-dashboard [accessed 11 June 2022]

4. Muenthaisong A, Nambooppha B, Rittipornlertrak A, Tankaew P, Varinrak T, Muangthai K, Atthikanyaphak K, Sawada T, Sthitmatee N. 2020. An Intranasal Vaccination with a Recombinant Outer Membrane Protein H against Haemorrhagic Septicemia in Swamp Buffaloes. Vet Med Int. 2020 May 26;2020:3548973. DOI: 10.1155/2020/3548973.

5. Shome R, Deka RP, Sahay S, Grace D, Lindahl JF. 2019. Seroprevalence of hemorrhagic septicemia in dairy cows in Assam, India. Infect Ecol Epidemiol. 9(1):1604064. DOI: 10.1080/20008686.2019.1604064

6. Clemmons EA, Alfson KJ, Dutton JW 3rd. 2021. Transboundary Animal Diseases, an Overview of 17 Diseases with Potential for Global Spread and Serious Consequences. Animals (Basel). 11(7):2039. DOI: 10.3390/ani11072039.

7. Noor SM, Prihandani SS, Desem MI, Purba HHS and Andriani. 2021. Antibody response in cattle after local isolate SE vaccine administration. IOP Conf. Series: Earth and Environmental Science. 860 012071. DOI:10.1088/1755-1315/860/1/012071

8. Nasution, SS, Azfirman LP, Hutagaol NM, Azizi RA. 2021. Investigasi Kasus Septicaemia Epizootica (SE) pada Ternak Kerbau dan Sapi di Kabupaten Aceh Singkil. Buletin Veteriner Tahun 2021 Edisi 2 URI: http://repository.pertanian.go.id/

handle/123456789/15518

9. Narcana IK, Suardana IW, Besung INK. 2020 Molecular characteristic of Pasteurella multocida isolates from Sumba Island at East Nusa Tenggara Province, Indonesia. Veterinary World, 13(1): 104-109. DOI: www.doi.org/10.14202/vetworld.2020.104-109

10. Berek HSD, Nugroho WS, Wahyuni AETH. 2015. Protektivitas Sapi di Kabupaten KupangTerhadap Penyakit Ngorok (Septicaemia Epizootica). J. Vet.16 (2): 167-173. URL: https://ojs.unud.ac.id/index.php/jvet/article/view/14604.

11. Tanwar H, Yadav AP, Brijbhushan, Shweta, Singh SB, et al. (2016) Immunity against Pasteurella multocida in Animals Vaccinated with Inactivated Pasteurella multocida and Herbal Adjuvant 'DIP-HIP'. J Vaccines Immun 2(1): 010-014. DOI: 10.17352/jvi.000014

12. Herliani, Abrani Sulaiman, and M. Ilmi Hidayat. 2020. Potency of Cell Wall Protein of Pasteurella multocida as Hemorrhagic Septicemia Vaccine on Swamp Buffaloes Journal of Wetlands Environmental Management. 8(1): 33–44. DOI: 10.20527/10.20527/jwem.v8i1.200

13. Varinrak T, Poolperm P, Sawada T, Sthitmatee N. 2017. Cross-protection conferred by immunization with an rOmpH-based intranasal fowl cholera vaccine. Avian Pathol. 46(5):515-525. DOI: 10.1080/03079457.2017.1321105.

14. Ahmad TA, Rammah SS, Sheweita SA, Haroun M, El-Sayed LH. 2014. Development of immunization trials against Pasteurella multocida. Vaccine. 32(8): 909-917. DOI: 10.1016/j.vaccine.2013.11.068.

15. Joshi, S., Tewari, K. & Singh, R. (2013). Comparative immunogenicity and protective efficacy of different preparations of outer membrane proteins of Pasteurella multocida (B:2) in a mouse model.. Veterinarski arhiv, 83 (6), 665-676. Retrieved from https://hrcak.srce.hr/111895

16. Okay S, Özcengiz E, Gürsel I, Özcengiz G. 2012. Immunogenicity and protective efficacy of the recombinant Pasteurella lipoprotein E and outer membrane protein H from Pasteurella multocida A:3 in mice. Res Vet Sci. 93(3):1261-5. DOI: 10.1016/j.rvsc.2012.05.011.

17. Muangthai K, Tankaew P, Varinrak T, Uthi R, Rojanasthien S, Sawada T, Sthitmatee N. 2017. Intranasal immunization with a recombinant outer membrane protein H based Haemorrhagic septicemia vaccine in dairy calves. J Vet Med Sci. 80(1):68-76. DOI: 10.1292/jvms.17-0176.

18. Maulana FK, Handijatno D, Plumeriastuti H, Ernawati R, Tyasningsih W, and Mufasirin. 2019. Sequence Homology and Epitope Prediction of 37 kDa Outer Membrane Protein H(ompH) Gene of Pasteurella multocida Type B Isolate from Nusa Tenggara Timur (NTT). Indian Journal of Public Health Research & Development. 10(12): 1708-1713. DOI:10.37506/v10/i12/2019/ijphrd/192109

19. Potocnakova L, Bhide M, Pulzova LB. 2016. An Introduction to B-Cell Epitope Mapping and In Silico Epitope Prediction. J Immunol Res. 6:6760830. doi: 10.1155/2016/6760830. Muenthaisong A, Rittipornlertrak A, Nambooppha B, Tankaew P, Varinrak T, Pumpuang M, Muangthai K, Atthikanyaphak K, Singhla T, Pringproa K, Punyapornwithaya V, Sawada T, Sthitmatee N. 2021. Immune response in dairy cattle against combined foot and mouth disease and haemorrhagic septicemia vaccine under field conditions. BMC Vet Res. 7(1):186. DOI: 10.1186/s12917-021-02889-8.

20. TopuzoĞullari M, Acar T, Pelİt Arayici P, UÇar B, UĞurel E, Abamor EŞ, ArasoĞlu T, Turgut-Balik D, Derman S. 2020. An insight into the epitope-based peptide vaccine design strategy and studies against COVID-19. Turk J Biol. 44(3):215-227. DOI: 10.3906/biy-2006-1.

21. Ganguly B. 2016. Computational Prediction of Immunodominant Epitopes on Outer Membrane Protein (Omp) H of Pasteurella multocida Toward Designing of a Peptide Vaccine. Methods Mol Biol. 2016;1404:51-57. DOI: 10.1007/978-1-4939-3389-1_3.

22. Pearson WR. 2013. An introduction to sequence similarity ("homology") searching. Curr Protoc Bioinformatics. 3:3.1. DOI: 10.1002/0471250953.bi0301s42.

23. Ghaffar A, Tariq A. 2016. In-silico analysis of Pasteurella multocida to identify common epitopes between fowl, goat and buffalo. Gene. 580(1): 58-66. DOI:10.1016/j.gene.2016.01.020.

24. Sanchez-Trincado JL, Gomez-Perosanz M, Reche PA. 2017. Fundamentals and Methods for T- and B-Cell Epitope Prediction. J Immunol Res. 2017:2680160. DOI: 10.1155/2017/2680160.

25. Oany AR, Emran AA, Jyoti TP. 2014. Design of an epitope-based peptide vaccine against spike protein of human coronavirus: an in silico approach. Drug Des Devel Ther. 2014 Aug 21;8:1139-49. DOI: 10.2147/DDDT.S67861.

26. Khan MT, Islam R, Jerin TJ, Mahmud A, Khatun S, Kobir A, et al. (2021). Immunoinformatics and molecular dynamics approaches: Next generation vaccine design against West Nile virus. PLoS ONE 16(6): e0253393. DOI: 10.1371/journal.pone.0253393

27. Doytchinova IA, Flower DR. VaxiJen: a server for prediction of protective antigens, tumour antigens and subunit vaccines. BMC Bioinformatics. 2007 Jan 5;8:4. DOI: 10.1186/1471-2105-8-4.

28. Wattimena MN, Wijanarka W. 2022 In Silico Analysis Prediction of B-Cell Epitope as a Vaccine Candidate for SARS-CoV-2 B.1.617.2 (Delta) Variant. Journal of Biomedicine and Translational Research [Online]. (1):7-15. DOI:10.14710/jbtr.v1i1.13113

29. Bui H-H, Sidney J, Li W, Fusseder N, Sette A. (2007). Development of an Epitope ConservancyAnalysis Tool to Facilitate the Design of EpitopeBased Diagnostics and Vaccines. BMC Bioinformatics 8:361. DOI: 10.1186/1471-2105-8-361

30. Azam F, Saad M, Rahim R, Chumnanpoen P, E-kobon T, Othman S. 2020. Antigenic outer membrane proteins prediction of Pasteurella multocida serotype B:2. AsPac J. Mol. Biol. Biotechnol. 28 (4) : 102-116. DOI: 10.35118/apjmbb.2020.028.4.

31. Maulana FK, Handijatno D, Plumeriastuti H, Ernawati R, Tyasningsih W, Mufasirin. Sequence Homology and Epitope Prediction of 37 kDa Outer Membrane Protein H(Omph) Gene of Pasteurella multocida Type B Isolate from Nusa Tenggara Timur (NTT). Indian Journal of Public Health Research and Development. 2019 Dec;10(12):1708-1713. DOI: 10.37506/v10/i12/2019/ijphrd/192109

32. Nouri MAA, Almofti YA, Abd-elrahman KA, & Eltilib EEM. 2019. Identification of Novel Multi Epitopes Vaccine against the Capsid Protein (ORF2) of Hepatitis E Virus. American Journal of Infectious Diseases and Microbiology. 7(1): 26-42. DOI: 10.12691/ajidm-7-1-5.

How to cite this article
Kurnia Maulana F, Handijatno D. Computational Evaluation of the B-Cell Epitope of 37-kDa Outer Membrane Protein H *Pasteurella multocida* Type B from Nusa Tenggara Timur, Indonesia . Iran J Vet Sci Technol.2024; 16(1): 19-26.
DOI: https://doi.org/10.22067/ijvst.2024.81545.1237
URL: https://ijvst.um.ac.ir/article_44759.html

Iranian Journal of Veterinary Science and Technology

Received: 2023- Nov-05
Accepted after revision: 2024-Jan- 24
Published online: 2024- Feb-01

RESEARCH ARTICLE

DOI: 10.22067/ijvst.2024.84563.1304

Recombinant Expression of Bornavirus P24 Protein for Enzyme-Linked Immunosorbent Assay Development

Seyedeh Narjes Sadat[a], Sahar Khalvand[a], Behzad Ramezani[b], Mahdi Habibi-Anbouhi[c], Fatemeh Kazemi-Lomedasht[a], Hajarsadat Ghaderi[a], Mahdi Behdani[a,d]

[a] Biotechnology Research Center, Venom & Biotherapeutics Molecules Lab, Pasteur Institute of Iran, Tehran, Iran.
[b] Kawsar Biotechnology Company, Tehran, Iran.
[c] National Cell Bank of Iran, Pasteur Institute of Iran, Tehran, Iran.
[d] Zoonoses Research Center, Pasteur Institute of Iran, Amol, Iran.

ABSTRACT

BDV is a neurotropic enveloped RNA virus that induces persistent neurologic disease in a wide host range, including several vertebrate species and humans. The BDV genome encodes six proteins but the P24 protein was identified at higher rates than other proteins in BDV-infected tissues. In this study, BDV-P24 protein was constructed and subcloned into expression plasmid pET22. Recombinant protein expression was confirmed by SDS-PAGE and western blotting. P24 protein was injected into rabbits with the aim of polyclonal antibody production and immunization. ELISA is a fast, cost-effective, and highly sensitive technique with a lower probability of contamination compared to other diagnostic methods. ELISA was performed to evaluate infection in laboratory rabbits and retrospective infection was examined in 50 rabbits. The obtained results in this study indicated that ELISA based on P24 protein has a high potential to detect BDV infection.

Keywords

Borna disease virus; ELISA; Polyclonal antibody; Borna-P24 protein; Diagnostic method

Number of Figures: 3
Number of Tables: 0
Number of References:: 36
Number of Pages: 6

Abbreviations

BDV: Borna disease virus
RNA: Ribonucleic acid
N: Nucleoprotein
P: Phosphoprotein
M: Matrix protein
G: Glycoprotein

Corresponding author: *Mahdi Behdani1*
Email: *Behdani@pasteur.ac.ir*
Tel: *+98(21)6648-0780*

Introduction

According to the definition of the World Health Organization, any infectious disease common between vertebrate animals and humans is classified as a zoonosis [1]. Zoonosis currently accounts for approximately 70% of emerging diseases [2] and causes 2.7 million human deaths worldwide annually [3]. The zoonotic pathogens are highly important due to the following reasons; the pathogen itself is compatible with other human hosts and is capable of causing resistant human-to-human infection without requiring to seed from the animal reservoir [4]. Early detection of the pathogens common between humans and animals through increasing laboratory capacity is a vital step toward the control and prevention of zoonosis [5, 6].

BDV is a highly neurotropic agent in mammalian species, such as horses, sheep, rabbits, rats, mice, guinea pigs, dogs, and cattle [7, 8]. More than 20 various genotypes from the Borna virus were extracted from different hosts, including humans, which creates a potential danger of sharing these viruses between humans and animals [9]. Selective tropism was exhibited by BDV in the nerve cells of the limbic system, especially the cortex and hippocampus, two primitive structures that control many behavioral and cognitive functions [10]. Clinical symptoms entail unusual behavior, sensorial changes, or miss of movement performance. In advanced steps, somnolence, lethargy, stupor, ataxia, and paralysis are observed. Death usually happens four weeks after the initial clinical symptoms [11]. Numerous neuropsychiatric entities have been indicated to be related to the potential markers of BDV infection in humans [12]. Several other studies have presented human cases of BDV infection in different psychiatric disorders, namely schizophrenia, learning problems, emotional disorders, and autism [13-15]. Some BDV-related antigens, antibodies, and RNAs were further detected in people with neurotropic symptoms, such as Parkinson's disease, chronic fatigue syndrome, Guillain-Barre syndrome, viral encephalitis, and multiple sclerosis [16]. Bornavirus was recently detected as the root reason for fatal human encephalitis following organ transplantation procedures, which remarkably enhanced the importance of this disease in humans [17].

BDV, as a negative-stranded RNA virus, has been enveloped by helical capsid [18]. BDV genome has six open reading frames, namely N, P, M, G, X, and L [19]. Molecular biological analysis has indicated that the P40/38 nucleoprotein, p10 protein, and P24 phosphoprotein are expressed continuously in the patient's cells [20]. The P24 protein has been identified at a higher ratio of P40 in the host tissue [21]. Techniques used for detecting BDV infection were indirect immunofluorescence with infected cells, western immunoblot, nested RT-PCR, real-time PCR, and ELISA [12]. Each of these methods faced problems; for example, nested PCR and real-time PCR cannot detect previous infection and there is a possibility of contamination, resulting in false positive results [22, 23]. The establishment of ELISA is facilitated by expressing and purifying large quantities of BDV recombinant antigens for the identification of BDV antibodies in biological samples [24]. ELISA for detecting BDV infection based on different BDV antigens has been performed in several vertebrate species, but so far this method based on P24 protein has not been investigated in rabbits [25, 26]. This study investigated the expression of P24 recombinant protein as well as the production of polyclonal antibodies against it in order to develop an ELISA for detecting BDV infection in laboratory rabbits.

Abbreviations-Cont'd

X: p10 protein
L: Large protein
PCR: Polymerase chain reaction
RT-PCR: Reverse transcription PCR
ELISA: Enzyme-linked immunosorbent assay
IPTG: Isopropyl-beta-d-thiogalactopyranoside
PBS: Phosphate-buffered saline
SDS-PAGE: Sodium dodecyl sulfate-polyacrylamide gel electrophoresis
HRP: Horseradish peroxidase
RT: Room temperature
TMB: Tetramethylbenzidine

Results

Borna-P24 Expression and Purification

The *pET22b-Borna-P24* construct was transformed to *E. coli* BL21. Expression of Borna-P24 protein was induced through IPTG for 16 hours. The product of recombinant Borna-P24 protein expression was observed in SDS-PAGE. The weight range of this protein was about 25 KDa (Figure 1A). These results were validated by western blotting through anti-His-tag antibodies (Figure 1B).

Investigation of Immunized Rabbit Serum Activity by ELISA

To evaluate the immunogenicity of the recombinant protein, Borna-P24 was injected into one rabbit in four immunizations, and then, ELISA was performed to assess the immune response. The Borna-P24 protein was coated on the well and various dilutions of immunized rabbit serum were added. According to the results of the fourth injection, the antibody titer was enhanced (Figure 2). Therefore, the recombinant Borna-P24 protein had immunogenicity

to induce rabbit immune response.

Investigation of Selected Rabbit's Serum Activity by ELISA

A total of 50 New Zealand white rabbits were selected from a herd of laboratories, and their previous borna virus infection was assessed by ELISA. After collecting a peripheral blood sample from the marginal vein, the serum was isolated. In this experiment, recombinant Borna-P24 protein was used as an antigen. The result of ELISA was negative for the P24-Borna virus antibody (Figure 3). These results were similar to the negative control and no antibodies were detected in the sera of the tested rabbits.

Discussion

BDV, as a neurotropic, enveloped, negative-stranded RNA virus is responsible for the severe infections of neuron cells [27]. Evidence indicates that BDV has a wide host range that spans several vertebrate species and humans [28, 29]. In previous studies, the P40 and P24 antibodies of the bornavirus were detected in the blood of patients with mental disorders [30]. The P40 values were higher in the chronic stage, whereas the P24 values increased in resistant infections [31].

In this study, for monitoring previous infections, we selected the P24 protein and produced polyclonal antibodies against the P24 recombinant protein for developing ELISA. The expression and purification of P24 protein were performed in large amounts. The recombinant protein was utilized for rabbit immunization. Polyclonal antibody generation in immunized rabbits was confirmed by ELISA. In addition, ELISA was performed in the selected laboratory rabbit herd, and no antibodies were detected. The results were obtained with high reproducibility.

Previous studies have proposed different methods for diagnosing BDV infection in diseased hosts. It is well known that whatever methodology is employed must be sensitive enough to diagnose the disease. Moreover, it is important to avoid the possibility of contamination and false positive results. In the past, some studies suggested diagnostic methods based on nested PCR [21, 22]. This method has inherent problems, such as the risk of contamination during the process and the inability to quantify the result. Other studies have suggested real-time PCR as an optimal way to diagnose BDV infection [23, 32, 33]. In this method, despite quantifying the results, there is still a risk of sample contamination and receiving false positive results. In addition, it should be noted that the mentioned techniques require a significant investment for the required machines. Furthermore, in all types of PCR, only an active infection is identified

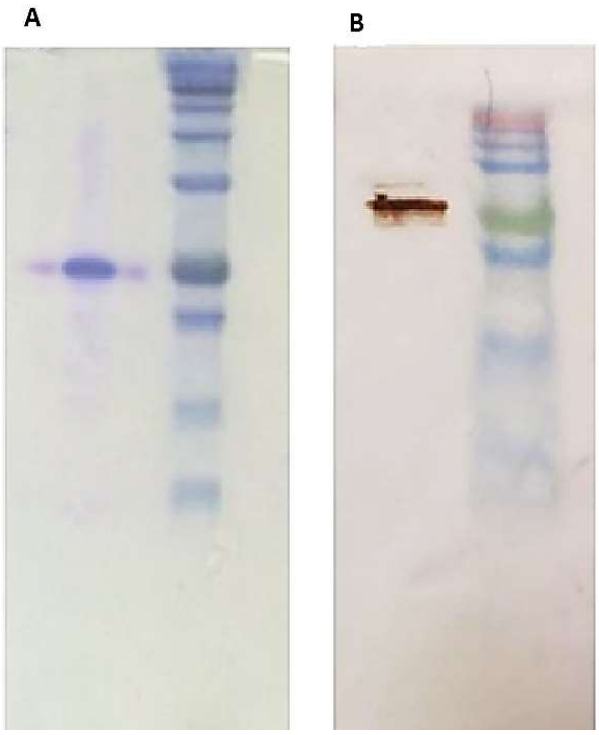

Figure 1.
Recombinant BDV P24 protein expression was induced with IPTG and evaluated by 12% SDS-PAGE (A) and western blotting (B). The MW of the marker lanes was from bottom 11, 17, 20, 25 kDa.

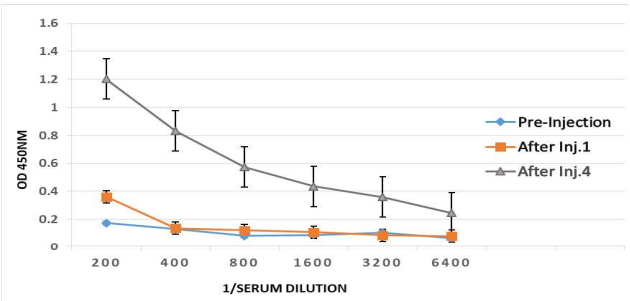

Figure 2.
Rabbit immune response monitoring by ELISA.

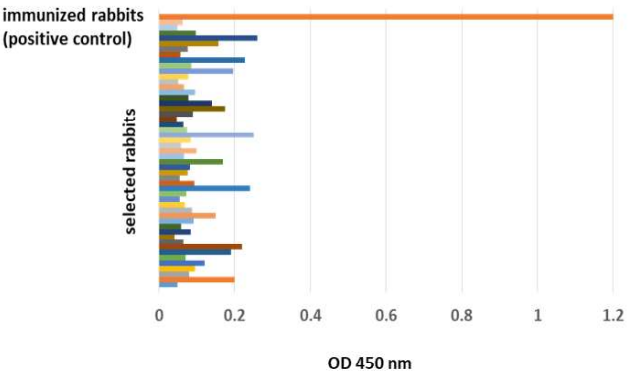

Figure 3.
Comparison of ELISA results of 50 selected rabbits from a laboratory herd and one rabbit immunized with Borna P24 Protein (positive control).

and no previous infection is detected. Today, ELISA is an optimal and applied method in medical diagnostic laboratories. It is low-cost and allows one to check many serum samples with minimum facilities in a few hours. In previous studies, P40 protein was used as an antigen in ELISA [34, 35]. According to other reports, the P24 protein has a higher diagnostic value than other components [16, 21, 36]. Therefore, the P24 protein is the preferred antigen in ELISA.

Conclusions

The results of our study indicated that ELISA based on P24 protein has a high potential for diagnosing BDV infection. These results were obtained from a study on one immunized rabbit and 50 selected rabbits.

Materials & Methods

Gene Construction, Expression, and Protein Purification

BDV *P24* gene sequence with a length of 615 bp subcloned to the expression plasmid *pET22* in frame with His-tag was purchased from Biomatik (Canada) and named *pET22b-Borna-P24*. This sequence is located between two restriction sites *NdeI* at the 5′ end and *XhoI* at the 3′ end. The construct was transformed into *E. coli* BL21 using heat-shock method and one colony was grown in 500 mL Luria-Bertani broth medium and expression of *P24* protein was induced through 0.05 mM concentration of IPTG for 16 hours. Bacterial sediment was collected by centrifugation for protein purification and suspension in lysis buffer (100 mM NaH2PO4, 10 mM Tris-HCl, 8 M Urea, pH 8.0). Eventually, bacteria were lysed by sonication method. After loading the lysate on the Ni-NTA resin (Qiagen, Germany) column, washing buffer was used to prepare the resin (8 M urea, 10 mM Tris–HCl, 100 mM NaH2PO4 adjust to pH 6.0) and borna P24 protein was separated using the elution buffer (8 M urea, 10 mM Tris–HCl, 100 mM NaH2PO4 adjusted to pH 4.3). Purified protein was dialyzed against PBS, and then, lyophilized and stored in -20°C. Finally, Protein concentration was determined with BCA method.

SDS-PAGE and Western Blot

To evaluate the expression of recombinant protein, 12% SDS-PAGE was used. Protein bands in polyacrylamide gel were stained by Coomassie blue. The expressed proteins in the gel were then transmitted to the nitrocellulose membrane for western blotting. The membrane was placed in 3% casein-blocking buffer overnight at 4°C and then, washed with PBS three times. The membrane was incubated with 1/1000 anti-His tag antibody as a primary antibody and then with 1/2000 anti-rabbit HRP-conjugated as a secondary antibody. The membrane was stained with 3, 3′-diaminobenzidine solution.

Production of P24 Polyclonal Antibody

A New Zealand female rabbit was used for immunization. Fifty micrograms of Borna-P24 recombinant protein were injected subcutaneously into the rabbit. Immunization was boosted four times at two-week intervals. A recombinant protein with complete Freund's adjuvant was used in the initial injection and incomplete adjuvant in others. Rabbits were bled from the marginal ear vein. Finally, specific polyclonal antibody titration was performed by ELISA. An amount of 1 µg/mL of recombinant Borna-P24 protein was coated in each well of the ELISA plate and was placed overnight at 4°C. Then, the plate was blocked by 3% skimmed milk and placed at room temperature for up to 1 h. PBS was used to wash the wells five times and 100 µL of serially diluted rabbit serum (1/100 to 1/3200) was added to each well and placed at room temperature for 1 h. With washing intervals, 100 µL of 1/2000 anti-rabbit HRP-conjugated was added and then, the plate was placed at room temperature for 1 h. One hundred microliter of 3, 3′, 5, 5′-tetramethylbenzidine substrate was added to all wells, and the plate was incubated at room temperature for 10 min in the dark. Finally, the reaction was stopped by adding 100 µL of stop buffer (H2SO4, 2N) into all wells. Optical density was read at the wavelength of 450 nm by a UV/Vis spectrophotometer (Epoch, BioTek, USA).

Investigation of Serum Titers Against Borna-P24 in Rabbits Herd

Fifty New Zealand rabbits were selected at the laboratory animal center of the Pasteur Institute of Iran (Karaj, Iran). After blood sampling and isolation of serum, ELISA was performed with 1/1000 serum dilution. Rabbit serum immunized with Borna-P24 was used as a positive control.

Authors' Contributions

Seyedeh Narjes Sadat performed a number of practical experiments, Writing - original draft, Writing - review & editing, and reduction of the manuscript. Sahar Khalvand, Behzad Ramezani and Hajarsadat Ghaderi performed a large number of practical experiments. Mahdi Habibi-Anbouhi and Fatemeh Kazemi-Lomedasht served as advisor. Mahdi Behdani; Writing - review & editing, served as advisors, supervision, formal analysis, reduction of the manuscript.

Acknowledgements

The authors wish to express their gratitude to all who provided support during the course of this research, especially Zahra Amirinia and Roghayeh Moghadam in KBC. This project was financially supported by KBC.

Conflict of interest

The authors declare that they have no known competing financial interests or personal relationships that could have appeared to influence the work reported in this paper.

References

1. Rahman MT, Sobur MA, Islam MS, Ievy S, Hossain MJ, El Zowalaty ME, et al. Zoonotic Diseases: Etiology, Impact, and Control. Microorganisms. 2020; 8(9). DOI:10.3390/microorganisms8091405.

2. Wang LF, Crameri G. Emerging zoonotic viral diseases. Rev Sci Tech. 2014; 33:569-581. DOI:10.20506/rst.33.2.2311.

3. Gebreyes WA, Dupouy-Camet J, Newport MJ, Oliveira CJ,

Schlesinger LS, Saif YM, et al. The global one health paradigm: challenges and opportunities for tackling infectious diseases at the human, animal, and environment interface in low-resource settings. PLoS Negl Trop Dis. 2014; 8:e3257. DOI:10.1371/journal.pntd.0003257.

4. Lo Iacono G, Cunningham AA, Fichet-Calvet E, Garry RF, Grant DS, Leach M, et al. A Unified Framework for the Infection Dynamics of Zoonotic Spillover and Spread. PLoS Negl Trop Dis. 2016; 10:e0004957. DOI:10.1371/journal.pntd.0004957.

5. Rabaa MA, Tue NT, Phuc TM, Carrique-Mas J, Saylors K, Cotten M, et al. The Vietnam Initiative on Zoonotic Infections (VIZIONS): A Strategic Approach to Studying Emerging Zoonotic Infectious Diseases. Ecohealth. 2015; 12:726-735. DOI:10.1007/s10393-015-1061-0.

6. Grant C, Lo Iacono G, Dzingirai V, Bett B, Winnebah TR, Atkinson PM. Moving interdisciplinary science forward: integrating participatory modelling with mathematical modelling of zoonotic disease in Africa. Infect Dis Poverty. 2016; 5:17. DOI:10.1186/s40249-016-0110-4.

7. Kinnunen PM, Palva A, Vaheri A, Vapalahti O. Epidemiology and host spectrum of Borna disease virus infections. J Gen Virol. 2013; 94:247-262. DOI:10.1099/vir.0.046961-0.

8. Zhang L, Wang X, Zhan Q, Wang Z, Xu M, Zhu D, et al. Evidence for natural Borna disease virus infection in healthy domestic animals in three areas of western China. Arch Virol. 2014; 159:1941-1949. DOI:10.1007/s00705-013-1971-5.

9. Komorizono R, Sassa Y, Horie M, Makino A, Tomonaga K. Evolutionary Selection of the Nuclear Localization Signal in the Viral Nucleoprotein Leads to Host Adaptation of the Genus Orthobornavirus. Viruses. 2020; 12(11):1291. DOI:10.3390/v12111291.

10. Bonnaud EM, Szelechowski M, Betourne A, Foret C, Thouard A, Gonzalez-Dunia D, et al. Borna disease virus phosphoprotein modulates epigenetic signaling in neurons to control viral replication. J Virol. 2015; 89:5996-6008. DOI:10.1128/JVI.00454-15.

11. Kupke A, Becker S, Wewetzer K, Ahlemeyer B, Eickmann M, Herden C. Intranasal Borna Disease Virus (BoDV-1) Infection: Insights into Initial Steps and Potential Contagiosity. Int J Mol Sci. 2019; 20(6). DOI:10.3390/ijms20061318.

12. Lipkin WI, Briese T, Hornig M. Borna disease virus - fact and fantasy. Virus Res. 2011; 162:162-72. DOI:10.1016/j.virusres.2011.09.036.

13. Honda T, Sofuku K, Matsunaga H, Tachibana M, Mohri I, Taniike M, et al. Detection of Antibodies against Borna Disease Virus Proteins in an Autistic Child and Her Mother. Jpn J Infect Dis. 2017; 70:225-227. DOI:10.7883/yoken.JJID.2016.277.

14. Honda T, Sofuku K, Matsunaga H, Tachibana M, Mohri I, Taniike M, et al. Prevalence of antibodies against Borna disease virus proteins in Japanese children with autism spectrum disorder. Microbiol Immunol. 2018; 62:473-6. DOI:10.1111/1348-0421.12603.

15. Williams BL, Hornig M, Yaddanapudi K, Lipkin WI. Hippocampal poly(ADP-Ribose) polymerase 1 and caspase 3 activation in neonatal bornavirus infection. J Virol. 2008; 82:1748-1758. DOIi:10.1128/JVI.02014-07.

16. Zhang L, Xu MM, Zeng L, Liu S, Liu X, Wang X, et al. Evidence for Borna disease virus infection in neuropsychiatric patients in three western China provinces. Eur J Clin Microbiol Infect Dis. 2014; 33:621-627. DOI:10.1007/s10096-013-1996-4.

17. Korn K, Coras R, Bobinger T, Herzog SM, Lucking H, Stohr R, et al. Fatal Encephalitis Associated with Borna Disease Virus 1. N Engl J Med. 2018; 379:1375-1377. DOI:10.1056/NEJMc1800724.

18. Lutz H, Addie DD, Boucraut-Baralon C, Egberink H, Frymus T, Gruffydd-Jones T, et al. Borna disease virus infection in cats: ABCD guidelines on prevention and management. J Feline Med Surg. 2015; 17:614-616. DOI:10.1177/1098612X15588452.

19. Briese T, Schneemann A, Lewis AJ, Park YS, Kim S, Ludwig H, et al. Genomic organization of Borna disease virus. Proc Natl Acad Sci U S A. 1994; 91:4362-4366. DOI:10.1073/pnas.91.10.4362.

20. McHugh JM, de Kloet SR. Bornavirus antigens in psittaciformes infected with psittaciform bornavirus and their use in diagnostic procedures. Archives of Veterinary Science and Medicine. 2020; 3:83-108.

21. Li Q, Wang Z, Zhu D, Xu M, Chen X, Peng D, et al. Detection and analysis of Borna disease virus in Chinese patients with neurological disorders. Eur J Neurol. 2009; 16:399-403. DOI:10.1111/j.1468-1331.2008.02516.x.

22. Soltani H, Mohammadzadeh S, Makvandi M, Pakseresht S, Samarbaf-Zadeh A. Detection of Borna Disease Virus (BDV) in patients with first episode of schizophrenia. Iranian Journal of Psychiatry. 2016; 11:257.

23. Zhang L, Liu S, Zhang L, You H, Huang R, Sun L, et al. Real-time qPCR identifies suitable reference genes for Borna disease virus-infected rat cortical neurons. Int J Mol Sci. 2014; 15:21825-39. DOI:10.3390/ijms151221825.

24. Ikuta K, Ibrahim MS, Kobayashi T, Tomonaga K. Borna disease virus and infection in humans. Front Biosci. 2002; 7:d470-95.

25. McHugh JM, de Kloet SR. The detection of bornavirus in birds, mammals and snakes by sandwich ELISA of bornaviral matrix protein. Archives of Veterinary Science and Medicine. 2021; 4:85-102.

26. Neumann B, Angstwurm K, Linker RA, Knoll G, Eidenschink

L, Rubbenstroth D, et al. Antibodies against viral nucleo-, phospho-, and X protein contribute to serological diagnosis of fatal Borna disease virus 1 infections. Cell Rep Med. 2022; 3:100499. DOI:10.1016/j.xcrm.2021.100499.

27. Liu S, Bode L, Zhang L, He P, Huang R, Sun L, et al. GC-MS-Based Metabonomic Profiling Displayed Differing Effects of Borna Disease Virus Natural Strain Hu-H1 and Laboratory Strain V Infection in Rat Cortical Neurons. Int J Mol Sci. 2015; 16:19347-68. DOI:10.3390/ijms160819347.

28. Hagiwara K, Tsuge Y, Asakawa M, Kabaya H, Okamoto M, Miyasho T, et al. Borna disease virus RNA detected in Japanese macaques (Macaca fuscata). Primates. 2008; 49:57-64. DOI:10.1007/s10329-007-0068-8.

29. He M, An TZ, Teng CB. Evolution of mammalian and avian bornaviruses. Mol Phylogenet Evol. 2014; 79:385-91. DOI:10.1016/j.ympev.2014.07.006.

30. Fukuda K, Takahashi K, Iwata Y, Mori N, Gonda K, Ogawa T, et al. Immunological and PCR analyses for Borna disease virus in psychiatric patients and blood donors in Japan. J Clin Microbiol. 2001; 39:419-29. DOI:10.1128/JCM.39.2.419-429.2001.

31. Geib T, Sauder C, Venturelli S, Hassler C, Staeheli P, Schwemmle M. Selective virus resistance conferred by expression of Borna disease virus nucleocapsid components. J Virol. 2003; 77:4283-90. DOI:10.1128/jvi.77.7.4283-4290.2003.

32. Barrantes X, Silva S, Macaya G, Bonilla JA. Detection of borna virus disease by real-time RT-PCR in Costa Rican equines and humans. Archives of Clinical Microbiology. 2012; 3(1). DOI: 10.3823/247.

33. Jin G, Xu X, Zhang L, Ma L, Huang R, Deng J, et al. Optimization of PCR buffer for Borna disease virus real-time PCR diagnostic kit. Journal of Third Military Medical University. 2011; 33:1323-27.

34. Zhai A-x, Li A-m, Song W-q, Kao W-p, Qian J, Li Y-j, et al. Infection of Borna disease virus in healthy animals in northern China. Asian Pacific Journal of Tropical Medicine. 2018; 11:S30.

35. de Kloet AH, Kerski A, de Kloet SR. Diagnosis of Avian bornavirus infection in psittaciformes by serum antibody detection and reverse transcription polymerase chain reaction assay using feather calami. J Vet Diagn Invest. 2011; 23:421-9. DOI:10.1177/1040638711403406.

36. Ma L, Deng R, Xu X, Yang H, Xie P. Preparation and identification of monoclonal antibody against phosphoprotein of Borna disease virus. Chinese Journal of Zoonoses. 2017; 33:779-783.

How to cite this article
Sadat S N, Khalvand S, Ramezani B, Habibi M, Kazemi-Lomedasht F, Ghaderi H, Behdani M. Recombinant Expression of Bornavirus P24 Protein for Enzyme-Linked Immunosorbent Assay Development. Iran J Vet Sci Technol.2024; 16(1): 27-32.
DOI: https://doi.org/10.22067/ijvst.2024.84563.1304
URL: https://ijvst.um.ac.ir/article_44851.html

Iranian Journal of Veterinary Science and Technology

Received: 2023- May- 29
Accepted after revision: 2024-Feb-04
Published online: 2024-Feb- 04

RESEARCH ARTICLE

DOI: 10.22067/ijvst.2024.82573.1255

Radiological and Anatomical Features of the Skull Bones of Adult Husky Dogs

Saman Ahani[a], Siamak Alizadeh[b], Mohammad Reza Hosseinchi[c]

[a] Doctor of Veterinary Medicine, Karaj Branch, Islamic Azad University, Karaj, Iran.
[b] Department of Clinical Sciences, Naghadeh Branch, Islamic Azad University, Naghadeh, Iran.
[c] Department of Basic Sciences, Urmia Branch, Islamic Azad University, Urmia, Iran.

ABSTRACT

Considering the role of skull bones in preserving vital organs, paying close attention to the shape and size of the skull is of great importance when various conditions, such as head trauma, are suspected. However, in order to confirm the suspicion radiologically, examiners need to have detailed information on the normal skull characteristics of each breed. This study aimed to evaluate the radiological and anatomical features of the skull in adult Husky dogs. The current descriptive cross-sectional study examined eight adult Husky dogs (four males and four females) that died due to different conditions, excluding those of the head. After the preparation of the skulls, radiographs were obtained on different views. In addition, the bones were examined in terms of morphological characteristics. Morphometric indices were also measured and the results were recorded. Based on the results of this study, the skull of Husky dogs consists of 11 cranial bones (Ossa cranii), and 21 facial bones (Ossa faciei). Three parameters, including the height and the length of tympanic bullae as well as the orbital index, were greater in females compared to males. However, the differences were not significant. Other parameters were greater in male dogs. The whole skull length and maximum width of the skull showed significant differences between the two genders ($p \leq 0.05$). The precise standards obtained in the current study can be used in interpreting the results to determine whether the presenting characteristics are abnormal or breed-dependent.

Keywords

Radiology, Anatomy, Dog, Husky, Skull

Number of Figures: 12
Number of Tables: 1
Number of References:: 27
Number of Pages: 12

Abbreviations

CT: Computed Tomography
TBH: Greatest height of the tympanic bulla
TBL: tympanic bulla length
WSL: Whole skull length
MWS: Maximum width of the skull

Corresponding author: *Siamak Alizadeh*
Email: *si.alizadeh@iau.ac.ir*
Tel: *+98(91)4189-1709*

Introduction

A variety of diseases, ranging from congenital to acquired ones, can affect the shape and size of the skull in dogs. Considering the importance of organs encased in the skull, such as the brain, changes in the architecture of this region are highly probable to be clinically significant [1]. This obligates examiners to pay close attention to the shape and size of the skull. However, owing to anatomical breed variations in dogs, it is not feasible to precisely realize whether the presenting shape of the skull is abnormal or breed-dependent unless there are thorough measurements of specific characteristics of each breed to serve as standards when needed [2]. Although different studies have examined skull morphology in Tarsus Çatalburun [3], Saarloos wolfdog [4], grey wolf [5], Lynx [6], red fox [7], vulpes [8], or golden jackals [9], no published article has studied that of Husky dogs.

Husky is known as a medium-sized, thickly furred, double-coated dog. It has erect triangular ears and distinctive markings on the head and has inherited the well-developed frontal sinuses of wolves, which is a useful way of distinguishing their skull from coyotes and foxes [10].

When skull examination is considered, CT is normally the modality of choice and helps operators to best appreciate subtle changes, such as small fractures [11]. This is mainly because of omitting the superimposition of the complex anatomy of the skull in CT [12]. However, despite its merits, CT is not usually available in all medical centers. Therefore, considering the ubiquity of radiology machines, radiography usually remains the only available choice in many medical centers at the time of this study.

The current research was conducted to investigate the radiological and anatomical features of the skull bones of adult Husky dogs.

Results

Morphological results

The skull of a Husky dog is composed of two parts: ossa cranii and ossa faciei. A total of 32 bones, including 11 cranial bones (three odd and four even bones) and 21 facial bones were assessed. Ossa cranii consisted of occipital, sphenoid, ethmoid, interparietal, parietal, frontal, and temporal bones. Facial bones consisted of maxilla, incisive, palatine, pterygoid, nasal, lacrimal, zygomatic, turbinate, mandible, vomer, and hyoid bones (Figure 1).

Cranial bones

Occipital bone: The whole nuchal surface of the skull was composed of occipital bone. This bone participates in the formation of the cranial surface and regions of the skull and contains a condyloid canal. Two short jugular processes were positioned on the sides of the condyles and hypoglossal canal. Muscular tubercles were also present. The intraparietal bone was completely joined with the nuchal bone and formed the interparietal process. The nuchal crest was relatively eminent and muscular prints were observable. The mastoid foramen was located on the caudal surface of the bone. The foramen magnum was relatively big and circular (Figure 1).

Sphenoid bone: There was more than one ethmoid foramen on the sphenoid bone. Round foramen was located on the alar canal and in the dorsal and internal parts of the alar canal. Oval foramen was observed in the caudal alar foramen. Spinous foramen was jointed with oval foramen.

Ethmoid bone: This bone was composed of three regions: the cribriform plate, crista galli, and ethmoidal fossa. Two ethmoidal foramina were seen on the sides of the plates and the optic canal. Cribriform plate had small foramina. A perpendicular plate was located between the nasal crest and crista galli. Lateral masses were positioned in the sides of the nose and composed of bone screws.

Interparietal bone: This bone was observed in the interparietal process jointed with the occipital bone (Figure 2).

Parietal bone: The results showed that this bone formed the major part of the skull. It has squamous, nasal, orbital, and temporal parts, as well as the zygomatic process. However, it did not contain supraorbital foramen. The zygomatic process was small and the frontal process was not jointed with the zygomatic bone. Two ethmoid foramina were observable in the frontal bone and on the edge of the sphenoid bone.

Frontal bone: It took part in the formation of orbits and had no special breed traits.

Temporal bone: This bone is composed of three parts; the tympanic part is located ventrally and comprises tympanic bullae. The squamous part possessed a zygomatic process which was jointed to the zygomatic bone and formed the zygomatic arc. No articular tubercle was found on this part. The mastoid process was located dorsally on the petrous part of the temporal bone.

Facial bones

Maxillary bone: On this bone, the facial crest and facial tuber were not detectable. The infraorbital foramen was located in the upper section of the third premolar teeth. Maxilla had frontal processes connected to the frontal bone. The alveolar process had cavities for premolar and molar teeth. The palatine process was joined with the median palatine suture. Palatine bone

Figure 1.
Oblique lateral view of adult male husky dog skull. Parietal bone (P), Temporal bone (T), Frontal bone (F), Premaxilla bone (pM), Lacrimal bone (L), Maxilla bone (M), Zygomatic bone (Z), Zygomatic process of temporal bone (ZpT), Temporal process of zygomatic bone (TpZ), Zygomatic process of frontal bone (ZpF), Coronoid process (crp), Condyloid process (cnp), Angular process (ap), Ramus of mandible (rM), Body of mandible (bM), External acoustic meatus (eam), Jugular process (jp), Occipital condyle (Oc), Mastoid foramen (maf), external sagittal crest (esc), Incisive teeth (iT), Canine tooth (cT), Premolar teeth (pT1-4), Molar teeth (mT1-3).

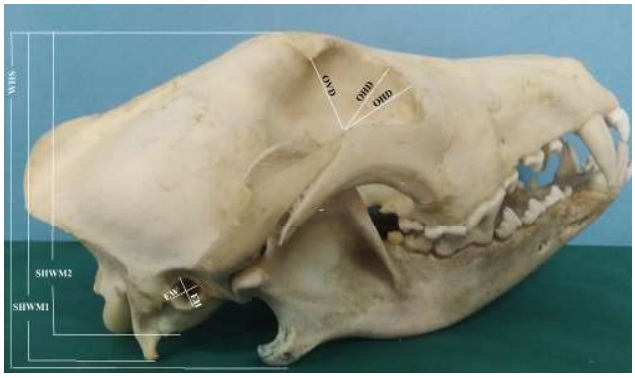

Figure 2.
Ventral view of adult female husky dog skull. Foramen magnum (fm), Jugular process (jp), Occipital condyle (Oc), tympanic bulla (tb), Basilar part of occipital bone (bO), zygomatic arch (Za), Basisphenoid bone (bS), Presphenoid bone (pS), Perpendicular part of palatine bone (pP), Horizontal part of palatine bone (hP), palatine process of maxilla (pM), Incisive teeth (iT1-3), Canine tooth (cT), Premolar teeth (pT1-4), Molar teeth (mT1-2).

and palatine process of the maxilla and also transverse palatine suture were observed. The ventral surface of the palatine process and palatine groove were seen within the major palatine foramen (Figure 3).

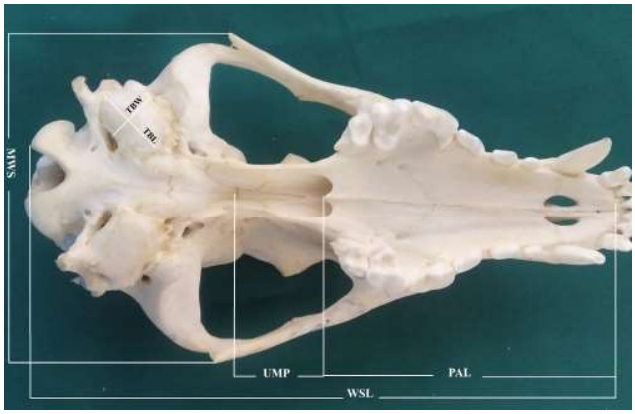

Figure 3.
Dorsal view of adult male husky dog skull. Parietal bone (P), Temporal bone (T), Frontal bone (F), Premaxilla bone(pM), Nasal bone (N), Maxilla bone (M), Zygomatic bone (Z), Zygomatic process of temporal bone (ZpT), zygomatic arch (Za), Zygomatic process of frontal bone (ZpF), external sagittal crest (esc).

Incisive bone: The body of incisive bone was formed as a thin palate with three alveoli for upper incisive teeth. Processes nasalis was observed jointed with nasal bone. The nasal process was well extended. The palatine process was formed as thin plates in the rostral part of the hard palate. Incisive sutures and palatine fissures were also observable in this region.

Palatine bone: It was formed by 33% of the length of the hard palate and formed the caudal part of this bone. The vertical plate of the bone participated in the formation of the lateral wall of the nasal foramen. The vertical palate was curved in the most ventral part toward the pterygoid process of the palatine bone.

Pterygoid bone: This bone was located lateral to the caudal foramen of the nasal bone. It terminated in the hock part of the hamulus.

Nasal bone: This bone formed the major part of the nasal cavity and its terminal part was concave in shape. Between nasal cavities were intranasal suture, nasal bone, and incisive bones.

Lacrimal bone: This bone was located in the frontal part of the orbital part. The bone was in contact with the frontal, palatine, maxilla, and zygomatic bones.

Zygomatic bone: This bone was positioned between the lacrimal bone and the maxilla. The bone participated in the formation of orbit parts. The temporal process of the zygomatic bone was jointed with the zygomatic process of the temporal bone, forming the zygomatic arch.

Vomer bone: The bone was positioned in the bottom of the nasal cavity as the septal sulcus. The bone was located in the distance with the nasopharyngeal meatus.

Turbinate bones: They were in the form of helix. Different parts of these bones were attached to their adjacent walls laterally.

Mandible bone: The Mandible was the largest facial bone and jointed with temporal condyles. Its ventral part was convex in shape. The alveolar border of the incisive part was composed of three alveoli for incisive teeth and one alveolus for canine teeth. The molar part had seven cavities for molar and premolar teeth. The external part of the mandible and its border had more than a mental foramen . In the perpendicular section, the mandibular canal was seen. Masseteric fossi were also observed as depressions on the ramus of the mandible. Mandibular foramen was terminated in mandibular canal. The articular extremity on the perpendicular section of the mandible had a coronoid process, condylar process, and mandibular notch. The angle of the mandible had an angular process (Figure 4).

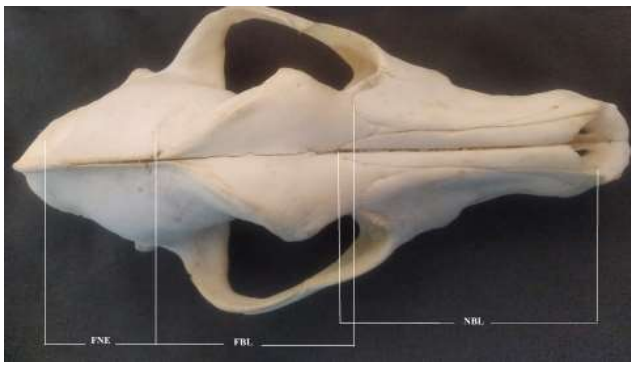

Figure 4.
Lateral view of adult male husky dog mandible. Coronoid process (crp), Condyloid process (cnp), Angular process (ap), Ramus of mandible (rM), Body of mandible (bM), Mental foramen (mf) (arrow). Incisive teeth (iT), Canine teeth (cT), Premolar teeth (pT1-4), and Molar teeth (mT1-3).

Hyoid bone: This bone was jointed with the styloid process of the temporal bone. It had basihyoid, thyrohyoid, ceratohyoid, epihyoid, and stylohyoid parts.

The results in Table 1 show that TBH, TBL, and orbital indices were higher in female dogs compared to male dogs; however, the differences were not significant. All other parameters were higher in male dogs, among which WSL and MWS had significant differences ($p \leq 0.05$).

Radiological results

Graphs taken in the dorsoventral position showed that the ethmoidal fossa, frontal sinus, brain cavity, external auditory canal, and tympanic bulla were detectable. Occipital bone was observable ventral to the nuchal bone. Ethmoid bone was located between the cranial cavity and nasal region, yet their foramina were not detectable. The bone was fused with pre-sphenoid, vomer, and palatine bones. In dorsoventral graphs, teeth, nasal bone, incisive bone, maxilla, mandible processes, condyloid process, zygomatic arch, frontal bone, tympanic bulla, and occipital bone were observed (Figure 5).

On the oblique open-mouth view, the frontal bone appeared convex in shape, especially in the cranial region. The supra-orbital groove was not detectable. The nasal bone was jointed with incisive bone in the rostral region and formed a nasal cavity. The anterior extremity of the bone was concave. The bone was connected with occipital bone in the cranial region, with parietal bone in the upper region, and with sphenoid bone in the lower part. According to the radiographs, squamous and petrous parts of the temporal bone were not detectable. Upper and lower teeth, maxilla, pre-maxilla, mandible zygomatic arch, frontal, parietal, intraparietal, tympanic bulla, and occipital bones were observable (Figure 6). In the alveolar border, the incisive part contained three alveoli for incisive teeth and one alveolus for canine tooth. The molar part had seven cavities for pre-molar and molar teeth. Mental foramen was observable, but the

Table 1.
Skull measurements of the male and female husky dog (Mean ± Standard deviation)

Parameters (mm)	Male, n= 4	Female, n= 4	Total, n= 8
WSH 1	98.42 ± 0.63	95.87 ± 0.79	97.14 ± 0.77
WSL 2	214.74 ± 1.21	203.37 ± 1.76*	209.05 ± 1.50
SHWM1 3	75.29 ± 0.62	71.32 ± 0.59	73.30 ± 0.64
SHWM2 4	81.15 ± 0.63	78.41 ± 0.72	79.78 ± 0.71
MWS 5	115.52± 0.69	107.20 ± 0.84*	111.36 ± 0.75
FBL 6	73.32 ± 0.39	70.23± 0.59	71.77 ± 0.51
NBL 7	84.82± 0.76	79.27 ± 0/72	82.04 ± 0/73
FNE 8	52.05± 0.32	49.16 ± 0/53	50.60 ± 0/51
MDL 9	158.87 ± 1.97	152.66 ± 1.51	155.76 ± 1.13
MSL 10	33.49 ± 0.25	32.14 ± 0.29	32.81 ± 0.26
PAL 11	47.96 ± 0.534	45.08 ± 1.024	46.52 ± 0.849
UMP 12	32.2 ± 0.192	31.2 ± 0.288	31.70 ± 0.241
TBL 13	22.38 ± 0.19	22.41 ± 0.22#	22.39 ± 0.23
TBW 14	16.55 ± 0.38	15.32 ± 0.30	15.93 ± 0.41
TBH 15	16.67 ± 0.20	16.70 ± 0.27#	16.68 ± 0.25
EAPH 16	6.19 ± 0.11	5.96 ± 0.08	6.07 ± 0.09
EAPW 17	6.72 ± 0.11	6.64 ± 0.09	6.68 ± 0.13
OVID 18	26.23 ± 0.18	25.95 ± 0.17	26.09 ± 0.15
OHD1 19	23.89 ± 0.18	23.76 ± 0.27	23.82 ± 0.26
OHD2 20	23.84 ± 0.29	22.12 ± 0.22	22.97 ± 0.31
Orbital index (%)	89.07 ± 4.27	90.32 ± 7.72#	89.67 ± 5.11
Cephalic index (%)	53.79 ± 2.89	52.85 ± 6.55	53.26 ± 5.01

$\chi^2(3)=1532$, $p =< 0.001$

[1] Whole skull height, [2] Whole skull length, [3] Skull height without the mandible: the height of skull from the most dorsal point of frontal bone to the most ventral point of sphenoid bone, [4] Skull height without the mandible: the highest point of frontal bone to the lowest point of Jugular processes, [5] Maximum width of the skull, [6] Total length of frontal bone, [7] Total length of the nasal bone, [8] Length of parietal bone, [9] Length of the mandibular bone, [10] Mandibular symphysial length, [11] Length of palate, [12] Length of the perpendicular plate of the palatine, [13] Tympanic bulla length, [14] Width of the tympanic bulla, [15] Greatest height of the tympanic bulla, [16] Height of the external auditory opening, [17] Width of the external auditory opening, [18] Orbital height/vertical diameter, [19] Orbital width/horizontal diameter: from the point of zygomatic arch, directed rostrally at 90o to the rim of the orbit, [20] Orbital width/horizontal diameter: from the point of the zygomatic arch, directed rostrally in a straight line to the rim of the orbit at the lacrimal fossa.

Superscript * shows statistically significant difference between male and female parameters. Superscript # shows values which were higher in females with no statistically significant differences ($P \leq 0.05$).

masseteric fossa was not detectable. Coronoid processes, condylar process, mandibular notch, and angle of the mandible with angular process were detectable (Figure 7).

Figure 5.
Dorso-ventral view (A) and ventro-dorsal view (B) of adult husky dog skull. 1: Incisor teeth, 2: Canine tooth of the lower jaw, 3: Canine tooth of the upper jaw, 4: Horizontal ramus of mandible, 5: Vomer bone, 6: Fourth premolar tooth of the upper jaw, 7: First molar tooth of lower jaw, 8: Nasal cavity, 9: Ethmoidal bone, 10: Frontal bone, 11: Zygomatic arch, 12: Coronoid process of mandible, 13: Parietal bone, 14: Mandibular condyle, 15: Brain cavity, 16: External auditory canal, 17: Tympanic bulla, 18: Occipital condyle.

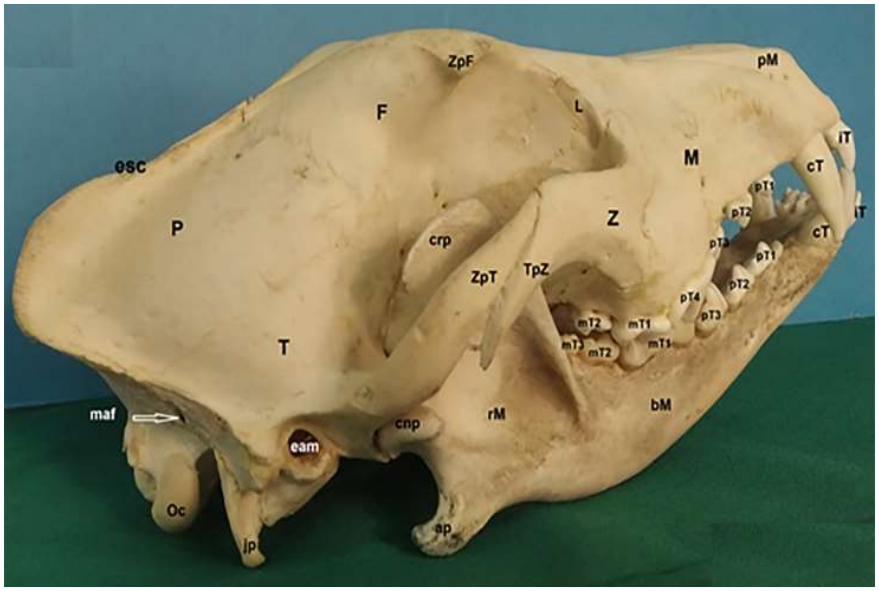

Figure 6.
Dorso-ventral view (A) and ventro-dorsal view (B) of adult husky dog skull. 1: Incisor teeth, 2: Canine tooth of the lower jaw, 3: Canine tooth of the upper jaw, 4: Horizontal ramus of mandible, 5: Vomer bone, 6: Fourth premolar tooth of the upper jaw, 7: First molar tooth of lower jaw, 8: Nasal cavity, 9: Ethmoidal bone, 10: Frontal bone, 11: Zygomatic arch, 12: Coronoid process of mandible, 13: Parietal bone, 14: Mandibular condyle, 15: Brain cavity, 16: External auditory canal, 17: Tympanic bulla, 18: Occipital condyle.

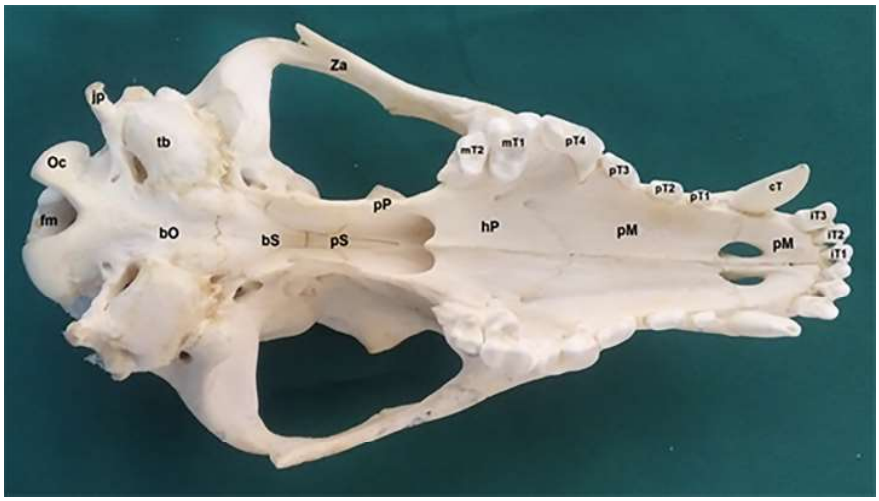

Figure 7.
Oblique-lateral view of the mandible of a husky dog. 1: Incisor teeth, 2: Inferior canine tooth, 3: Inferior premolar 1, 4: Inferior premolar 2, 5: Inferior premolar 3, 6: Inferior premolar 4, 7: Inferior molar 1, 8: Inferior molar 2, 9: Inferior molar 3, 10: Mental foramina, 11: Horizontal ramus of mandible, 12: Vertical ramus of mandible, 13: Coronoid process, 14: Condylar process and 15: Angular process.

Discussion

This study was conducted to evaluate the radiological and anatomical features of the skull bones in adult Husky dogs. Several studies have reported measures, locations, and shapes of skull bones in other species, such as wolves, foxes, and Aksaray Malakli dogs [4, 13, 14].

Previous studies on the skull morphometry of German shepherds showed that the length of the skull is 14.38 cm, while it is 16.22 cm in the Nigerian local dog, both of which are smaller than that of Husky (25.65 cm). In another study conducted on the Kangal dog, the skull was reported to be 25.87 cm in length which is roughly the same size as Husky in the current study [15].

The current research revealed that the skull width of Huskies was 11.13 cm which was larger than that of the Nigerian local dog (8.49 cm), but smaller than that of the Kangal breed dog (13 cm) [15, 16]. These variations indicate the normal breed variants in different breeds of dogs.

The head index in our study was calculated to be 53.26% ± 5.01%, whereas the corresponding values for the Russian Dolicocephalic Collie, Wolfhound, Mesaticephalic German Shepherd, and Brachycephalic Boston Terrier breeds were 48%, 56%, 58%, and 81%, respectively. As a result, head index in Husky dog was closer to the Wolfhound's [17, 18]. The Niger dog's orbital index was 80.87. More precisely, orbital indices of males were higher (81.57) than females (80.35) [16]. The orbital indices of huskies, on the other hand, were lower in males (89.07) than in females (89.67).

Couturier et al. (2005) reported that the nuchal crest in medium-sized dogs was slightly prominent and had no tubercles, while the results of the current study revealed that the nuchal crest was quite prominent in the Husky dog, beneath which were two distinct tubercles (muscular print). The mastoid foramen was located on the caudal surface of this bone [19].

Andreis et al. (2016), in a study on mesaticephalic dogs, reported only one small irregular foramen on the cribriform plate of the ethmoid bone, while there were two distinct holes on the cribriform plate of the ethmoid bone of Husky dogs. The cribriform plate itself had numerous small foramina with round edges being located next to the alar canal [20].

Our results are in agreement with the findings of Hermanson et al. (2018), stating that the temporal bone of medium-sized dogs has squamous, tympanic, and petrous parts in addition to a zygomatic process. This process joins with the temporal process of the zygomatic bone to form the zygomatic arch. The tympanic bulla was very large and a small muscular process was extended to its front. Based on our findings in the Husky breed, the mastoid process, as well as the muscular process of the temporal bone, were atrophied and the styloid process was also very small [21].

In 2020, Watson reported tuberosities of the maxillary bone, such as facial crest, in small- and large-sized dogs, and outlined their characteristics. However, according to the radiological findings of our study, the maxilla of Husky dogs did not have a facial crest and facial tuber. The infraorbital foramen was shown to be located dorsal to the third premolar tooth [22]. The radiological findings were confirmed in anatomical studies. This bone only had a frontal appendage which was attached to the frontal bone.

Some diagnostic imaging studies showed that the ethmoid bone in dogs has recognizable foramen [23, 24]. The results of the current study revealed that the ethmoid bone was located between the cranial cavity and nose and no foramen was recognizable. In addition, it was found that the ethmoid bone was fused to the caudal part of the presphenoid. It was also rostroventrally merged with vomer and palatine, and rostrodorsally with frontal bones.

It has been stated that different factors, such as nutrition, influence the skull morphology; high-quality diets may help bones grow to a larger extent [25]. According to the owners, cases in this study were fed on a mixed diet, including chicken and skeleton. The authors did not manage to find other studies investigating the radiological and anatomical features of the skull bone in adult Husky dogs fed on different types of diets. Therefore, no comparative conclusion could be made in this regard.

The results showed that the cephalic index was 53 in both genders. The findings were parallel with several studies on the cephalic index of other species and breeds. Urošević et al. (2021) reported a skull index of 64 in Yugoslav shepherd dogs [26]. Moreover, Gál et al. (2022) reported a value of 53.13±3.35 in grey wolf which was in agreement with our findings [9]. Another study also reported the values of 52.52 and 52.53 in red foxes which were close to our findings [7].

In conclusion, this study was conducted to investigate the radiological and anatomical features of the skull bones in adult Husky dogs. The results showed both similarities and differences between Husky and other breeds of dogs. The findings of the current study can be used in making diagnostic and clinical decisions to distinguish the normal and abnormal size and shape of the skull bones of adult Husky dogs.

Materials & Methods

Animals

In the current descriptive cross-sectional study, eight adult husky dogs (four males and four females), with an average age of 6.40 ± 1.50 years, and a mean weight of 23.37 ± 3.65 kg were studied. In order to collect the skulls, the objectives of this study were explained to the officials of veterinary hospitals. Following their agreements, Husky dogs, dead or euthanized due to different disorders, were sent to the center where the current study was held. None of the cases died due to diseases related to the head. The approximate age of each dog was confirmed using the dental formula [27].

Description of the method

Radiographs of the skulls were obtained on dorsoventral, ventrodorsal, and left and right lateral recumbency. The focal film distance was 100 cm, and the applied kVp and mAs were 55 and 4, respectively. The radiographs were taken using a digital device (Ralco-S.r.l DR, Italy). The detector was a SCI flat panel type with a size of 24×30 cm, and the software used to process images and measure the structures was Varian and Drgem.

In order to prepare the skulls, the skin and muscles of the head and neck were removed using dissection tools. Skull bones were then flushed with water, soaked in KOH for 5 days, and whitened using H_2O_2 (Figure 8). The skull was dried by sunlight for 7 days. Morphometric parameters were measured by a caliper and the mean was reported [15, 16]. Whole skull height was considered as the distance between the most dorsal surface of the frontal bone and the most ventral surface of the mandible bone. Skull height without the mandible was considered as the height of the skull from the most dorsal point of the frontal bone to the most ventral point of the sphenoid bone in the foramen magnum. Skull heights without the mandible were measured from the highest point of the frontal bone to the lowest point of the jugular processes. Height of the external auditory opening and width of the external auditory opening were calculated as the distance between the dorsal and ventral regions of the open-

Figure 8.
Skull preparation. A: The Skull was bleached using 3% H_2O_2 for 24-48 hours B: The skull was left to be dried.

ing and the distance between the two regions, respectively. Orbital height/vertical diameter was measured from the ventral region of the orbit. Orbital width/horizontal diameter was calculated from the point of the zygomatic arch directed rostrally at 90º to the rim of the orbit. Orbital width/horizontal diameter was considered from the point of the zygomatic arch directed rostrally in a straight line to the rim of the orbit at the lacrimal fossa. The orbital index was calculated as the width to the height of the orbit and reported as a percent. The cephalic index was reported as the width to the length of the skull in percent (Figure 9). The maximum width of the skull was considered as the width of the skull from one zygomatic bone to the other. The whole skull length was considered as the distance of the rostral part

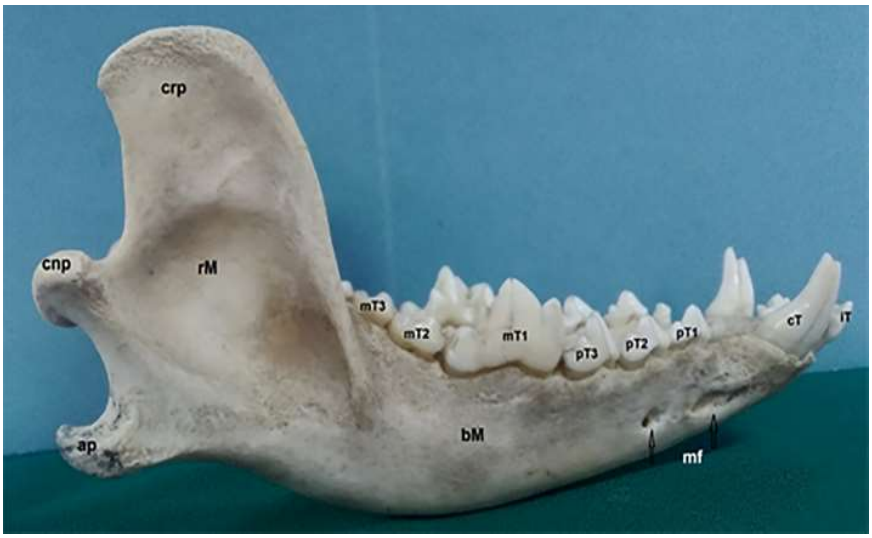

Figure 9.
Lateral view of the adult male husky dog skull. Whole skull height (WSH), Skull height without the mandible (SHWM1), Skull heights without the mandible (SHWM2), Height of the external auditory opening (EH), Width of the external auditory opening (EW), Orbital height/vertical diameter (OVD), and Orbital width/horizontal diameter (OHD).

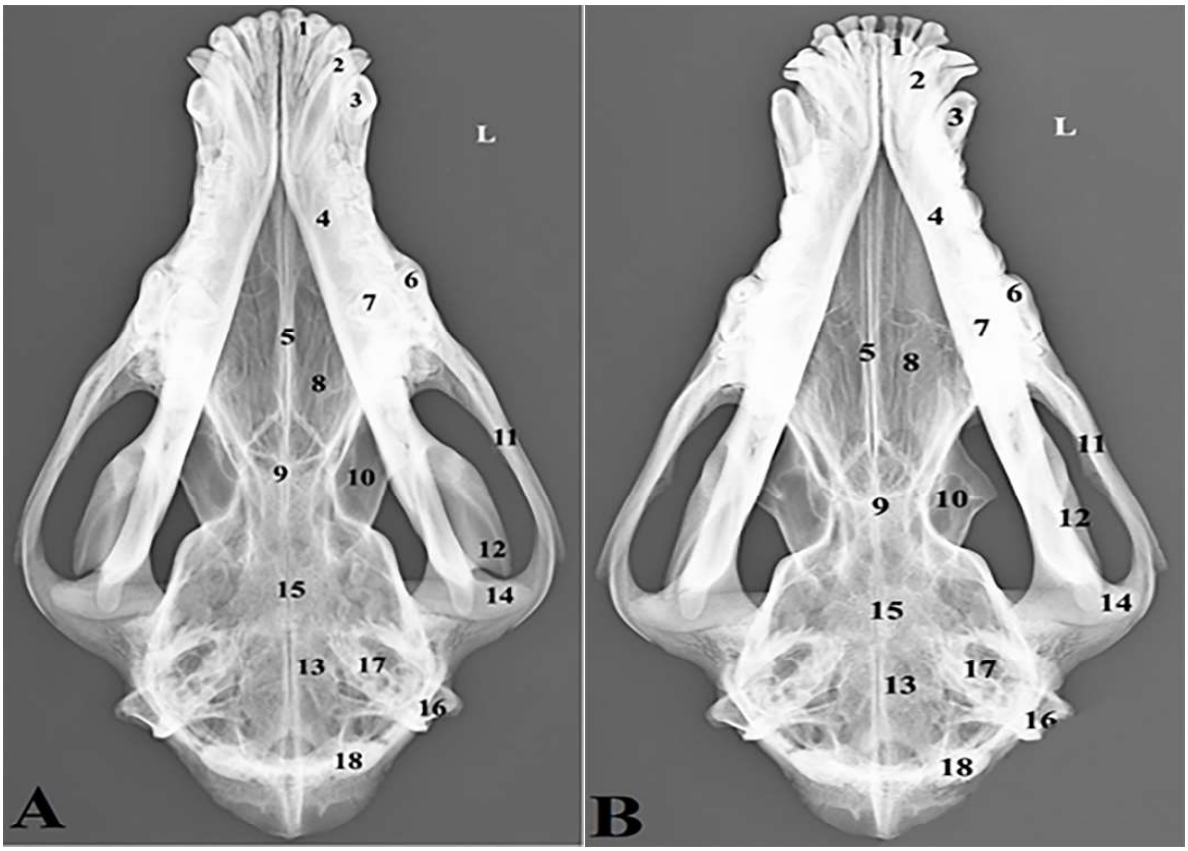

Figure 10.
Ventral view of the adult male husky dog skull. Maximum width of the skull (MWS), Whole skull length (WSL), Length of the palate (PAL), Length of the perpendicular plate of the palatine (UMP), Tympanic bulla length (TBL), and Width of the tympanic bulla (TBW).

of incisive alveoli to the most caudal region of the occipital bone. The length of the palate was evaluated in the median line from the palatine bone to the caudal foramen. The length of the perpendicular plate of the palatine bone is considered the most caudal part of the caudal bone foramen to the suture of the vertical plate of the palatine bone. The greatest height of the tympanic bulla, tympanic bulla length, and width of the tympanic bulla were also measured (Figure 10). The total length of the frontal bone was measured as the anterior section of bone to the suture region of this bone. The overall length of the nasal bone was assessed as the terminal part of the frontal bone to the rostral part of the nasal bone. The length of the parietal bone was considered as the length of the frontoparietal suture to nuchal eminence (Figure 11). The length of the mandibular bone was evaluated as the length of the mandible to the caudal part of the condyloid. The mandibular symphysial length was evaluated as the symphysial length of the mandible, originating from the rostral to the cranial part of the region (Figure 12).

Statistical Analysis

Data were analyzed using SPSS v.24 and expressed as mean ± SD. The student t-test and ANOVA were used to compare the means. P-value < 0.05 was considered statistically significant.

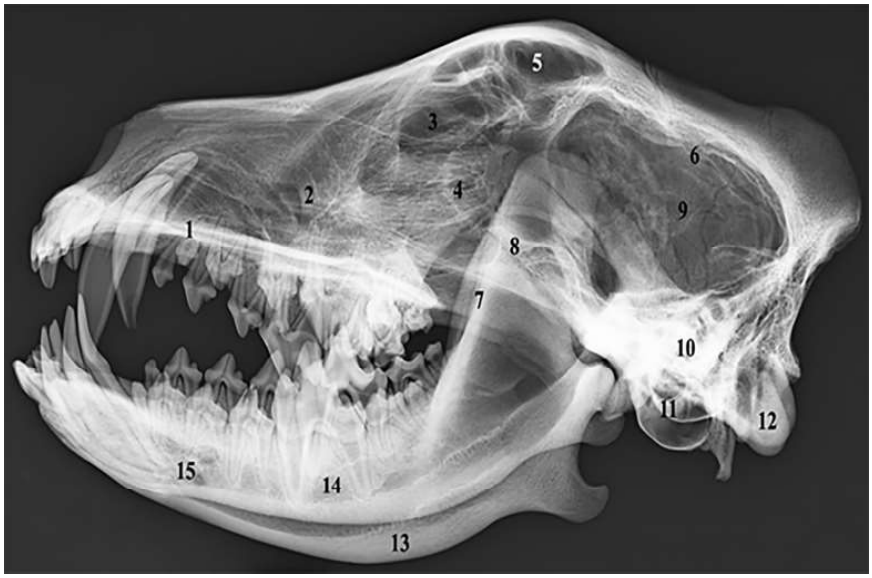

Figure 11.
Dorsal view of the adult male husky dog skull. The total length of frontal bone (FBL), length of the nasal bone (NBL), and Length of parietal bone (FNE).

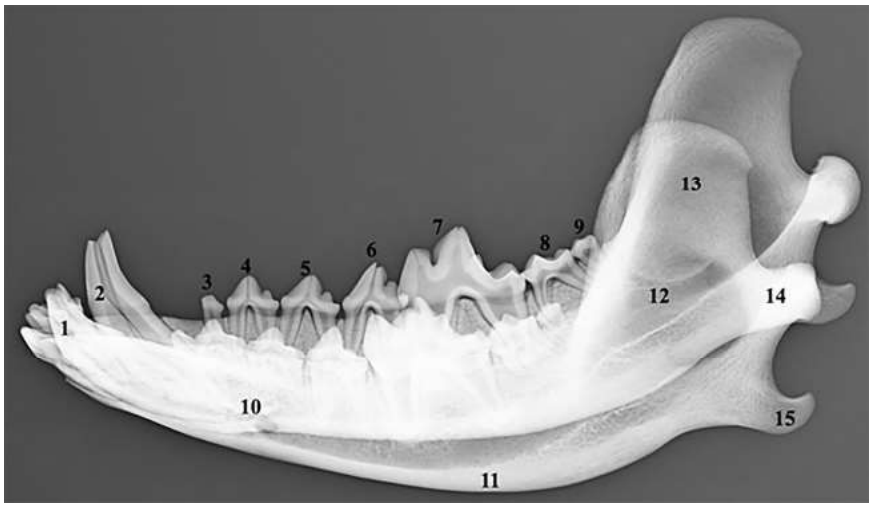

Figure 12.
Oblique lateral view of the adult male husky dog mandible. Length of the mandibular bone (MDL).

Authors' Contributions

SA and MRH conceived and planned the experiments. SA and MRH, ALA contributed to sample preparation. SA, MRH contributed to the interpretation of the results. SA and SA took the lead in writing the manuscript. All authors provided critical feedback and helped shape the research, analysis and manuscript.

Acknowledgements

The authors thank the Faculty of Veterinary Medicine, Urmia Branch, Islamic Azad University, Urmia, Iran, for all of the facilities.

Conflict of interest

The authors declare that there is no conflict of interest.

References

1. Dasilveira EE, Dasilvalisboaneto AF, CarlosSabinoPereira H, Ferreira JS, DosSantos AC, Siviero F. Canine skull digitalization and three-dimensional printing as an educational tool for anatomical study. Journal Of Veterinary Medical Education. 2021;48(6):649-55. DOI: 10.3138/jvme-2019-0132.

2. Bannasch DL, Baes CF, Leeb T. Genetic variants affecting skeletal morphology in domestic dogs. Trends in genetics. 2020;36(8):598-609. DOI: 10.1016/j.tig.2020.05.005.

3. Ograk Y, Urosevic M, Drobnjak D. Tarsus Çatalburun Breed of Turkish Hunting Dog (Turkish Pointer). Agriculture, Zemun-Belgrade (Serbia). 2012;6(1):22-24. UDC: 639.1.081.31.

4. Geiger M, Evin A, Sánchez-Villagra MR, Gascho D, Mainini C, Zollikofer CP. Neomorphosis and heterochrony of skull shape in dog domestication. Scientific Reports. 2017;7(1):1-9. DOI: 10.1038/s41598-017-12582-2.

5. Krofel M, Hatlauf J, Bogdanowicz W, Campbell L, Godinho R, Jhala Y. Towards resolving taxonomic uncertainties in wolf, dog and jackal lineages of Africa, Eurasia and Australasia. Journal of Zoology. 2022;316(3):155-68. DOI: 10.1111/jzo.12946.

6. Gál E, Bartosiewicz L, Kiss V. A fifth–sixth century CE lynx (Lynx lynx L., 1758) skeleton from Hungary: Cranial morphology and zoological interpretations. International Journal of Osteoarchaeology. 2022;32(4):41-49. DOI: 10.1002/oa.3101.

7. Hadžiomerović N, Gündemir O, Kovačevi, S. Mandible size and shape of the red fox (Vulpes vulpes) and golden jackal (Canis aureus). Adv Anim Vet Sci. 2022;10(2):364-8. DOI: 10.17582/journal.aavs/2022/10.2.364.368.

8. Martín-Serra A, Nanova O, Varón-González C, Ortega G, Figueirido B. Phenotypic integration and modularity drives skull shape divergence in the Arctic fox (Vulpes lagopus) from the Commander Islands. Biology letters. 2019;15(9):406-12. DOI: 10.1098/rsbl.2019.0406.

9. Srinivas Y, Jhala Y. Morphometric variation in wolves and golden jackal in India (Mammalia, Carnivora). Biodiversity Data Journal. 2021;27(9):48-62. DOI: 10.3897/BDJ.9.e67677.

10. Wan M, Hejjas K, Ronai Z, Elek Z, Sasvari-Szekely M, Champagne FA. DRD 4 and TH gene polymorphisms are associated with activity, impulsivity and inattention in Siberian Husky dogs. Animal genetics. 2013;44(6):717-27. DOI: 10.1111/age.12058.

11. Rohleder JJ, Jones J, Duncan R, Larson MM, Waldron DL, Tromblee T. Comparative performance of radiography and computed tomography in the diagnosis of middle ear disease in 31 dogs, Vet Radiol Ultrasound. 2016;47(1):45-52. DOI: 10.1111/j.1740-8261.2005.00104.x.

12. Wisner E, Zwingenberger A. Atlas of small animal CT and MRI. 1st ed. Iowa, USA: Wiley Blackwell; 2015.

13. Widyananta BJ, Saleh CP, Noviana D, Rahmiati DU, Ulum MF, Soehartono RH. Atlas of Normal Radiography in the Dogs and Cats. PT Penerbit: IPB Press; 2017.

14. İlgün R, Özüdoğru Z, Karabulut O, Can M. Macroanatomical and morphometric study on the skull bones of Aksaray Malakli dogs. Folia Morphologica. 2022;81(1):157-63. DOI: 10.5603/FM.a2021.0011.

15. Onar V, Pazvant S. Skull typology of adult male Kangal dogs. Anatomia, histologia, embryologia. 2001;30(1):41-8. DOI: 10.1046/j.1439-0264.2001.00292.x.

16. Igado OO. Skull typology and morphometrics of the Nigerian local dog (Canis lupus familiaris). Niger J Physiol Sci. 2017;32(2):153-8. PMID: 29485635.

17. Onar V, Çakırlar C, Janeczek M, Kızıltan Z. Skull Typology of Byzantine Dogs from the Theodosius Harbour at Yenikapı, Istanbul. Anat. Histol. Embryol. 2012;41(1): 341-52. DOI: 10.1111/j.1439-0264.2012.01143.x.

18. Evans HE, Christensen C. Miller's Anatomy of the Dog: The skeletal system (skull). 3rd ed. Philadelphia, W.B: Saunders Press; 1993.

19. Couturier L, Degueurce C, Ruel Y, Dennis R, Begon D. Anatomical study of cranial nerve emergence and skull foramina in the dog using magnetic resonance imaging and computed tomography. Veterinary Radiology & Ultrasound. 2005;46(5):375-83. DOI: 10.1111/j.1740-8261.2005.00068.x.

20. Andreis ME, DiGiancamillo M, Faustini M, Veronesi MC, Modina SC. Dog craniometry: a cadaveric study. Università dehli Studi di Milano. 2016;6(1):23-33. DOI: 10.13130/2283-3927/7082.

21. Hermanson JW, Evans HE, DeLahunta A. Miller and Evans'

anatomy of the dog. Health Sciences: Elsevier; 2018.

22. Watson E. Veterinary forensic radiology and imaging. Forensic Sciences: CRC Press; 2020.

23. DePaolo MH, Arzi B, Pollard RE, Kass PH, Verstraete FJ. Craniomaxillofacial trauma in dogs—Association between fracture location, morphology and etiology. Frontiers Vet. Sci. 2020;242(7):1-15. DOI: 10.3389/fvets.2020.00242.

24. Dunand L, Belluzzi E, Bongartz A, Caraty J. Application of a bilateral temporal fascia free graft in a dog with multifragmented frontal sinus and nasal bone fracture. Veterinary Surgery. 2022;32(1):127-44. DOI: 10.1111/vsu.13804.

25. Chirchir H. Trabecular bone in domestic dogs and wolves: Implications for understanding human self-domestication. The Anatomical Record. 2021;304(1):31-41. DOI: 10.1002/ar.24510.

26. Urošević MM, Drobnjak D, Stojic P, Urošević MB. Craniological parameters of Yugoslav shepherd dog Sharplanina. Mediterranean Agricultural Sciences. 2017;30(3):269-74. DOI: 10.24925/turjaf.v8i7.1571-1576.3452.

27. Gracis M. Dental anatomy and physiology. BSAVA manual of canine and feline dentistry and Oral surgery: BSAVA; 2018.

How to cite this article
Ahani S, Alizadeh S, Hosseinchi MR. Radiological and Anatomical Features of the Skull Bones of Adult Husky Dogs. Iran J Vet Sci Technol.2024; 16(1): 33-44.
DOI: https://doi.org/ 10.22067/ijvst.2024.82573.1255
URL: https://ijvst.um.ac.ir/article_44886.html

Iranian Journal of Veterinary Science and Technology

Received: 2023- Aug- 01
Accepted after revision: 2023- Dec-31
Published online: 2024-Feb-01

RESEARCH ARTICLE

DOI: 10.22067/ijvst.2023.83414.1280

Molecular Identification of *Mycobacterium avium* subsp. *Paratuberculosis* isolated from ELISA-Positive Samples by Nested PCR

Mahsa Soleimani[a], Alireza Shahrjerdi[b], Mitra Salehi[a]

[a] Department of Microbiology, Faculty of Biological Sciences, North Tehran Branch, Islamic Azad University, Tehran, Iran.
[b] National Institute for Genetic Engineering and Biotechnology, Tehran, Iran.

ABSTRACT

Paratuberculosis (Johne's disease) is a chronic granulomatous small intestine disease caused by MAP. Diagnosing and isolating infected animals is the most important measure for controlling the disease. Therefore, this study aimed to molecularly identify mycobacterium isolated from ELISA-positive cows with Johne's disease by nested PCR from the samples from Markazi Province, Iran. For this purpose, 2938 samples were decontaminated and then cultured on the Herrold egg culture medium containing mycobactin and no mycobactin. After DNA extraction, PCR for *16S rRNA* was first performed, followed by nested PCR on positive samples. Of 2938 samples, 87 were positive, and 26 were suspected. All positive isolates were observed in Ziehl-Neelsen staining in microscopic expansion. A 543-bp band was observed in 26 tested samples and mycobacterium strains in PCR for *16S rRNA*, indicating the presence of mycobacterium in the above samples. Nested PCR was performed for all isolates and positive and negative control strains. A 398-bp band was obtained in the first stage, and a 298-bp fragment was obtained in the second stage, indicating the presence of MAP in the samples. Accordingly, nested PCR is suggested as a proper method for the quick and definitive diagnosis of disease cases.

Keywords

Mycobacterium avium, Johne's disease, 16S rRNA, Nested PCR

Number of Figures: 2
Number of Tables: 2
Number of References:: 22
Number of Pages: 7

Abbreviations

MAP: Mycobacterium avium subsp. paratuberculosis
RVSRI: Razi Vaccine and Serum Research Institute
bp: base pair
TE: Tris/EDTA

Corresponding author: *Alireza Shahrjerdi*
Email: *drshahrjerdi@rvsri.ac.ir*
Tel: *+98(91)8162-1955*

Introduction

Johne's disease is a progressive chronic granulomatous enterocolitis in ruminants caused by MAP. MAP is a 0.5-2 µm, very slow-growing, acid-fast, mycobactin-dependent, and very stable pathogen that can survive in various media for a long time [1]. This bacterium enters the intestinal epithelial cells of cattle and other mammals, causing irreversible damage to infected animals, such as indigestion, diarrhea, vomiting, reduced reproduction, and death in various cases [2]. MAP is a silent, chronic, surprising infection considered a serious risk for the animal husbandry industry. Dealing with this disease is very costly and causes the early elimination of breeding livestock, reduction of livestock products, and heavy economic damage to stockbreeders.

Culturing is the technique used to precisely identify this bacterium, but this technique faces numerous challenges. The disease cannot be diagnosed in the early stages of culturing, and ELISA screening is recommended during this period. Furthermore, the incubation period of this disease is very long, with very slow growth. Consequently, molecular methods are used for the diagnosis and epidemiological investigations of this disease [3].

Johne's disease has existed for many years in Iran's ruminants. Considering similar clinical symptoms and molecular isolation and diagnosis of this bacterium in most patients with Crohn's disease, this bacterium is assumed to play a role in Chron's disease in humans. Therefore, scientists consider this bacterium a potentially serious threat to public health. Despite the high frequency of MAP in Iran's livestock [4-6], it is challenging to study the actual prevalence of the disease due to the high insensitivity of diagnostic methods and different testing and sampling methods in distinct countries. Notably, comprehensive research has not been conducted in Iran, but scattered studies have been performed using diverse methods.

A high-efficiency vaccine is required to prevent the disease caused by this bacterium. The disease situation in Iran must be first identified to run the disease control program, and control programs should be then performed accordingly.

This study aimed to isolate and determine the molecular identity of mycobacterium from ELISA-positive suspicious cows with Johne's disease from the samples of Markazi Province sent to RVSRI.

Results

ELISA. Of 2938 cow samples from dairy farms in Markazi and Alborz provinces, 87 positive and 26 suspicious samples were obtained using ELISA.

Culture. Initial isolation and MAP recultivation were performed using the Herrold egg culture medium (Figure 1; A). Ziehl–Neelsen staining confirmed the accumulation of acid-fast bacilli in 26 suspicious samples (Figure 1; B). Bright bacteria were also observed in the fluorochrome method (Figure 1; C).

PCR. The quantity (a concentration of 300-800 ng/mL and a wavelength of 260 nm) and quality (an obvious bond) of extracted DNA were suitable.

PCR for *16S rRNA*. At this stage, the 16S rRNA gene amplification confirmed isolates belonging to the mycobacterium genus. The PCR product length for this gene was 543 bp (Figure 2; A).

Nested PCR. The product length of 398 bp confirmed that isolates belonged to MAP (Figure 1; A). Finally, MAP was identified by producing a 298-bp fragment (Figure 1; C).

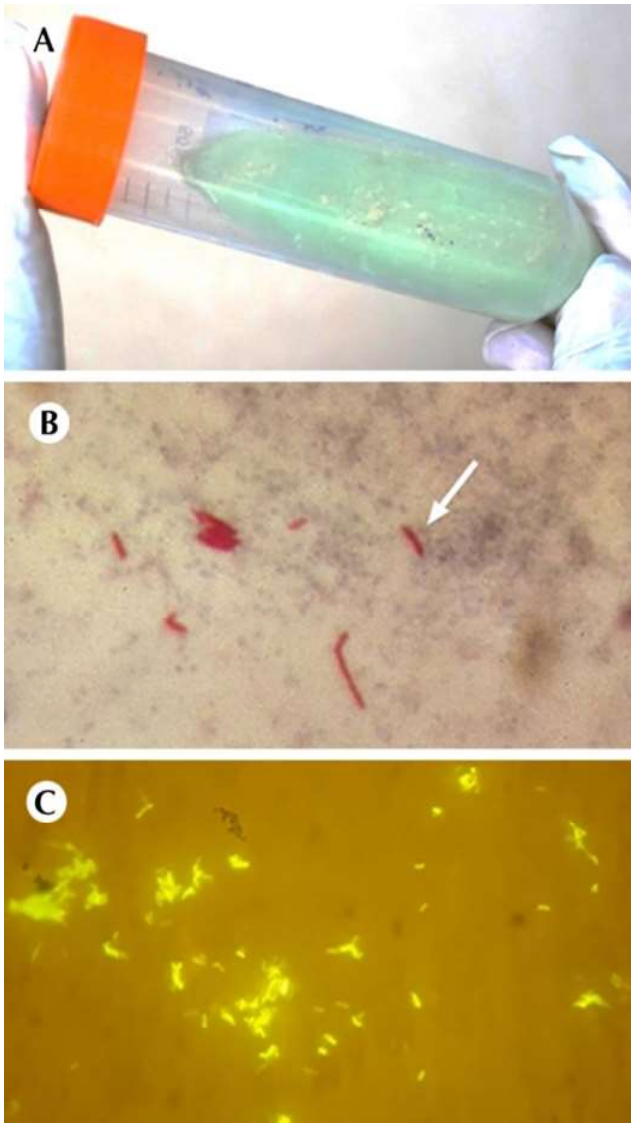

Figure 1.
MAP culture on Herald's egg yolk medium with mycobactin-J (A), Ziehl-Neelsen (B), and fluorochrome (C) staining of isolates

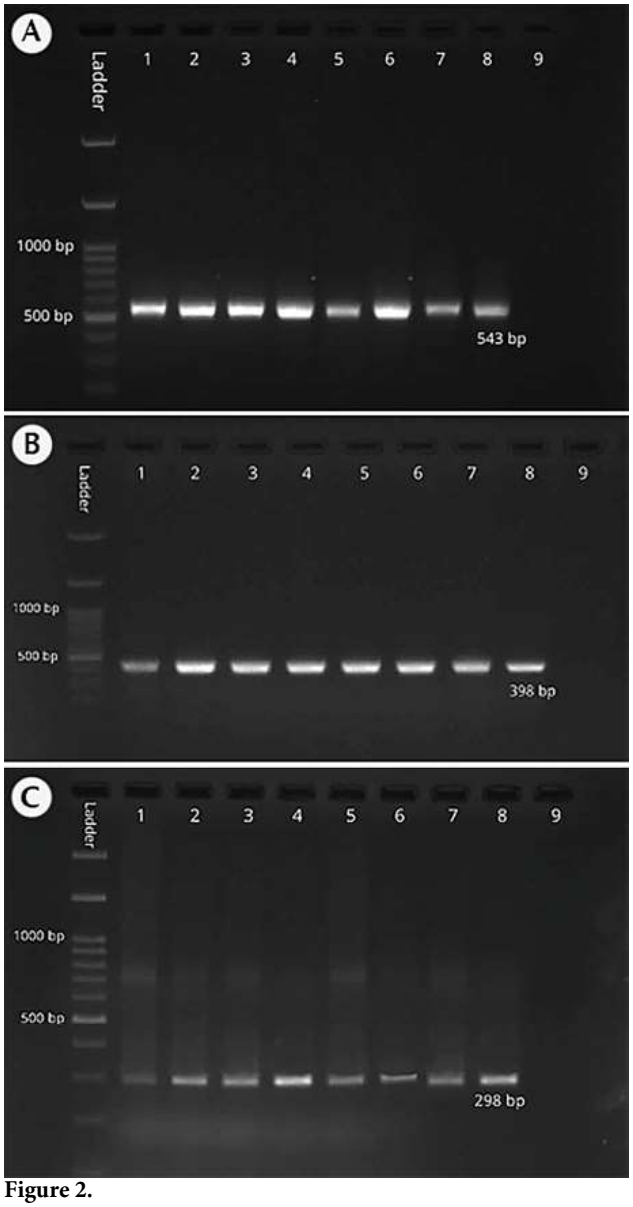

Figure 2.
PCR for identifying the isolates
PCR for 16S rRNA (A); Nested PCR for P90 & P91 (B); Nested PCR for AV1 & AV2 (C); [1-8: Isolates; 9: Negative control]

Discussion

Johne's disease is a serious problem due to the economic damage it causes to the livestock industry worldwide. Paratuberculosis also causes significant economic damage to the industry in Iran, but its extent is still unknown. Therefore, the diagnosis and control of diseases in ruminant herds is very important [8, 11]. The clinical symptoms of livestock are not solely reliable, as confirmed by the results of various studies on cows examined by the Johnin test, because this test fails to diagnose infected livestock among the suspected cases. Consequently, using molecular methods in Iran as a complementary test considerably helps dairy herds' health and, thereby, human society's health [10, 12].

Culturing on specific solid media is the most sensitive and specific method for diagnosing Paratuberculosis in livestock. However, culture-based methods are time-consuming and experimentally challenging for this bacterium [11]. Accordingly, new PCR-based molecular methods are used as proper alternatives for detecting the bacterium. Moreover, secondary contamination and drying of the culture medium may occur during long incubation periods, causing false negative results [10, 12].

The IS900 marker is specific to the MAP genome. However, unrealistic results may be observed depending on the type of selected primers due to the genetic similarity of the insertion sequence and its similar genetic units, known as pseudo-IS900 factors. There are reports on this case [13]. As a result, using equivalent genetic markers can improve the precision and correctness of identity tests. For this reason, in addition to the PCR-IS900 test in this study, nested PCRs using the P90 and P91 primers on the samples, and then the primers AV1 and AV2 were used.

Numerous PCR-based molecular techniques with high sensitivity and specificity have been proposed to quickly detect the bacterium [14]. However, nested PCR was used to confirm the isolates due to the lower sensitivity of usual PCR than nested PCR. Numerous studies have been recently conducted in this area, reporting the higher sensitivity of nested PCR than other methods in some cases. Abdolmohammadi et al. [8], Corti and Stephan [15], Haghkhah et al. [5], Jafari [16], and Doosti [17] identified MAP-infected cases using this technique.

Seyyedin et al. designed three primer pairs for the IS900 sequence, including Para1F/Para4R, Para2F/Para3R, and P90F/P91R, producing a 210-bp fragment. Their results showed that, except in one case, all positive cultured cases were consistent with nested PCR [18]. Soumya et al. reported a higher sensitivity of nested PCR than culture and ELISA [19].

Comparing the results of direct observation, ELISA, culturing, and nested PCR in examining the contamination of the milk tanks of dairy farms to MAP showed that 82 samples (82%) were positive in culture, 94 (94%) in nested PCR, 98 (98%) in ELISA, and only 33 (33%) in direct observation. Four samples were positive in ELISA but were negative in PCR. These 4 samples, along with the other 12 samples whose ELISA was positive (16 samples), did not have bacterial growth in the culture medium.[8]. Overall, the results of this study confirmed the superiority of nested PCR over other methods employed in this study. The contamination of the dairy cows of Kerman Province to MAP was examined and identified using microbial culture, PCR, and nested PCR [10]. Comparing these methods showed the superiority of nested PCR in detecting MAP, as confirmed by our results.

Abdolmohammadi et al. isolated MAP from

suspicious samples and examined them using nested PCR. Of 142 suspicious samples, 47 isolates were obtained. All positive isolates were acid-fast bacilli in Ziehl-Neelsen staining. In 83 samples of 142 samples and mycobacterium strains in PCR for 16S rRNA, a 543-bp band was observed, indicating the presence of mycobacterium in the samples. Nested PCR was performed on all isolates and positive and negative control strains, confirming the presence of MAP by generating a 398-bp fragment in the first stage and a 298-bp fragment in the second stage [8]. The consistency of our results with those reported by Abdolmohammadi et al. suggests that nested PCR can be used as a quick and definitive method for diagnosing the disease.

Some recent studies showed that the simple, one-step PCR cannot detect MAP in some cases, particularly at low DNA templates [20]. Single PCR is not sensitive enough as a diagnostic test for clinical samples. This low sensitivity of single PCR has been reported previously and was attributed to the presence of amplification inhibitors. Research on MAP has, however, found that this lower sensitivity of the standard amplification protocol when applied to clinical samples is neither solely due to the presence of inhibitors nor to the extraction of mycobacterial DNA [21]. It was found that when a standard amplification protocol is used, the technique can detect DNA from MAP in samples containing >100 CFU/mL but is frequently negative for samples containing fewer organisms [22]. An amplification of the latter samples was possible using nested PCR.

Consequently, the more reliable and sensitive nested PCR was used in this study to detect this infectious factor. This test was used due to its ability to search and amplify very low DNA contents. We have tested nested PCR for the rapid detection of paratuberculosis infection in suspicious clinical samples and compared its performance with bacteriological culture and single PCR. Nested PCR had an increased sensitivity for the detection of MAP, approaching that of culture.

Conclusion

It can be argued that ELISA can be very helpful in examining the status of samples and monitoring the progress of disease control programs. It is recommended as a screening method for Johne`s disease. However, this test may produce false positives and negative results. Therefore, culture or PCR should be used after detecting the infected cases by ELISA for the definitive diagnosis of the disease. Nested PCR significantly improves the sensitivity of detecting MAP and can be useful for the quick diagnosis of paratuberculosis. However, PCR inhibitors are a major hindrance. Accordingly, nested PCR is suggested as a proper method for the quick and definitive diagnosis of disease cases.

Materials & Methods

Collection of samples

Of 2938 cows from Markazi Province dairy farms (Arak: 497, Khomein: 101, Shazand: 66, Delijan: 328, Komijan: 26, Farahan: 17, Saveh: 498, and Zarandiye: 1405 samples), 6 mL blood was taken from the Jugular vein and sent to the RVSRI reference laboratory where the sera were separated. Microtubes were stored at -20°C for ELISA and PCR.

ELISA

ELISA was performed for all 2938 serum samples using an ELISA paratuberculosis kit (Cat No. RVJ99001, RVSRI) according to the standard instructions [7]. To this end, the wells were coated with MAP316F antigen. In the next step, 10 µL of the serum samples was mixed with 300 µL dilution buffer in a blank plate and then, the mixture was incubated at 25°C for 30 min, and 100 µL of this mixture was transferred to the main plate and the plate was incubated at 25°C for 30 min. After 5 times of washing, 100 µL of the conjugated bovine antibody was added to the mixture, and the mixture was incubated at 25°C for 30 min. After washing once again, 100 µL of substrate was added and the plate was incubated in a dark room at 25°C for 10 min. Finally, 100 µL of stop solution was added and the absorbance was read at 450 nm by an ELISA reader.

Culture

Initial isolation and MAP recultivation were performed using the Herrold egg culture medium containing mycobactin and without mycobactin, along with amphotericin B (5 mg), chloramphenicol (50 mg), and penicillin (100,000 units) [8]. The isolates were microscopically examined using the Ziehl–Neelsen (acid-fast) and fluorochrome methods.

Genomic DNA extraction

Bacterial DNA was extracted by Van Solingen's method using CTAB, isoamyl alcohol, and chloroform. Two complete loops of bacterial colonies were taken from the surface of the Herrold egg medium and slowly transferred into a microtube containing 400 µL of TE buffer. The resultant suspension was kept at 85°C for 30 min to deactivate bacteria [8, 9].

To extract DNA, 50 µL lysozyme (10 mg/mL) was added to each microtube containing mycobacterium suspension and stored overnight at 37°C after vortexing. Thereafter, 110 µL of protease K and SDS 10% was added to each microtube, vortexed, and incubated overnight at 50°C. Afterwards, 100 µL of 5 M NaCl and 100 µL of CTAB/NaCl solution were added and vortexed until a milky white solution appeared. The solution was stored at 65°C for 10 min. Then, 750 µL isoamyl alcohol-chloroform (1:24) was added to each microtube and vortexed for 10 min and then centrifuged at 11000 g for 8 min at 25°C. A volume of 450 µL of cold isopropanol was added to the aqueous phase (containing DNA) and kept at -20°C for 30 min. The microtubes were centrifuged at 11000 g for 15 min at 25°C, and the supernatant was discarded. One milliliter of cold ethanol 70% was added, and the microtubes were vortexed several times. The solution was then centrifuged at 11000 g for 5 min at 25°C, and the supernatant was discarded. Next, 20 µL of TE buffer was poured on the DNA precipitates, and the DNA quantity and quality were examined by electrophoresis and nanodrop.

PCR

PCR was first performed for the 16S rRNA gene (confirming that the isolates belonged to the mycobacterium genus) with primers 5'ACGGTGGGTACTAGGTGTGGGTTTC3' and 5'TCTGCGATTACTAGCGACTCCGACTTCA3'. After that, Nested PCR was performed using primers IS900 P90 (5'GTTCGGGGCCGTCGCTTAGG3') and IS900 P91 (5'GAGGTCGATCGCCCACGTGA3'), confirming that the isolates were MAP. The product was used as a pattern for the subsequent PCR using primers IS900 AV1 (5'ATGTGGTTGCTGTGTTGGATGG3') and IS900 AV2 (5'CCGCCGCAATCAACTCCAG3'). The final PCR volume was set at 12.5 µL (Table 1). In addition to the positive and negative mycobacterium DNA samples, a distilled water microtube containing all PCR components except DNA was used as a negative control. The microtubes were then placed in a thermocycler, and the temperature program of PCR was set according to Table 2 [8-10]. Electrophoresis was performed using Red Safe pre-stained 1% MP agarose with a genetic marker size of 100 bp for 90 min at 2 V/cm.

Table 1.
Thermal cycle conditions

PCR reaction	Initial heating	Denaturation	Annealing	Extension	Final extension	No. of cycles
16S rRNA	5 min, 94 °C	1 min, 94 °C	1 min, 60 °C	1min, 72 °C	10 min, 72 °C	25
MAP1	5 min, 95 °C	1 min, 95 °C	90 sec, 58 °C	90 sec, 72 °C	10 min, 72 °C	35
MAP2	5 min, 95 °C	1 min, 95 °C	90 sec, 58 °C	90 sec, 72 °C	10 min, 72 °C	35

Table 2.
PCR Materials

PCR reaction 16S rRNA	PCR buffer (µl)	dNTPs (µl)	MgCl2 (µl)	Primer forward (µl)	Primer reverse (µl)	DMSO (µl)	Taq polymerase (µl)	DNA template (µl)	PCR water (µl)
IS900 P	1.25	0.25	0.4	1	1	0.5	0.3	3	4.8
IS900 AV	1.25	0.25	1.25	0.4	0.4	0.5	0.5	3	4.95

Authors' Contributions

A.S. conceived and planned the experiments. M.S. carried out the experiments. M.S., and M.Sa. contributed to sample preparation. A.S., and M.Sa. contributed to the interpretation of the results. M.S. took the lead in writing the manuscript. All authors provided critical feedback and helped shape the research, analysis and manuscript.

Acknowledgements

The authors of the article express their gratitude to the management and personnel of the tuberculin department of the Razi Vaccine and Serum Research Institute as well as the herd owners who provided the necessary help and cooperation to collect the samples for this study.

Conflict of interest

The authors declare that there is no conflict of interest.

References

1. Hassani M. Johne's disease in Iran: A systematic review and meta-analysis. Veterinary Research and Biological Products. 2017;30(1):139-147. DOI: 10.22034/VJ.2017.107807.

2. Charavaryamath C, Gonzalez-Cano P, Fries P, Gomis S, Doig K, Scruten E, Potter A, Napper S, Griebel PJ. Host responses to persistent Mycobacterium avium subspecies paratuberculosis infection in surgically isolated bovine ileal segments. Clinical and Vaccine Immunology. 2013;20(2):156-165. DOI: 10.1128/CVI.00496-12.

3. Nadalian M, Hasani tabatabei A, Mir arefeyn M. A Retrospective study of econimic losses due to bovine Paratuberculosis (John's disease) in two dairy herds around Tehran. Veterinary Research and Biological Products. 1996;9(4):128-131. DOI: 10.22092/VJ.1996.112758.

4. Shahmoradi A, Mosavari N, Aref Pajouhi R, Heidari M, Noamaan V, Nabinejad A, et al. Study of John's disease in industrlal and semi-industrial cattle husbandry of Esfahan province. Veterinary Research and Biological Products. 2009;82:13-17. DOI: 20.1001.1.24235407.1388.22.1.2.0.

5. Haghkhah M, Ansari-Lari M, Novin-Baheran AM, Bahramy A. Herd-level prevalence of Mycobacterium avium subspecies paratuberculosis by bulk-tank milk PCR in Fars province

(southern Iran) dairy herds. Preventive Veterinary Medicine. 2008;86(1-2):8-13. DOI: 10.1016/j.prevetmed.2008.03.010.

6. Ghaem Maghami S, Khosravi M, Ahmadi M, Denikoo A, Haghdin M, Koochakzadeh A. Study of the prevalence rate of John's disease in Markazi province and evaluation of absorbed ELISA for adoption as a diagnostic method. Iranian Veterinary Journal. 2012;8(3):54-59.

7. Keshavarz R, Mirjalili A, Mosavari N, Tadayon K. Development and optimization a high sensitive and specific ELISA system for rapid detection of paratuberculosis in cattle. International Journal of Advanced Biotechnology and Research. 2016;7(1):1-9.

8. Abdolmohammadi Khiav L, Haghkhah M, Tadayon K, Mosavari N. Isolation of Mycobacterium avium subsp. paratuberculosis and confirmation of cases by Nested-PCR. Veterinary Research and Biological Products. 2019;32(1):41-47. DOI: 10.22092/VJ.2018.122621.1472.

9. Johansen TB, Olsen i, Jensen MR, Dahle UR, Holstad G, Djonne B. New probes used for IS1245 and IS1311 re-striction fragment length polymorphism of Mycobacterium avium subsp. avium and Mycobacterium avium subsp. hominissuis isolates of human and animal origin in Norway. BMC Microbiology. 2007;7:11-14. DOI: 10.1186/1471-2180-7-14.

10. Soltani M. Detection of Mycobacterium avium subsp. paratuberculosis in Kerman province's dairy cows using microbial culture, PCR and Nested-PCR Methods. Iranian Journal of Animal Science Research. 2018;10(2):263-273. DOI: 10.22067/IJASR.V10I2.65920.

11. Badiei A, Mousakhani F, Barin A, Hamidi A, Zafari M. Comarison of direct microscopic examination, Enzyme Linked Immunosorbent Assay (ELISA), culture and Nested-PCR for diagnosis of herds bulk tank milk infection with Mycobacterium avium subspecies paratuberculosis. Veterinary Clinical Pathology. 2012;5(4):1369-1378.

12. Shrafati-chaleshtori F, Sharafati-chaleshtori R, Shakerian A, Momtaz H. Detection of Mycobacterium paratuberculosis using polymerase chain reaction (PCR) in cow raw milk samples in shahre-kord. Medical Laboratory Journal. 2009;3(1):1-6.

13. Nassiri M, Jahandar M, Soltani M, Mahdavi M, Mahdavi M. Identification and strain determination of M. paratuberculosis (MAP) by PCR and REA methods based on IS900 and IS1311 insertion segments. Agricultural Biotechnology Journal. 2012;4(1):83-96. DOI: 10.22103/JAB.2012.469.

14. Mahmoodi Koohi P, Sadeghi-nasab A, Mohammadzadeh A, Sharifi A, Bahari A, Mosavari N. Identification of Mycobacterium avium subsp paratuberculosis infection in industrial dairy farms of Hamedan. Iranian Veterinary Journal. 2018;14(1):55-61. DOI: 10.22055/IVJ.2017.67340.1832.

15. Corti S, Stephan R. Detection of Mycobacterium avium subspecies paratuberculosis specific IS900 insertion sequences in bulk-tank milk samples obtained from different regions throughout Switzerland. BMC Microbiology. 2002;2:9-15. DOI: 10.1186/1471-2180-2-15.

16. Jafari B, Moosakhani F, Jamshidian M. Subtype genotyping characterization of Mycobacterium avium subspecies paratuberculosis isolated from dairy cattle of Tehran province. Advanced BioResearch. 2015;6:60-64. DOI:10.15515/abr.0976-4585.6.2.6064.

17. Doosti A. Moshkelani S. Detection of Mycobacterium paratuberculosis by Nested-PCR in dairy cattles suspected to john's disease. Journal of Microbial World. 2009;2:19-22.

18. Seyyedin M, Tadjbakhsh H, Salehi T. Identification of Mycobacterium avium subsp. paratuberculosis in fecal samples of Holstein-Friesian cattle using molecular and cultivation methods. Journal of Veterinary Research. 2010;65:135-171.

19. Soumya MP, Pillai RM, Antony PX, Mukhopadhyay HK, Rao VN. Comparison of faecal culture and IS900 PCR assay for the detection of Mycobacterium avium subsp. paratuberculosis in bovine faecal samples. Veterinary Research Communications. 2009;33:781-791. DOI: 10.1007/s11259-009-9226-3.

20. Sadeghi N, Jamshidi A, Seyyedin M. Detection of Mycobacterium avium Subsp. paratuberculosis in pasteurized milk samples in Northeast of Iran by culture, direct Nested PCR and PCR Methods. Iranian Journal of Chemistry and Chemical Engineering. 2020;39(6):251-258. DOI: 10.30492/IJCCE.2019.36497.

21. Vary PH, Andersen PR, Green E, Hermon-Tayler J, McFadden J. Use of highly specific DNA probes and the PCR reaction to detect Mycobacterium paratuberculosis in Johne's disease. Journal of Clinical Microbiology. 1990;28:933-937. DOI: 10.1128/jcm.28.5.933-937.1990.

22. Pierre C, Lecossier D, Boussougant Y, Bocart D, Joly V, Yeni P, et al. Use of a reamplification protocol improves sensitivity of detection of Mycobacterium tuberculosis in clinical samples by amplification of DNA. J Clin Microbiol. 1991;29(4):712-717. DOI: 10.1128/jcm.29.4.712-717.1991.

How to cite this article
Soleimani M, Shahrjerdi A, Salehi M.Molecular Identification of *Mycobacterium avium* subsp. *Paratuberculosis* isolated from ELISA-Positive Samples by Nested PCR. Iran J Vet Sci Technol.2024; 16(1): 45-51.
DOI: https://doi.org/10.22067/ijvst.2023.83414.1280
URL:https://ijvst.um.ac.ir/article_44766.html

Iranian Journal of Veterinary Science and Technology

Received: 2023- Sep-13
Accepted after revision: 2024- Feb-04
Published online: 2024-Feb-04

RESEARCH ARTICLE

DOI: 10.22067/ijvst.2024.84426.1300

Effects of the Hydroalcoholic Extract of *Peganum harmala* Against the Venom of the Iranian *Snake Naja naja oxiana* in Mice

Behrooz Fathi

Department of Basic Sciences, Faculty of Veterinary Medicine, Ferdowsi University of Mashhad, Mashhad, Iran.

ABSTRACT

Peganum harmala contains pharmacologically active compounds and has been utilized for various purposes over the years. Due to public health concerns about snakebite envenoming, this study aimed to assess the potential antagonistic effects of this plant against the lethal impact of snake (*Naja naja oxiana*) venom. This study used five protocols and 56 adult albino mice in seven equal groups (A, B1, B2, C, D, E, and F). In protocol I (control), group A received only 4 mg/kg of venom, while groups B1 and B2 received the *P. harmala* extract at doses of 15 and 30 mg/kg, respectively. In protocol II, group C was simultaneously administered 15 mg/kg of the extract and 4 mg/kg of venom. In protocol III, group D received 4 mg/kg of venom, followed by the administration of 15 mg/kg of the extract after 20 min. In protocol IV, group E was treated with venom-extract pre-incubated for 20 min at the same doses. In protocol V, group F received 30 mg/kg of the extract orally 60 min before the injection of venom at 4 mg/kg. The route of injection was IP. The average time of death after venom injection was 31 ± 5 min. Groups B1 and B2 survived, while the animals in group C died after 29 ± 7 min, group D after 18 ± 4 min, group E after 17 ± 5 min, and group F after 22 ± 3 min. In conclusion, *P. harmala* does not protect against *Naja naja* venom and accelerates its lethal effect in an unknown way.

Keywords

Snakebite, Peganum harmala, Naja naja oxiana, Venom, Synergist

Number of Figures: 2
Number of Tables: 1
Number of References:: 40
Number of Pages: 9

Abbreviations

IP: Intraperitoneal
WHO: World Health Organization
LD50: Lethal dose 50%
IV: Intravenously
PLA2: Phospholipase A2
LD100: Lethal dose 100%
MAO: Monoamine oxidase

Corresponding author: *Behrooz Fathi*
Email: *b-fathi@um.ac.ir*
Tel: *+98(91)5976-5651*

Introduction

Snakebite envenomation is a global public health issue recognized by WHO, especially in tropical and subtropical regions. Over five million people are affected annually, resulting in 135,000 deaths. Survivors often face long-term disabilities, exceeding the fatality rate [1-3].

Iran, a temperate region, exhibits an impressive biodiversity with a notable presence of 81 snake species. Among these, 25 are venomous and hold significant medical importance. In a period spanning from 2002 to 2011, Iran witnessed a substantial number of reported snakebite incidents, which reached a staggering figure of 53,787 cases, resulting in 67 deaths.

The Caspian cobra (*Naja naja oxiana*) (Figure 1), belonging to the Elapidae family, is primarily found in the northeastern part of Iran, mainly in Khorasan province [4-7]. It is one of the most venomous snakes in Iran and in some neighboring countries. Its venom contains a highly potent neurotoxin with an exceptionally low LD50, making it more deadly than other cobra venoms. Studies have indicated that its LD50 is 10 µg/mouse when administered IV and recorded after 24 hours [8, 9]. Mortality due to Iranian cobra bites is 70%-75% if not treated, which is the highest rate among cobras, especially the Naja genus [10]. While N. n. oxiana is responsible for numerous fatal snakebites in Iran, the exact number of individuals envenomed by this snake has not been officially reported.

Antivenoms are considered the most conventional and effective treatment for venomous bites, as they can neutralize the toxins present in the venom and alleviate its effects. They play a crucial role in reducing the severity of envenomation, preventing complications, and promoting recovery.

However, it is important to acknowledge that antivenoms also have certain disadvantages. These include the risk of allergic reactions, such as early potentially life-threatening anaphylactic reactions and delayed reactions of the serum sickness type. Limited availability, high cost, specificity to particular types of venom, time limitations for administration, and the potential for other side effects should be noted [11-13]. Moreover, antivenoms have demonstrated limited efficacy in effectively treating the local destructive effects induced by venoms. Consequently, there exists a continuing and significant medical need pertaining to venomous bites and stings. It is paramount for scientists to persist in their endeavors to explore and develop more potent alternatives, as well as make advancements in the field of antivenom research.

In regions with a high frequency of snakebite incidence and limited access to medical facilities, the utilization of herbal medicines may be the only hope for saving the lives of victims [14, 15].

One illustrative example involves the employment of Indian Rauvolfia serpentina within traditional Ayurvedic medicine to address snakebite complications. Another notable plant is *Andrographis paniculata*, also known as the "King of Bitters," which has a longstanding history in traditional medicine for its use in treating snakebites and venomous envenomation. *Azadirachta indica*, commonly referred to as Neem, can be topically applied to mitigate the swelling and inflammation triggered by snakebites. *Aloe barbadensis*, commonly recognized as aloe vera, offers pain alleviation and support in wound healing when applied topically to the site of snakebite. Moreover, Curcuma longa, also known as turmeric, possesses curcumin, which exhibits considerable anti-inflammatory and antioxidant properties that can facilitate wound healing by reducing inflammation when topically administered [16]. Certain traditional medicines, that contain natural PLA2 inhibitors, possess potent anti-snake venom properties. For instance, the ashwagandha plant (*Withania somnifera*) has been found to neutralize the venom of the speckled cobra (*Naja naja*) [17], and the leaf extract of *Acalypha indica* has been shown to have the potential to neutralize the venom of the Russell's viper [18].

The scientific investigation of herbal antidotes for snake venom holds significant importance in the management of snakebites, while the effectiveness of this traditional treatment approach remains largely unproven in most cases.

Peganum harmala L. (*P. harmala*) (Figure 1), a perennial plant, is commonly known as Syrian Rue, harmala, or Espand in Iranian traditional folklore, and belongs to the family Zygophyllaceae [19]. While its primary origin is central Asia, it has scattered and now grows in various regions, including Australia, northern Africa, and southwestern America. *P. harmala* thrives in semiarid conditions similar to those found in Iran [20, 21].

Recent research has shown that *P. harmala* contains numerous *phytoconstituents* largely in its seed [22]. The bioactive alkaloids, including harmine, harmaline, harmol, vasicine, vasicinone, deoxyvasicine, and deoxyvasicinone are responsible for their therapeutic functions, such as anticancer, antidiabetic, antimicrobial, anti-inflammatory, antiviral, antidiarrheal, antiemetic, antidepressant, anthelmintic, and antioxidant properties, which have been vastly documented [23-25].

In Iran, the most popular traditional use of P. *harmala* seeds is as a disinfectant by burning the seeds and producing smoke through direct heat. While there are reports of individuals in various regions utilizing *P. harmala* to treat snake bites, these claims lack

scientific and research-based evidence.

This study was conducted to assess the potential of *P. harmala* as a remedy for snakebites, representing the first investigation into its efficacy in countering the lethal effects of snake venom. Accordingly, we aimed to investigate the possible antagonistic impact of *P. harmala* on the venom of the Iranian cobra, *N. n. oxiana.*

Results

Evaluation of Peganum Hermala extract for its antivenom activity

Protocol I, acute toxicity study

Prior to the main tests, several pilot studies were conducted to determine the LD100 of Naja naja oxiana venom in mice. Control groups, were including Group A, B1, and B2. In Group A, all mice were administered a dose of 4 mg/kg of *N. n. oxiana* venom alone and animals in group B1 and B2 received only the *Peganum Hermala* extract at doses of 15 mg/kg and 30 mg/kg, respectively. The mortality rate in group A was 100%, and the average time to death was 31 ± 5 minutes (Figure 2). Conversely, all mice in Groups B1 and B2, survived. This observation indicates a lack of toxic effects of the extract at the concentrations tested (Table 1).

Protocol II, the effect of Peganum Hermala extract were injected simultaneously with the venom of N. n. oxiana

All mice in Group C were treated with 15 mg/kg of *Peganum Hermala* extract along with 4 mg/kg of venom simultaneously. In this group, the mortality rate was 100%, and the average time to death was 29 ± 7 minutes. These values were not significantly different from the time to death of animals in Group A. (Figure 1) (Table 1).

Protocol III, the effect of Peganum Hermala extract were injected 20 min after the venom of N. n. oxiana

In this protocol, animals in Groups D received 15 mg/kg of *Peganum Hermala* extract, 20 minutes after being treated with 4 mg/kg of venom. The average time to death in Group D was 18 ± 4 minutes, which was significantly different from the time to death of animals in Group A ($p < 0.001$) (Figure 2) (Table 1).

Protocol IV, effect of a mixture of N. n. oxiana venom and Peganum Hermala extract

In this protocol, group E was treated with a mixture of 4 mg/kg of venom and 15 mg/kg of *Peganum Hermala* extract were incubated for 20 min. The average time to death in this group was 17 ± 5 minutes, which was significantly different from the time to death of animals in group A ($p < 0.01$) (Figure 2) (Table 1).

Protocol V, effect of oral administration Peganum Hermala extract against N. n. oxiana venom

In this protocol, group F was treated with 4 mg/kg of venom and 30 mg/kg of *Peganum Hermala* extract orally. The average time to death in group F was 22 ± 3 minutes, which was significantly different from the time to death of animals in group A ($p < 0.01$) (Figure 2) (Table 1).

Figure1.
A) Peganum harmala seeds, B) Iranian snake Naja naja oxian (Prepared by B. Fathi)

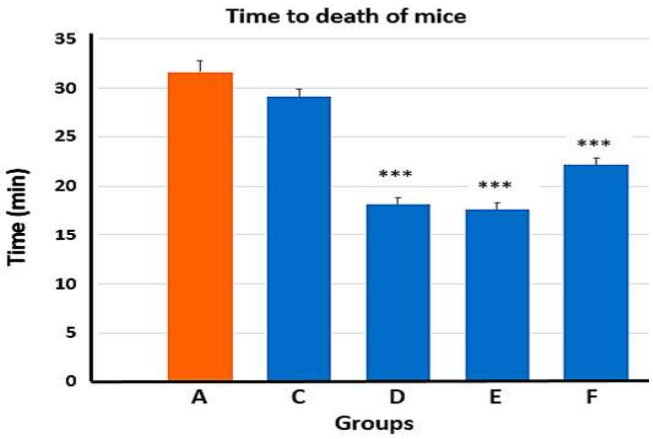

Figure 2.
Time to death of mice after application of venom (V) and Peganum Hermala extract in different experimental protocols.
Protocols: I (groups A): Only venom was injected at dose of 4 mg/kg (control). II (group C): Venom at 4 mg/kg and plant extract at 15 mg/kg have been injected simultaneously. III (group D): The plant extract has been injected 20 minutes after the venom injection at the pervious doses. IV (group E): Venom and plant extract have been incubated for 20 min prior to being injected at the pervious doses. V (group F) treated with venom at 4 mg/kg (ip) 60 minutes after administration of plant extract at 30 mg/kg orally. The level of significance considered was $p < 0.05$.

Table 1.
Application of different protocols and summary of the experiment results

Protocols	NO of mice	Venom Mg/kg	P. Harmala Mg/kg	Average time to death
A	8	4	-	31 ± 5
B1	8	-	15	Live
B2	8	-	30	Live
C	8	4	15	29 ± 7
D	8	4	15	18 ± 4
E	8	4	15	17 ± 5
F	8	4	30/orally	22 ± 3

Discussion

There is limited scientific research available regarding the specific interaction between *P. harmala and* cobra venom. The results of the present study showed that *P. harmala* extract does not have a protective effect and increases the speed of the deadly effect of the *N. n. oxiana* venom in an unknown way. In other words, it has a synergistic effect on this venom.

The *N. n. oxiana* venom exhibits neurotoxic properties and also possesses cytotoxic effects [26]. The inhibitory effect of cobra venom on nicotinic acetylcholine receptors results in the prevention of post-synaptic neurotransmitter connections, ultimately leading to respiratory muscle paralysis, particularly preventing the crucial function of the diaphragm, which clinically is the reason for victim death [27, 28].

P. harmala contains a variety of chemical compounds, including amino acids, such as phenylalanine, valine, histidine, and glutamic acid; flavonoids, such as coumarin, tannins, and sterols; and is rich in toxic alkaloids of the β-carboline type, such as Harmine, Harmaline, Harmol, and Harmalol [29-31]. In several studies on traditional herbal treatments, the toxicity and interactions of this plant have been identified [31]. Beta-carbolines bind to receptors, such as serotonin, muscarinic, histamine, and beta-adrenergic. Therefore, it seems that it cannot interfere with the blocking of acetylcholine receptors by venom. In other words, *P. harmala* extract does not have an inhibitory effect on specific receptors of active substances of *N. n. oxiana* venom.

According to a report, *P. harmala* has been associated with the clinical symptoms of intoxication. Animals experiencing intoxication exhibit various manifestations, including increased excitability, trembling, muscle stiffness, and an unsteady gait. Following a short narcotic state and heightened activity, animals may also encounter difficulties in breathing, mydriasis, hypothermia, and urinary problems [32, 33]. In severe cases, paralysis, depression of the central nervous system, dyspnea, and arterial hypotension have been observed. However, it is important to note that in this particular study, the administration of two different doses of *P. harmala* (15 and 30 mg/kg) did not result in any signs of intoxication. This lack of intoxication could potentially be attributed to the low concentration of *P. harmala* used in the study. The LD50 (lethal dose required to kill 50% of test subjects) of its alkaloid harmane in mice has been reported as 50 mg/kg [29]. Therefore, we assumed that the toxic effects of *P. harmala*, even at low doses, manifest by intensifying the toxic effect of cobra venom. Furthermore, previous studies have demonstrated that *P. harmala* seed extract possesses antispasmodic effects, inducing a myorelaxant effect on rabbit and guinea pig smooth muscles in vitro [29]. It is probable that the synergistic effect between *P. harmala* and *N. n. oxiana* venom, which accelerates the paralysis caused by the venom, is associated with these toxic activities.

The results showed that the venom incubated with the *P. harmala* extract (group E) kills the animals at a faster rate compared to the control group A and group C. It can be concluded that the P. harmala extract can react with the venom molecules and change the structure of these molecules so that they can react more easily to their receptors or more receptors are caught in an unknown way. However, such facilitation has been also observed in group D, in which the admin-

istration of extract and venom had a 20-min interval. Moreover, the time to death in group C, in which extract and venom were administrated simultaneously, was very close to the control group. This may indicate that extract interaction is different in vitro and in vivo.

Other possibilities may help to explain this synergic effect. *P. harmala* affects the cardiovascular system, reducing blood pressure that may accelerate the time to death of animals [34]. In severe cases, paralysis, CNS depression, dyspnea, hypothermia, and low blood pressure occur. Moreover, its notable alkaloids encompass beta-carbolines (e.g., harmaline, harman, harmalol, and harmine), as well as quinazoline derivatives (vasicine and vasicinone) that have mild hallucinogenic effects and are known for their ability to inhibit monoamine oxidase enzyme which breaks down certain neurotransmitters, namely serotonin, dopamine, and noradrenaline. Inhibiting MAO can lead to increased levels of these neurotransmitters, which can have various effects on the body [35-39].

Therefore, it is reasonable that the MAO-inhibiting properties of *P. harmala* may disrupt the metabolism of venom toxins. Such disruption has the potential to augment the concentration of toxins, thereby raising the severity and duration of venom-induced toxic effects. As a consequence, accelerated and intensified neurotoxic and cardiotoxic effects may occur within the organism. However, it should be noted that the interactions between MAO inhibitors and venom toxins can be complex and depend on multiple factors, including the specific venom toxins, concentration of MAO inhibitors, and the individual's physiological responsiveness. Regarding the route of administration, although it has been reported that the alkaloids of *P. harmala* are readily absorbed by the digestive system [32], the findings of the current study indicated no significant difference in the time of animal mortality when administering *P. harmala* extract orally or intraperitoneally.

Conclusion

The results of the present study indicated that the extract of *P. harmala* not only lacks a protective effect against *Naja naja* venom but also enhances the speed of the venom's lethal effect in an unknown manner. Although the extract alone had no toxic effect, interaction with venom exhibited a synergistic effect with the venom. The extract may increase the susceptibility of animals to this venom in an unclear way. These findings suggested that the plant extract has either a lower competitive ability with the neurotoxin or no competitive ability at all. Further investigation, particularly at the molecular level, is essential to enhance result clarity and gain a deeper understanding of the underlying mechanisms involved in these interactions.

Materials & Methods

Venom

The freeze-dried crude venom of *N. n. oxiana* was kindly provided by the Razi Vaccine and Serum Research Institute, Karaj, Iran. The Lyophilized venom was stored at 4°C and freshly prepared by dissolving it in a sterile physiological saline solution (0.9 % NaCl) to a final volume of 500 µl before injection into the animals.

Preparation of P. harmala extract

The fresh plant was harvested during early summer from agricultural fields located in the vicinity of Sabzevar city (36°12'45"N and 57°40'35"E) in the western region of Razavi Khorasan province, Iran. The plant specimen was precisely identified as *P. harmala* at the Ferdowsi University of Mashhad Herbarium (13613-FUMH). Subsequently, the plant material was subjected to drying in a dark room at a temperature of 28°C ± 4°C for two weeks. Following the drying process, the black seeds were carefully separated and finely ground into a powder. methanolic extract of *P. harmala* was prepared in the Department of Pharmacognosy at the Pharmacy College of Ferdowsi University of Mashhad.

A total of 100 g of powder was dissolved in 300 ml of 70% methanol and left to stand for 48 h. The solution was stirred for 30 min at room temperature and then filtered through Whatman filter paper no. 1. An additional 200 ml of methanol was added to the remaining mixture, and the process was repeated three times. The resulting solution was protected from light by placing it in an aluminum-covered glass container. Using a vacuum rotary evaporator (IKARV 10, Germany) set at 50°C and 60 rpm, methanol evaporated from the solution. The resulting solution was a highly viscous, dark red honey-like liquid. The solution was poured onto a plate and transferred to an oven for one week until it dried into a solid form. Afterwards, it was covered with aluminum foil and stored in a refrigerator at 4°C until use.

To dissolve the extract, we conducted tests using various solutions, including saline solution, a mixture of saline solution, and 2-3 drops of DMSO 0.01%. In addition, we employed diverse methods, such as heating, shaking, and centrifugation in attempts to dissolve the extract. However, none of these approaches yielded successful results. Ultimately, we achieved dissolution by using 2 normal HCL while adjusting pH to 7.5 with NaOH.

Animals

For this study, 56 adult albino mice of both sexes aged 8-10 weeks and weighing 28-40 g were purchased from the Animal House of Mashhad University of Medical Sciences. The animals were housed in the animal facility of the Faculty of Veterinary Medicine under controlled environmental conditions, including a 12:12 light-dark cycle, a temperature of 23°C ± 2°C, and a relative humidity of 55% ± 10%. They were kept in standard rodent cages and provided with food and water ad libitum. The experimental protocol was conducted following the guidelines of the Animal Ethics Committee of the Faculty of Veterinary Medicine, Ferdowsi University of Mashhad. The protocol was approved by this Ethics Committee with the code IR.UM.REC.1401.171.

Experimental protocols

The ability of *P. Harmala* extract to antagonize the lethal effects of *N. n. oxiana* venom was investigated using five different protocols (I, II, III, IV, and V) (Table 1).

For this study, 56 mice were divided into seven equal groups (A, B1, B2, C, D, E, and F).

In protocol I (controls), group A received *N. n. oxiana* venom only at a dose of 4 mg/kg and groups B1 and B2 received only P. harmala extract at the doses of 15 and 30 mg/kg, respectively.
In protocol II, group C was treated simultaneously with 15 mg/kg of *P. harmala* extract, along with 4 mg/kg of venom.
In protocol III, group D was treated with 15 mg/kg of *Peganum Harmala* extract, 20 min after the administration of *N. n. oxiana* venom at 4 mg/kg.

In protocol IV, group E was treated with the mixture of venom and *P. harmala* extract which was preincubated for 20 min at room temperature (26°C ± 2°C) prior to injection into animals. The route of administration in this study was IP.

It has been reported that the main route of administration for *P. harmala* is the oral route, as its alkaloids are well absorbed by the digestive system (Tahri et al., 2011). Therefore, in protocol VI, group F received the extract orally at a dose of 30 mg/kg after 24 h of food deprivation. After one hour, they received a dose of 4 mg/kg of venom. The survival time of each animal (in minutes) after the injection of venom, extract, and venom/extract was recorded and statistically compared with the control groups.

Statistical analysis

The data are presented as mean ± SEM and all the results were analyzed using SPSS-22 (SPSS Inc., Chicago, Illinois). One-way analysis of variance was used to analyze the data, followed by a post-hoc analysis using a Tukey test. The level of significance was considered $p < 0.05$.

Acknowledgements

We thank Razi Vaccine and Serum Research Institute, Tehran-Iran, for generously provided the Lyophilized crude venom of *Naja naja Oxiana*. We also thank Dr. Fatemeh Salami for statistical analysis.

Funding

This research has been financially supported by Ferdowsi University of Mashhad-Iran

Conflict of interest

The authors declare that there is no conflict of the interest

References

1. Chippaux JP. Snakebite envenomation turns again into a neglected tropical disease. J. Venom Anim Toxins Incl Trop Dis. 2017; 8:23-38. DOI:10.1186%2Fs40409-017-0127-6.

2. Longbottom J, Shearer FM, Devine M, Alcoba G, Chappuis F, Weiss DJ. et al. Vulnerability to snakebite envenoming: a global mapping of hotspots. The Lancet. 2018 392:673-684. DOI:10.1016/S0140-6736(18)31224-8.

3. World Health Organization. Snakebite Envenoming: a Strategy for Prevention and Control. World Health Organization, Geneva. Available: 2019.

4. Latifi, M. The Snakes of Iran. Published by Environment Protection organization, Tehran, 2000. 478 pp. (in Persian, with Latin index).

5. Vazirianzadeh B, Chitins P, Vahabe A, Mozafari A. Epidemiological study of patients with snake biting in the hospitals of Ahvaz, Iran. J. Exp. Zool, India. 2008 11(2):497-500.

6. Dehghani R, Fathi B, Shahi MP, Jazayeri M. Ten years of snakebites in Iran. Toxicon. 2014 90:291-298. DOI:10.1016/j.toxicon.2014.08.063.

7. Monzavi SM, Dadpour B, Afshari R. Snakebite management in Iran: Devising a protocol. J. Res. Med. Sciences: the official journal of Isfahan University of Medical Sci. 2014 19(2):153-163.

8. Akbari A, Rabiei H, Hedayat A, Mohammadpour N, Zolfagharian H, Teymourzadeh S. Production of effective antivenin to treat cobra snake (Naja naja oxiana) envenoming. Archives of Razi Institute. 2010 65(1):33-37.

9. Kazemi-Lomedasht F, Yamabhai M, Sabatier JM, Behdani M, Zareinejad MR, Shahbazzadeh D. Development of a human scFv antibody targeting the lethal Iranian cobra (Naja oxiana) snake venom. Toxicon. 2019 171:78-85. DOI:10.1016/j.toxicon.2019.10.00.

10. Gopalkrishnaknoe, P., Chou ML. (1990) snakes of medical importance (Asia-Pacific Region). Singapore: National University of Singapore.

11. de Silva HA, Ryan NM, de Silva HJ. Adverse reactions to snake antivenom, and their prevention and treatment. Brit J Clin Pharm. 2016 81(3):446-452. DOI:10.1111/bcp.12739.

12. Gutiérrez JM, Calvete JJ, Habib AG, Harrison RA, Williams DJ, Warrell DA. Snakebite envenoming. Nat Rev Dis Primers. 2017 3(1): 1-21. DOI:10.1038/nrdp.2017.63.

13. Pucca MB, Cerni FA, Janke R, Bermúdez-Méndez E, Ledsgaard L, Barbosa JE, Laustsen AH. History of envenoming therapy and current perspectives. Front. Immunol. 2019 10(10):1598. DOI:10.3389/fimmu.2019.01598.

14. Soares AM, Ticli FK, Marcussi S, Lourenço MV, Januário AH, Sampaio SV, Giglio JR, Lomonte B, Pereira PS. Medicinal plants with inhibitory properties against snake venoms. Curr Med Chem. 2005;12(22):2625-41. DOI:10.2174/092986705774370655.

15. Félix-Silva J, Silva-Junior AA, Zucolotto SM, Fernandes-Pedrosa MF. Medicinal plants for the treatment of local tissue damage induced by snake venoms: An overview from traditional use to pharmacological evidence. Evid Based Complement Alternat Med. 2017; 5748256. DOI:10.1155/2017/5748256.

16. Dey A, De JN. Traditional use of plants against snakebite in Indian subcontinent: a review of the recent literature. Afr J Tradit Complement Altern Med. 2011;9(1):153-74. DOI:10.4314%2Fajtcam.v9i1.20.

17. Lizano S, Domont G, Perales J. Natural phospholipase A2

myotoxin inhibitor proteins from snakes, mammals and plants. Toxicon. 2003; 42:963–77.

18. Shirwaikar A, Rajendran K, Bodla R, Kumar CD. Neutralization potential of Viper russelli russelli (Russell's viper) venom by ethanol leaf extract of Acalypha indica. J Ethnopharmacol. 2004; 94 (23): 267-73. DOI: 10.1016/j.jep.2004.05.010. PMID: 15325729.

19. Niroumand MC, Farzaei MH, Amin GH. Medicinal properties of Peganum harmala L. in traditional Iranian medicine and modern phytotherapy: a review. J. Tradit Chin Med. 2015 ;35(1): 104–109, DOI:10.1016/S0254-6272(15)30016-9.

20. Moloudizargari M, Mikaili P, Aghajanshakeri Sh, Asghari MH, Shayegh J. Pharmacological and therapeutic effects of Peganum harmala and its main alkaloids. Pharmacogn Rev 2013; 7(14): 199-212. DOI:10.4103%2F0973-7847.120524.

21. Bahmani M, Rafieian-kopaei M, Parsaei P, Mohsenzade- gan A. The anti-leech effect of Peganum harmala L. extract and some anti-parasite drugs on Limnatis nilotica. Afr J Microbiol Res. 2012; 6(10): 2586-2590. DOI:10.5897/AJMR12.201.

22. Aghili MH. Makhzan-al-Advia (Persian). Tehran: Tehran University of Medical Sciences. 2009; 328.

23. Lamchouri F, Settaf A, Cherrah Y, et al. Antitumour principles from Peganum harmala seeds. Therapie. 1999; 54(6): 753–758.

24. Farouk L, Laroubi A, Aboufatima R, Benharref A, Chait A. "Evaluation of the analgesic effect of alkaloid extract of Peganum harmala L.: possible mechanisms involved". J Ethnopharmacol. 2008; 115 (3): 449–54.

25. Asgarpanah J, Ramezanloo F. Chemistry, pharmacology and medicinal properties of Peganum harmala L. African Journal of Pharmacy and Pharmacology. 2012; 6 (22).

26. Grishin EV, Sukhikh AP, Adamovich TB, Ovchinnikov YuA. The isolation and sequence determination of a cytotoxin from the venom of the middle-asian cobra Naja naja oxiana. FEBES. 1974; 48: 179-83.

27. Mikhailov AM, Nickitenko AV, Trakhanov SD, Vainshtein BK, Chetverina EV. Crystallization and preliminary x-ray diffraction study of neurotoxin-I from Naja naja oxiana venom. FEBS. 1990; 269(1): 255-57.

28. Nickitenko AV, Michailov AM, Betzel Ch, Wilson KS. Three-dimentional structure of neurotoxin-1 from Naja naja oxiana venom at 1.9 A resolution. FEBS. 1993; 320: 111-17.

29. Mahmoudian M, Jalipour H, Dardashti PS. Toxicity of Peganum harmala: Review and a case report. Iranian Journal of Pharmacology and Therapeutics. 2002; 1:1-4.

30. Lamchouri F, Settaf A, Cherrah Y, El Hamidi M, Tligui N, Lyoussi B, et al. Experimental toxicity of Peganum harmala seeds. Annales Pharmaceutiques Françaises. 2002;60:123-29.

31. Rachid D. Intoxication by Harmel [Internet]. Medical Toxicology. Intech Open; 2021. Available from: http://dx.doi.org/10.5772/intechopen.92936.

32. Tahri N, Rhalem R, Soulaymani A, Achour S, Rhalem N, Khattabi A. Peganum harmala L. poisoning in Morocco: About 200 cases. Thérapie. 2011; 67(1):53-58.

33. El Bahri L, Chemli R. Peganum harmala L. A poisonous plant of North Africa. Veterinary and Human Toxicology. 1991; 33:276-277.

34. Aarons DH, Victor Rossi G, Orzechowski RF. Cardiovascular actions of three harmala alkaloids: Harmine, harmaline, and harmalol. Journal of Pharmaceutical Sciences. 1977 ;66(9):1244-1248.

35. Abdel-Fattah AFM, Matsumoto K, Murakami Y. Central serotonin level-dependent changes in body temperature following administration of tryptophan to pargyline- and harmaline- pretreated rats. Gen Pharmacol 1997; 28: 405-409.

36. Mirzaie M, Nosratabadi SJ, Derakhshanfar A, Sharifi I. Antileishmanial activity of Peganum harmala extract on the in vitro growth of Leishmania major promastigotes in comparison to a trivalent antimony drug. Veterinarski Arhiv. 2007; 77(4): 365-375.

37. Karasawa MMG, Mohan C. Fruits as prospective reserves of bioactive compounds: A Review. Nat Prod Bioprospect. 2018 ;8(5):335-346. DOI:10.1007/s13659-018-0186-6.

38. Sharifi-Rad J, Quispe C, Herrera-Bravo J, Semwal P, Painuli S, Özçelik B et al. Peganum spp. A Comprehensive Review on Bioactivities and Health-Enhancing Effects and Their Potential for the Formulation of Functional Foods and Pharmaceutical Drugs. Oxid Med Cell Longev. 2021; 27;5900422. DOI:10.1155/2021/5900422.

39. Berlowitz I, Egger K, Cumming P. Monoamine Oxidase Inhibition by Plant-Derived β-Carbolines; Implications for the Psychopharmacology of Tobacco and Ayahuasca. Front. Pharmacol. 2022; 13:886408. DOI:10.3389/fphar.2022.886408.

40. Tahri N, Rhalem R, Soulaymani A, Achour S, Rhalem N, Khattabi A. Peganum harmala L. poisoning in Morocco: About 200 cases. Thérapie. 2011;67(1):53-58.

Online supplemental material

[Describe available supplemental material here, including brief legends for these materials, if applicable, for example Figure S1., Movie M1, …]

How to cite this article
Fathi B. Investigation the Effects of hydroalcoholic extract of *Peganum harmala* Against the Venom of the Iranian Snake *Naja naja oxiana* in Mice . Iran J Vet Sci Technol.2024; 16(1): 52-59.
DOI: https://doi.org/10.22067/ijvst.2024.84426.1300
URL: https://ijvst.um.ac.ir/article_44882.html

Iranian Journal of Veterinary Science and Technology

Received: 2023- Aug- 09
Accepted after revision: 2023-Dec- 06
Published online: 2024- Feb-01

CASE REPORT

DOI: 10.22067/ijvst.2023.83244.1276

Large colon volvulus due to meconium impaction in a neonatal foal: a case report

Omid Azari [a], Seyed mahdi Ghamsari [a], Ali Roustaei [a], Omid Koohestani [b], Ahad Hassani [c]

[a] Department of Surgery and Radiology, Faculty of Veterinary Medicine, University of Tehran, Tehran, Iran.
[b] Student of Veterinary Medicine, Faculty of Veterinary Medicine, University of Tehran, Tehran, Iran.
[c] Doctor of Veterinary Medicine, Equine Practitioner in Tehran Province, Tehran, Iran .

ABSTRACT

A 36 hours old foal was presented with abdominal pain and undefication that did not respond to medical treatment. Physical examination revealed marked abdominal distension, mild tachycardia, tachypnea and high rectal temperature. Radiographic and ultrasonographic investigations confirmed the meconium impaction and large colon involvement. The case was recommended for urgent exploratory celiotomy. Close observation during surgery showed distention of small and large intestine and 360° volvulus of left colon associated with meconium impaction in small colon. After decompression and correction of large colon, impacted meconium was removed from the lumen via small colon enterotomy. The foal was recovered uneventfully and did not show any complication during 2 weeks follow up. This report suggested failure to pass meconium can cause other gastrointestinal disorders in neonatal foals.

Keywords

Neonate foal, Meconium impaction, Colon volvulus, Colic pain

Number of Figures: 2
Number of Tables: 0
Number of References:: 20
Number of Pages: 7

Abbreviations

LCV: large colon volvulus

Corresponding author: *Omid Azari*
Email: : *Omid.azari@ut.ac.ir*
Tel: *+98(91)2318-5781*

Introduction

Colic is a prevalent condition in equine neonates, which is a significant concern due to vast differential diagnosis possibilities, management difficulty, and non-pathognomonic clinical signs[1]. Abdominal pain may be caused by gastrointestinal origin (e.g., impactions, gastric ulcer) or extra-gastrointestinal one (e.g., mesenteric abscess, ovarian tumor) [2]. Studies revealed that most foals' gastrointestinal colic can be solved medically and will not require surgery[3]. Concurrent disorders, nonspecific clinical signs, and potential post-surgery medical problems, along with decreasing survival rate over time since the condition occurred, make the judgment intricate[1,3]. Surgical abdominal pains in foals are mainly associated with the small intestine. Large colon illnesses also include medical (Acute and chronic diarrhea) and surgical (obstruction). Large intestine obstructions are classified into simple, non-strangulating, and strangulating[1,4]. Meconium impaction is the simple and non-strangulating obstruction, and one of the most common causes of colic in equine neonate[5]. Retention of meconium may happen due to delayed ingestion of colostrum, dystocia, prematurity, low birth weight, birth asphyxia, and dehydration[6]. Impaction of meconium often resolved medically, and surgical intervention should be performed in unresponsive cases[6]. Large colon volvulus (LCV) and intussusception are strangulating obstructions, and both are reported rarely in neonate foals[1,4]. Despite the difficulty of making differentiating between surgical and medical therapy, foals with strangulating obstruction must be operated in the minimum time owing to the time-dependent success rate[3,4].

LCV usually begins rapidly and may lead to luminal obstruction and strangulating colic[4]. In this regard, neonates may show respiratory and cardiovascular signs, which can be helpful in diagnosis along with paraclinical evaluations. Generally, colon volvulus in horses with a degree exceeding 270° has a poor prognosis which even becomes lesser through time[7]. Many studies stated the fact that with faster referring and diagnostic processes and, eventually, operation, the survival rate will increase significantly[1,3,7].

In this case report, the clinical sign, diagnostic testing, and surgical findings of a 36 hours old neonate foal with a meconium retention followed by 360° large colon volvulus, will be described.

Case Presentation

A 36 hours old male thoroughbred neonate foal weighing 48 kg, was presented with signs of abdominal pain and failure to pass the meconium to the large animal veterinary hospital, University of Tehran. This case was referred to surgery after failure of medical therapy including enema by a veterinary practitioner. The colt demonstrated diminished appetite and was also letargic. No obvious abnormality had been found in the childbearing and gestation period. At the time of physical examination, the foal was alert and abdominal distension and moderate colic pain was evident. A digital examination of the rectum did not reveal meconium retention. On physical examination, the foal showed tachycardia (135 beats/min) and tachypnea (62 breaths/min), and high rectal temperature (40.2°C). Hematological examination revealed normal in red blood cell count (10.2×1012/L), hemoglobin concentration (125 g/L) and hematocrit (43%). White blood cell count mildly increased (12×109/L) with neutrophilia.

Standing Radiography projection showed marked gaseously distended intestinal loops in caudoventral and middle aspect of abdomen measuring 1.5 to 1.7 times of first lumbar vertebrae with meconium retention in distal colon (Figure 1.A). For further examination, transabdominal ultrasonography was performed when the foal was in the lateral position that revealed gas-fluid distended, hypomotile and circular appearance of large and small intestinal loops with normal wall thickness (Figure 1.B). A multiple hyperechoic immobile well-defined curved surface with dirty distal shadowing artifacts was prominent in the small colon represented the meconium impaction. Free fluid was not noted in the peritoneal or retroperitoneal cavities. Meconium impaction was the primary diagnosis and we did not correlate severe distention of intestinal loops observing in Ultrasonography and radiography with retention of meconium, so based on paraclinical findings, and because the meconium impaction did not respond to medical treatment, an emergency exploratory celiotomy was recommended that accepted by the owner.

Surgical Treatment

Intravenous catheters were placed in an aseptic fashion and sterile isotonic fluid (Sodium Chloride 0.9%, Intravenous Infusion) were given pre and intra-operatively (8mL/kg/h). The foal was pre-medicated with intravenous injection of flunixin meglumine (1.1 mg/kg BW) and Midazolam (0.1 mg/kg BW). Anaesthesia was induced using ketamine (2.2 mg/kg BW, IV) and maintained with isoflurane in medical oxygen on a semi-closed circle system. Then, the foal was positioned in dorsal recumbency and ventral surface of abdomen was prepared for aseptic surgery. A ventral midline incision (15 cm length) was created through the linea alba starting at the umbilicus and extending cranially.

Figure 1.
A: Radiology, Standing radiography of foal abdomen shows marked gaseously distended intestinal loops (arrow) in caudoventral and middle aspect of abdomen. B: sonography, Sonographic imaging shows large intestinal loops (L) are dilated with fluid and gas echogenicity. Wall thickness is normal.

Initial exploration of abdominal cavity revealed marked distention of large colon. Also, mild non-specific small intestinal distension was present presumably due to the secondary ileus. The colon was decompressed of gas using an 18-gauge needle attached to a suction unit. Further exploration confirmed meconium impaction at distal region of small colon, and also 360° volvulus of left colons at the level of the sternal and diaphragmatic flexures (Figure 2). The twisted colon was corrected and the pelvic flexure was replaced in the correct orientation. Clinical evaluation of the colon including serosal colour, pulses in the ventral and dorsal colic arteries and colon motility showed that the tissue was alive. After that, the impaction of meconium was tried to break down by careful trans-luminal massage in combination with a warm water enema, but the attempt was unsuccessful and consequently, the enterotomy incision was performed in small colon and impacted meconium was removed. The enterotomy was closed in interrupted lembert pattern with 2–0 polyglactin 910 (Vicryl). The small intestinal contents were decompressed into the caecum, followed by decompression of both colon and caecum of free gas, using needle and suction unit. The abdominal viscera were copiously lavaged with warm normal saline and ventral midline incision was closed, routinely.

The foal recovered without any problem. Postoperative treatment included intravenous administration of 22000 IU/kg sodium benzylpenicillin QID, 6.6 mg/kg gentamicin SID and 1.1 mg/kg flunixin-meglumine SID, for 3 days. The foal discharged from the hospital, 3 days after the surgery. During two week follow up, the owner declared that the foal defecated normally and had good appetite.

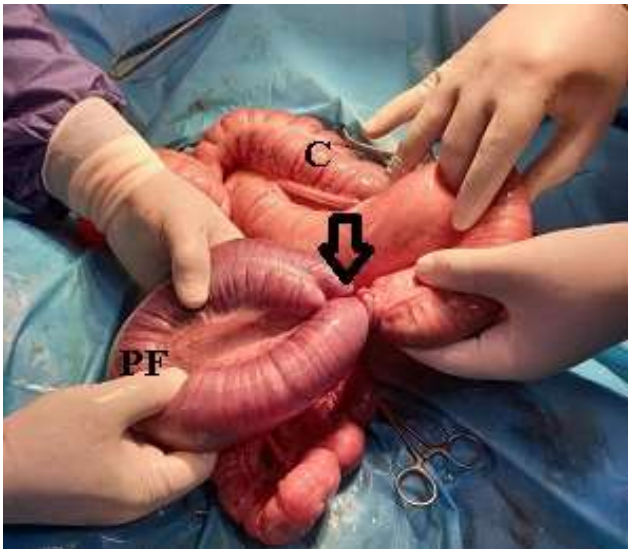

Figure 2.
On laparotomy exploration, a 360 degree volvulus (arrow) was observed in the left colon of neonate foal. PF: Pelvic flexure; C:Cecum

Discussion

This study describes the clinical findings and surgical intervention of volvulus and meconium impaction occurring in 36 hours old foal. The simultaneous occurrence of these disorders is relatively rare in foals.

Among the colic origins, large colon volvulus have been reported rarely in foals[7]. Colon volvulus observed by Abutarbush et al. is the fourth most common cause of colic on presentation of adult hors-

es with an incidence of 7.3%[8]. In adult horses, LCV has an incidence of 10-21% among the surgical colics[9,10]. Large colon volvulus is 1st cause of euthanasia in surgical colics of mature horses. Mair and Smith (2005) revealed that volvulus is an important and killing condition, so initial recognition of this deadly disease is highly advisable [9]. Phillips and Walmsley (1993) reported that 53% of horses with surgical colic had a lesion of the large intestine of which one-third had LCV[11]. Although LCV is a common cause of surgical colic in adult horses, but less commonly reported in foals [12].

Vatistas et al. (1996) reported 5 foals among the 67 surgical colic had LCV[13]. In the study conducted by Adams et al. (1988) including 20 neonatal foals, torsion at the sternal and diaphragmatic flexures was observed in 3 foals[14]. In a review article of 119 abdominal surgery in foals , 5 foals had LCV, of which 4 patients were older than 3 months[15]. LCV was not reported in 137 neonate foals was reviewed in the University of Pennsylvania[3].

There are rare reports of LCV in 3 day-old neonates same as our report that the location of volvulus was the sternal and diaphragmatic flexures [1,12,14] reflecting these flexures may be a main site for LCV in neonatal foals. However, in adult horses, most of the volvulus occurs in cecal base or near the cecocolic fold because the colon region is freely movable in abdominal cavity and has a few attachments to the abdominal wall. Contributing factors for colonic motility is unknown in foals although differences in the morphology and density of myenteric plexuses between foals and adult horses have been reported and could influence colon motility pattern with animal age [1].

In a recent study concurrent large colon volvulus and atresia coli in 18 hours old foal was described and atresia coli result to hypoxia and inflammation may cause of LCV through the colon motility change [12]. A 360° LCV with meconium retention and intestinal incarceration has been described in 36 hours old colt [16]. We speculated that impaction in distal part of colon may cause of ileus and subsequently inflammation and vascular damage result in altered colon motility causing LCV.

Large-breed horses, post foaling, multiple colic episodes, feeding hey and restricted grazing are the risk factors for colonic volvulus in adult horses[12]. These factors are not contributed for the foals, but congenital malformation, undiagnosed colitis, abnormalities of the myenteric plexuses and intrauterine hypoxic injury to the colon put at foals to risk of LCV [1]. In the current patient, congenital malformation of the colon was not observed.

Due to small size of ponies and foals, transrectal palpation of the abdominal organs is out of the mind, and it is suggested that paraclinical examinations such as radiography and transcutaneous abdominal ultrasound be used to make a correct diagnosis. Radiography is a good diagnostic tool for distinguishing lesions of the large and small intestines and had a sensitivity of 96% for detecting gastrointestinal disease in foals and the width of enlarged intestinal loops was measured with the length of the first lumbar vertebral body[17]. In the current patient markedly distention of intestinal loops measuring 1.5 to 1.7 times the L1 body length vertebrae showed obstruction caused by meconium impaction. For further evaluation, ultrasound was done and gaseous/fluid distention of the intestinal loops was noted and we did not speculate the LCV in this patient. Large colon volvulus diagnosis by transabdominal ultrasound in foals associated with difficulties reported by others [12,18]. However, Pease et al (2004) described that ultrasound finding in colon torsion in adult horses, including wall thickening in ventral site ≥9 mm, had a sensitivity of 67 % and a specificity of 100 % with high positive predictive value 100%, and also in another recent study marked large colon wall thickening proposed strangulated large intestine in neonatal foals [1,19]. It is suggested to measure colon wall thickening in colic foals that may support the colon strangulation, although no sign of wall thickening was observed in our ultrasound findings. Meconium impaction as described in the ultrasound of nonmoving sharp-edged particle in this report, close to description of sand impaction in adult horses, however, radiography is the gold standard for diagnosis of sand colic[20].

It is believed that survival rate in LCV surgery in horses depends on serosal colour of affected colon, degree of rotation and some laboratory and cardiopulmonary parameters. In more reports about the LCV in foals, euthanasia is selected for patients as the vascular compromise of colon and serosal colour changes[1], although patient in our study has no sign of discoloration of strangulated colon and survived two weeks follow up.

In conclusion, according to the current case report, distention of colon due to the meconium impaction may increase the risk of colon displacement or volvulus in foals that it urgently needs to surgical intervention.

Authors' Contributions

O.A and S.G performed surgery and manuscript writing. A.R and O.K performed paraclinical examinations, review literature and manuscript draft. A.H performed clinical examination and case follow-up.

Acknowledgments

Many thanks to the technical staff of the large animal hospital of Veterinary Faculty of Tehran University.

Conflict of Interests

The authors declare that there is no conflict of interest.

References

1. du Preez S, Trope GD, Owens C, Hughes KJ. Volvulus of the large colon in a neonatal foal. Equine Vet Educ. 2018;30[6]:306–11. DOI: 10.1111/eve.12730.

2. Nikahval B, Vesal N, Ghane M. Surgical correction of small colon faecalith in a Dare-Shuri foal. Turkish J Vet Anim Sci. 2009;33[4]:357–61. DOI: 10.3906/vet-0802-14.

3. MacKinnon MC, Southwood LL, Burke MJ, Palmer JE. Colic in equine neonates: 137 cases [2000–2010]. J Am Vet Med Assoc. 2013;243[11]:1586–95. DOI: 10.2460/javma.243.11.1586.

4. Constable PD, Hinchcliff KW, Done SH, Grünberg WBT-VM [Eleventh E, editors. 8 - Diseases of the Alimentary Tract–Ruminant. In W.B. Saunders; 2017. p. 436–621. Available from: https://www.sciencedirect.com/science/article/pii/B9780702052460000085.

5. Prange T. Small colon obstructions in foals. Equine Vet Educ. 2013;25[6]:293–6. doi: 10.1111/eve.12040.

6. Auer JA, Stick JA. Equine surgery-E-book. Elsevier Health Sciences; 2018.

7. Jones SL, Fecteau G, Hullinger PJ, Bickett-Weddle DA, St. Jean G, Nichols S, et al. • Chapter 32 - Diseases of the Alimentary Tract. In: Smith BP, Van Metre DC, Pusterla NBT-LAIM [Sixth E, editors. St. Louis [MO]: Mosby; 2020. p. 702-920.e35. Available from: https://www.sciencedirect.com/science/article/pii/B978032355445900032X.

8. Abutarbush SM, Carmalt JL, Shoemaker RW. Causes of gastrointestinal colic in horses in western Canada: 604 cases [1992 to 2002]. Can Vet J. 2005;46[9]:800.

9. Mair TS, Smith LJ. Survival and complication rates in 300 horses undergoing surgical treatment of colic. Part 1: Short-term survival following a single laparotomy. Equine Vet J. 2005 Jul;37[4]:296–302. DOI: 10.2746/0425164054529409.

10. Gonzalez LM, Fogle CA, Baker WT, Hughes FE, Law JM, Motsinger-Reif AA, et al. Operative factors associated with short-term outcome in horses with large colon volvulus: 47 cases from 2006 to 2013. Equine Vet J. 2015;47[3]:279–84. DOI: 10.1111/evj.12273.

11. Phillips TJ, Walmsley JP. Retrospective analysis of the results of 151 exploratory laparotomies in horses with gastrointestinal disease. Equine Vet J. 1993;25[5]:427–31. DOI: 10.1111/j.2042-3306.1993.tb02985.x.

12. McGovern KF, Gough RL. Large Colon Volvulus in a Neonatal Foal Secondary to Atresia Coli. J Equine Vet Sci. 2022;119:104114. DOI: 10.1016/j.jevs.2022.104114.

13. Vatistas NJ, Snyder JR, Wilson WD, Drake C, Hildebrand S. Surgical treatment for colic in the foal [67 cases]: 1980-1992. Equine Vet J. 1996 Mar;28[2]:139–45. doi: 10.1111/j.2042-3306.1996.tb01606.x.

14. Adams R, Koterba AM, Brown MP, Cudd TC, Baker WA. Exploratory celiotomy for gastrointestinal disease in neonatal foals: a review of 20 cases. Equine Vet J. 1988 Jan;20[1]:9–12. DOI: 10.1111/j.2042-3306.1988.tb01442.x.

15. Cable CS, Fubini SL, Erb HN, Hakes JE. Abdominal surgery in foals: a review of 119 cases [1977-1994]. Equine Vet J. 1997 Jul;29[4]:257–61. DOI :10.1111/j.2042-3306.1997.tb03120.x.

16. Lillich JD, Goggin JM, Valentino LW, Flaminio M, Rush BR. Volvulus of the large colon in a foal. Equine Vet Educ. 2000;12[1]:18–9. DOI: 10.1111/j.2042-3292.2000.tb01757.x

17. Fischer Jr AT, Kerr LY, O'Brien TR. Radiographic diagnosis of gastrointestinal disorders in the foal. Vet Radiol. 1987;28[2]:42–8. DOI: 10.1111/j.1740-8261.1987.tb01722.x

18. McAuliffe SB. Abdominal ultrasonography of the foal. Clin Tech Equine Pract. 2004;3[3]:308–16. DOI: 10.1053/j.ctep.2005.02.008.

19. Pease AP, Scrivani P V, Erb HN, Cook VL. Accuracy of increased large-intestine wall thickness during ultrasonography for diagnosing large-colon torsion in 42 horses. Vet Radiol Ultrasound. 2004;45[3]:220–4. DOI: 10.1111/j.1740-8261.2004.04038.x.

20. Korolainen R, Ruohoniemi M. Reliability of ultrasonography compared to radiography in revealing intestinal sand accumulations in horses. Equine Vet J. 2002;34[5]:499–504. DOI: 10.2746/042516402776117764.

How to cite this article
Azari O, Ghamsari SM, Roustaei A, Koohestani O, Hassani A. Large colon volvulus due to meconium impaction in a neonatal foal: a case report. Iran J Vet Sci Technol.2024; 16(1): 60-65.
DOI: https://doi.org/10.22067/ijvst.2023.83244.1276
URLhttps://ijvst.um.ac.ir/article_44563.html

Iranian Journal of Veterinary Science and Technology

Received: 2023- Jun- 10
Accepted after revision: 2024- Jan-10
Published online: 2024- Feb-01

Abstracts (in Persian)

علل حذف لاشه های طیور کشتاری در کشتارگاه های صنعتی نمین، استان اردبیل، ایران

آیدین عزیزپور*[1]، زهرا امیرعجم[2]

۱گروه گیاهان دارویی، دانشکده کشاورزی مشگین شهر، دانشگاه محقق اردبیلی، اردبیل، ایران.
۲ گروه قلب، دانشکده پزشکی، دانشگاه علوم پزشکی اردبیل، اردبیل، ایران.

چکیده

تولید گوشت طیور در سراسر جهان طی دو دهه گذشته در حال گسترش است. در این راستا، بازرسی بهداشتی گوشت و پایش بیماری ها در خط کشتار به عنوان یکی از راه های ارزیابی وضعیت گله‌ها شناخته شده است. هدف از این مطالعه تعیین میزان و علل اصلی حذف طیور کشتار شده و محاسبه خسارت اقتصادی ناشی از حذفیات لاشه در کشتارگاه صنعتی نمین، استان اردبیل بود. داده ها توسط بازرس دامپزشکی در کشتارگاه جمع آوری شد. تعداد طیور کشتار شده و وزن آنها و تعداد و وزن لاشه های حذفی و همچنین دلایل مختلف ضبط لاشه ها ثبت شد. در این بررسی، ۳۴۸۸۹۱۶ قطعه طیور کشتار شد و ۴۲۳۱۰ لاشه (۱.۲۰۲ درصد) با وزن ۶۶۳۸۵ کیلوگرم ضبط گردید. بیشترین درصد لاشه های ضبطی در پاییز (۱/۶۱ درصد) و کمترین آن در بهار (۰.۹۳ درصد) مشاهده شد. خسارت اقتصادی مستقیم ناشی از حذف لاشه ها تا ۱۵۳۰۶۷ دلار برآورد شد. سپتی سمی و تلفات قبل کشتار (DOA) شایع‌ترین علل حذف لاشه ها بودند که به ترتیب ۴۷/۵۸ درصد و ۰.۵۸۰ از کل لاشه های ضبطی و کل کشتار را شامل شدند. بیشترین درصد فراوانی لاشه های ضبطی ناشی از بیماری ها در پاییز اتفاق بود. در حالی که تابستان بیشترین میزان حذف را در ارتباط با DOA داشت. نتایج بررسی حاضر نشان داد که بیشترین ضبط لاشه ها مربوط به بیماری ها در مقایسه با سایر علل می باشد. بنابراین، بهبود برنامه های کنترل بیماری ها در گله ها و افزایش رفاه پرندگان قبل از کشتار توصیه می شود.

واژگان کلیدی

لاشه حذفی، سپتی سمی، تلفات قبل کشتار، نمین

* نویسنده مسئول: آیدین عزیزپور
Aidin_azizpour@uma.ac.ir

Iranian Journal of Veterinary Science and Technology

Abstracts (in Persian)

Received: 2023- Oct- 01
Accepted after revision: 2023- Dec-06
Published online: 2024- Feb-01

تغییرات تظاهرات بالینی لیشمانیوز جلدی در ظرفیت های مختلف آنتی اکسیدانی تام: یک مطالعه حیوانی با استفاده از موش BALB/c

مجتبی یوسفی[1]، سید مسعود ذوالحواریه[2]*، علیرضا نوریان[1]، حسین رضوان[1]، علی صادقی نسب[2]

[1] گروه پاتوبیولوژی، دانشکده دامپزشکی، دانشگاه بوعلی سینا، همدان، ایران.
[2] گروه علوم درمانگاهی، دانشکده دامپزشکی، دانشگاه بوعلی سینا، همدان، ایران.

چکیده

شدت تظاهرات بالینی لیشمانیوز جلدی بسته به عواملی مانند گونه لیشمانیای درگیر، گونه میزبان و پاسخ ایمنی آنها می تواند متفاوت باشد. این مطالعه با هدف بررسی رابطه بین شدت علائم بالینی مختلف، تغییرات هیستوپاتولوژیک و شاخص های ژنتیکی با ظرفیت آنتی اکسیدانی تام در موش های آزمایشگاهی آلوده به لیشمانیا ماژور انجام شد. تعداد ۱۰۵ سر موش BALB/c هشت هفته‌ای از هر دو جنس در ۷ گروه آزمایشی (۱۵ سر در هر گروه) به شرح زیر قرار گرفتند: ۱) موش سالم، ۲) موش آلوده به لیشمانیا و تحت درمان با ۱۰۰ SC GlucantimeTM ، mg/kg/day تا بهبودی کامل، ۳) موش ها به مدت ۱۰ روز قبل از عفونت برای افزایش ظرفیت آنتی اکسیدانی تام، ویتامین Eبا دوزاژ 20 SC ، IU/kg/day دریافت کردند وپس از عفونت با گلوکانتیم درمان شدند، ۴) موش های آلوده به لیشمانیا ویتامین E و گلوکانتیم را روزانه تا بهبودی کامل را دریافت کردند، ۵) موشها ویتامین E ، به مدت ۱۰ روز، قبل از عفونت دریافت کردند و ۶) موش های آلوده به لیشمانیا، ویتامین E، تا پایان آزمایش دریافت کردند و ۷) موش ها روزانه ویتامین E را تا پایان آزمایش دریافت کردند. ارزیابی اندازه زخم، بیان ژن های پیش التهابی (IFN-γ و EGF) و بهبود (KGF و TNF-α) و یافته های هیستوپاتولوژیک و میزان مرگ و میر، سه بار در روزهای ۳۱، ۳۸ و ۷۲ پس از عفونت انجام شد. تقریباً ۳۱ روز پس از تلقیح انگل، ضایعات پوستی در تمام موش‌های آلوده، ایجاد شد. در گروه ۳ ، تظاهرات بالینی، زمان بهبودی و تغییرات هیستوپاتولوژیک به طور معنی داری مطلوب تر بود، در حالی که گروه ۴ از نظر شاخص های ارزیابی شده بدترین وضعیت را نشان داد. در حالی که سطح بالای ظرفیت آنتی اکسیدانی تام قبل از شروع بیماری نقش موثری در شاخص های بهبودی دارد، افزایش همزمان آن در ابتدای عفونت باعث کاهش توانایی بدن در پاکسازی موثر انگل، التیام بافت شده، موجب بدتر شدن تظاهرات بالینی بیماری می شود.

واژگان کلیدی

TNF-α و IFN-γ ،تظاهرات بالینی، لیشمانیا، لیشمانیوز جلدی، ظرفیت آنتی اکسیدانی

* نویسنده مسئول: سید مسعود ذوالحواریه
mzolhavarieh@basu.ac.ir

Iranian Journal of Veterinary Science and Technology
Abstracts (in Persian)

Received: 2023- Nov-05
Accepted after revision: 2024- Jan-24
Published online: 2024- Feb-01

بیان پروتئین نوترکیب P24 ویروس Borna برای توسعه روش الایزا

سیده نرجس سادات[1]، سحر خالوندا[1]، بهزاد رمضانی[2]، مهدی حبیبی انبوهی[3]، فاطمه کاظمی لمعه دشت[1]، هاجر سادات قادری[1]، مهدی بهدانی[1,4]

۱ مرکز تحقیقات بیوتکنولوژی، آزمایشگاه ونوم و مولکول های درمانی، انستیتو پاستور ایران، تهران، ایران.
۲ شرکت زیست فناوری کوثر، تهران، ایران.
۳ بانک سلولی ایران، انستیتو پاستور ایران، تهران، ایران.
۴ مرکز تحقیقات زئونوز، انستیتو پاستور، آمل، ایران.

چکیده

ویروس بیماری برنا (BDV) یک ویروس RNA نوروتروپیک، پوشش دار و رشته منفی است. این ویروس باعث بیماری سیستم عصبی مرکزی در طیف وسیعی از گونه‌های مهره‌دار و انسان می‌شود. ژنوم ۶BDV پروتئین را کد می کند، اما ژن پروتئین p24 با نرخ بالاتری نسبت به سایر پروتئین ها در بافت های آلوده به BDV شناسایی شده است. در این مطالعه، پروتئین BDV-p24 سنتز شده و در پلاسمید بیانی pET22 ساب کلون شد. بیان پروتئین نوترکیب با الکتروفورز ژل سدیم دودسیل سولفات-پلی آکریل آمید و وسترن بلات تایید شد. پروتئین P24 برای تولید آنتی بادی پلی کلونال و ایمن سازی به خرگوش تزریق شد. الایزا در مقایسه با سایر روش های تشخیصی روشی سریع، مقرون به صرفه با حساسیت بالا و همچنین احتمال آلودگی کمتری دارد. روش الایزا برای بررسی عفونت در خرگوش های آزمایشگاهی و عفونت گذشته نگر در ۵۰ خرگوش ازمایشگاهی مورد بررسی قرار گرفت. نتایج مطالعه ما نشان داد که روش الایزا مبتنی بر پروتئین p24 پتانسیل بالایی برای تشخیص عفونت BDV دارد.

واژگان کلیدی

ویروس بیماری برنا، الایزا، آنتی بادی پلی کلونال، پروتئین Borna-P2

* نویسنده مسئول: مهدی بهدانی
Behdani@pasteur.ac.ir

Iranian Journal of Veterinary Science and Technology

Received: 2023-May-29
Accepted after revision: 2024-Feb-04
Published online: 2024- Feb-04

Abstracts (in Persian)

ویژگی‌های رادیولوژیک و آناتومیک استخوان‌های جمجه در سگ‌های بالغ نژاد هاسکی

سامان آهنی [۱]، سیامک علیزاده [۲]، محمدرضا حسینچی [۳]

[۱] دانش آموخته دکترای دامپزشکی، واحد کرج، دانشگاه آزاد اسلامی، کرج، ایران.
[۲] گروه علوم درمانگاهی، واحد نقده، دانشگاه آزاد اسلامی، نقده، ایران.
[۳] گروه علوم پایه، واحد ارومیه، دانشگاه آزاد اسلامی، ارومیه، ایران.

چکیده

با توجه به نقش استخوان‌های جمجه در محافظت از اندام‌های حیاتی بدن، معاینه دقیق این استخوان‌ها در شرایط مختلفی مانند آسیب‌های ناحیه سر ضروری می‌باشد. حال آنکه با توجه به تنوع نژادی میان سگ‌ها، انجام این معاینه نیازمند اطلاعات کاملی از ویژگی‌های اختصاصی جمجمه در نژاد مورد نظر می‌باشد. هدف از انجام این پژوهش بررسی دقیق و شناسایی ویژگی‌های رادیولوژیک و آناتومیک استخوان‌های جمجه در سگ‌های هاسکی بالغ بود. در مطالعه توصیفی-گذشته‌نگر حاضر از هشت سگ بالغ نژاد هاسکی (چهار نر و چهار ماده) - که به دلایلی غیر از آسیب‌های ناحیه سر تلف شده بودند - استفاده شد. بعد از آماده‌سازی جمجمه، از نماهای مختلف این ساختار رادیوگراف تهیه شد. همچنین جهت بررسی آناتومیک، جمجمه‌ها از نظر ریخت‌شناسی مورد بررسی قرار گرفتند. در ادامه اندازه‌های مرفومتریک استخوان‌ها بدست آمد و نتایج حاصله ثبت و بررسی شد.

جمجه سگ‌های هاسکی بالغ از ۱۱ استخوان جمجمه‌ای و ۲۱ استخوان صورتی تشکیل شده بود. مقادیر سه پارامتر طول و عرض تیمپانیک بولا و اندیس استخوان اربیتال در جنس ماده نسبت به جنس نر بیشتر بود درحالیکه مقایسه این مقادیر اختلاف معناداری را نشان نداد. سایر پارامترهای بررسی شده در جنس نر دارای مقادیر بالاتری نسبت به جنس ماده بود. اختلاف دو پارامتر طول و عرض جمجه در دو جنس معنادار گزارش شد ($P \leq 0.05$).

یافته‌های بدست آمده در مطالعه حاضر می‌تواند به عنوان استاندارد برای معاینه جمجمه سگ‌های هاسکی بالغ مورد استفاده قرار گیرد و در تشخیص و مقایسه نمونه‌های سالم و بیمار به کار رود.

واژگان کلیدی

رادیولوژی، آناتومی، سگ، هاسکی، جمجمه

* نویسنده مسئول: سیامک علیزاده
Si.alizadeh@iau.ac.ir

Iranian Journal of Veterinary Science and Technology

Abstracts (in Persian)

Received: 2023- Aig-01
Accepted after revision: 2023- Dec-31
Published online: 2024- Feb-01

تعیین هویت مولکولی مایکوباکتریوم اویوم زیرگونه پاراتوبرکلوزیس جدا شده از نمونه‌های الایزا مثبت توسط Nested-PCR

مهسا سلیمانی [۱]، علیرضا شهرجردی *[۲]، میترا صالحی [۱]

۱گروه میکروبیولوژی، دانشکده علوم زیستی، واحد تهران شمال، دانشگاه آزاد اسلامی، تهران، ایران.
۲ مؤسسه ملی مهندسی ژنتیک و بیوتکنولوژی، تهران، ایران.

چکیده

پاراتوبرکلوزیس (بیماری یون) بیماری مزمن گرانولوماتوزی روده باریک توسط مایکوباکتریوم اویوم تحت گونه پاراتوبرکولوزیس (MAP) ایجاد می‌شود. در کنترل بیماری، مهم‌ترین اقدام تشخیص و جداسازی حیوانات آلوده می‌باشد. لذا هدف این بررسی، شناسایی مولکولی مایکوباکتریوم جدا شده از گاوهای الایزا مثبت بیماری یون از نمونه‌های ارسالی استان مرکزی به روش Nested-PCR بود. ۳۵۰ نمونه ارسالی پس از آلودگی‌زدایی بر روی محیط کشت هرالداگ حاوی مایکوباکتین و بدون مایکوباکتین کشت داده شدند. پس از استخراج DNA،PCR-*16S rRNA* و سپس از نمونه‌های مثبت Nested-PCR انجام شد. از تعداد ۳۵۰ نمونه، تعداد ۸۷ نمونه مثبت و ۲۶ نمونه مشکوک بدست آمد. در گسترش میکروسکوپی همه جدایه‌های مثبت در رنگ‌آمیزی زیل-نلسون باسیل مشاهده گردید. در ۲۶ نمونه مورد آزمایش و همچنین از سویه‌های مایکوباکتریایی در PCR-*16S rRNA*، باندی به اندازه ۵۴۳ جفتباز مشاهده شد که نشان‌دهنده حضور مایکوباکتریوم در نمونه‌های فوق بود. Nested-PCR برای تمامی جدایه‌ها و سویه‌های کنترل مثبت و منفی انجام پذیرفت که در مرحله اول باند ۳۹۸ جفت‌باز و در مرحله دوم قطعه‌ای به طول ۲۹۸ جفت‌باز حاصل گردید که نشان‌دهنده وجود MAP در نمونه‌ها بود. براساس این مطالعه Nested-PCR به عنوان روش مناسب تشخیص سریع و قطعی موارد بیماری پیشنهاد می‌گردد.

واژگان کلیدی

Nested-PCR، PCR-*16S rRNA*،مایکوباکتریوم اویوم، بیماری یون

* نویسنده مسئول: علیرضا شهرجردی
drshahrjerdi@rvsri.ac.ir

Iranian Journal of Veterinary Science and Technology

Abstracts (in Persian)

Received: 2023- Sep-13
Accepted after revision: 2024- Feb-04
Published online: 2024- Feb-04

بررسی اثرات عصاره هیدروالکلی اسپند در مقابل زهرمارکبرای ایرانی "ناجا ناجا اکسیانا" در موش سوری

بهروز فتحی

گروه علوم پایه، دانشکده دامپزشکی، دانشگاه فردوسی مشهد، مشهد، ایران.

چکیده

اسپند حاوی ترکیبات فعال دارویی است و در طول سال ها برای اهداف مختلف مورد استفاده قرار گرفته است. این مطالعه با هدف ارزیابی اثرات این گیاه در برابر تأثیر کشنده زهر مار کبرای ایرانی انجام شد. در این مطالعه از ۵ پروتکل و ۵۶ موش آلبینو بالغ در۸ گروه مساوی شامل A ، B1، B2، C، D، E و F استفاده گردید. در پروتکل I گروه A (کنترل) تنها ۴ mg/kg زهر، و گروههای B1 و B2 عصاره اسپند را به ترتیب با دوز ۱۵mg/kg و ۳۰ دریافت کردند. در پروتکل II، گروه C به طور همزمان۱۵ mg/kgعصاره را به همراه ۴ mg/kg زهر دریافت کرد. در پروتکل III، به گروه D ابتدا ۴ mg/kg زهر و پس از ۲۰ دقیقه ۱۵ mg/kg عصاره تزریق شد. در پروتکل IV، به گروه E عصاره اسپند و زهر که به مدت ۲۰ دقیقه با هم انکوبه شده بودند با دوزهای قبلی تزریق شد. در پروتکل V، گروهF ابتدا ۳۰ mg/kg عصاره اسپند به صورت خوراکی و ۶۰ دقیقه بعد، زهر با دوز ۴ mg/kg تزریق شد. تزریقات به روش داخل صفاقی انجام شد. میانگین زمان مرگ پس از تزریق زهر ۵ ± ۳۱ دقیقه بود. گروه B1 و B2 زنده ماندند، در حالی که گروه C پس از ۷ ± ۲۹ دقیقه، گروه D پس از ۴ ± ۱۸ دقیقه، گروه E ، پس از ۵ ± ۱۷ دقیقه و گروه F پس از ۳ ± ۲۲ دقیقه تلف شدند. در نتیجه، اسپند در برابر زهرمار کبرای ایرانی نه تنها قدرت حفاظتی ندارد بلکه اثر کشنده آن را به روشی ناشناخته تسریع می کند.

واژگان کلیدی

مارگزیدگی، اسپند، مارکبرای ایرانی، زهر، هم افزایی

* نویسنده مسئول: بهروز فتحی
b-fathi@um.ac.ir

Iranian Journal of Veterinary Science and Technology

Received: 2023- Aug-09
Accepted after revision: 2023- Dec-06
Published online: 2024- Feb-01

Abstracts (in Persian)

چرخش کولون متعاقب انباشتگی مکونیوم در یک کره نوزاد: گزارش موردی

امید آذری*[۱]، سید مهدی قمصری[۱]، علی روستایی[۱]، امید کوهستانی[۲]، احد حسنی[۳]

۱گروه جراحی و رادیولوژی، دانشکده دامپزشکی، دانشگاه تهران، تهران، ایران.
۲ دانش آموخته دکترای حرفه ای، دانشکده دامپزشکی، دانشگاه تهران، تهران، ایران.
۳ دکترای حرفه ای دامپزشکی، دامپزشک طب اسب، استان تهران، تهران، ایران.

چکیده

یک کره اسب، ۳۶ ساعت پس از تولد با علائم اولیه درد شکمی و عدم توانایی دفع که به درمان پاسخ نمی داد؛ به بیمارستان ارجاع گردید. در طی معاینه اتساع شکم، افزایش خفیف ضربان قلب، افزایش سرعت تنفس و دمای بالای رکتوم مشخص شد. بررسی های رادیوگرافی و اولتراسونوگرافی انباشتگی مدفوع و درگیری روده بزرگ را تایید کرد. سپس سلیوتومی اکتشافی به شکل اورژانسی با رهیافت خط وسط صورت گرفت. مشاهدات اولیه در طی عمل اتساع کولون کوچک و بزرگ و همچنین سکوم را نشان داد. در طی بررسی چرخش ۳۶۰ درجه کولون چپ که همراه با انباشتگی مدفوع در کولون کوچک بود کاملا آشکار شد. بعد از اصلاح وضعیت آناتومی، از طریق انتروتومی در کولون کوچک مدفوع انباشته شده، خارج گردید. کره اسب طی دو هفته بعد از جراحی تحت نظر قرار گرفت ودر طول این مدت هیچگونه عارضه ای را نشان نداد. این مطالعه نشان می دهد که عدم توانایی در دفع مدفوع می تواند باعث بروز مشکلات گوارشی متعدد ثانویه گردد.

واژگان کلیدی

کره نوزاد، انباشتگی مکونیوم، چرخش کولون، کولیک

* نویسنده مسئول:امید آذری
omid.azari@ut.ac.ir

Author Index

Guide for authors

SCOPE

Iranian journal of Veterinary Science and Technology (IJVST) publishes important research advances in veterinary medicine and subject areas relevant to veterinary medicine including anatomy, physiology, pharmacology, bacteriology, biochemistry, biotechnology, food hygiene, public health, immunology, molecular biology, parasitology, pathology, virology, large and small animal medicine, poultry diseases, diseases of equine species, and aquaculture. Articles can comprise research findings in basic sciences, as well as applied veterinary findings and experimental studies and their impact on diagnosis, treatment, and prevention of diseases. IJVST publishes four kinds of manuscripts: Research Article, Review Article, Short Communication, and Case Report.

Guide for Authors

GENERAL GUIDELINES

1. Submitted manuscripts should not be previously published elsewhere and should not be under consideration by any other journal.
2. The corresponding author should provide all co-authors with information regarding the manuscript, and obtain their approval before submitting any revisions.
3. The submitted manuscript should be accompanied by a written statement signed by the corresponding author on behalf of all the authors that its publication has been approved by all co-authors, stating that the whole manuscript or a part of it has not been published.
4. Ethics: Authors must state that the protocol for the research project has been approved by the Ethics Committee of the institution within which the work was undertaken. Authors are responsible for animal welfare and all statements made in their work.

OPEN ACCESS POLICY

Iranian Journal of Veterinary Science and Technology is a fully Open Access journal in which all the articles are available Open Access. There is no cost to the reader or author. All costs are covered by the Ferdowsi University of Mashhad Press.

COPYRIGHT

Copyright on any open access article in the Iranian Journal of Veterinary Science and Technology, published by Ferdowsi University of Mashhad Press is retained by the author(s).

- Authors grant Ferdowsi University of Mashhad Press a license to publish the article and identify itself as the original publisher.
- Authors also grant any third party the right to use the article freely as long as its integrity is maintained and its original authors, citation details, and publisher are identified.

The Creative Commons Attribution License 4.0 formalizes these and other terms and conditions of publishing articles. The Copyright assignment form can be downloaded from the IJVST website.

SUBMISSION

Authors should submit their manuscript in electronic format directly through the IJVST website (ijvst.um.ac.ir) along with a letter to the editor signed by the author to whom correspondence should be addressed. Please ensure that Email addresses are university/governmental addresses and full postal addresses are included on the title page of the manuscript. The following files and forms can be downloaded from the IJVST website:

Manuscript (template file can be downloaded from the IJVST website)
Title page (template file can be downloaded from the IJVST website)
Tables (template file can be downloaded from the IJVST website)
Endnote manuscript library file (Vancouver style can be downloaded from the IJVST website)

Guide for Authors

Copyright assignment form (can be downloaded from IJVST website)
Conflict of interest and author agreement form (can be downloaded from the IJVST website)

For further information, please contact the Editorial Office:
Iranian Journal of Veterinary Science and Technology
Email: ijvst@um.ac.ir;
Tel: +98 51 3880-3742

PREPARATION OF MANUSCRIPT

Manuscripts should be written in English, with Abstract in both English and Persian (where applicable), typewritten in MS Word program, double-spaced, in 12-point "Times New Roman" font on A4 paper size. Authors are requested to reserve margins of 2.5 cm all around the pages. Manuscript should also have line numbers. All pages of the manuscripts should also be enumerated.

Research Articles should contain Title page, Abstract, Keywords, List of Abbreviations, Introduction, Results, Discussion, Materials and methods, References, and Figure legends. Tables and figures should be appended as individual files.

Review Articles should contain Title page, Abstract, Keywords, List of Abbreviations, Introduction, appropriate sections dependeing to the subject, Conclusions and future directions. Tables and figures should be appended as individual files. The review article should provide an update on recent advances in a particular field. Authors wishing to submit review articles should contact the Editor with an outline of the proposed paper prior to submission.

Case Reports should include Title page, Abstract, Keywords, List of Abbreviations, Introduction, Case Presentation, Results and Discussion, and References. Case reports should not exceed 2000 words (excluding the references) and should include no more than two tables or figures. Tables and figures should be appended as individual files.

Short Communications should not exceed 2000 words (excluding the references) and include no more than two tables or figures. They should include Title page, Abstract, Keywords, List of Abbreviations, the text summarizing results with no other divisions, and References. Tables and figures should be appended as individual files.

Title Page

Full Title Page should include title (concise and informative), author(s) (including the complete name, department affiliation, and institution), running head (condensed title) (≤ 50 characters, including spaces), name and address of the authors to whom correspondence and reprint requests

should be addressed, Acknowledgements, Author contributions, and Conflict of interest.

Acknowledgements: Personal acknowledgement, sources of financial support, contributions and helps of other researchers and everything that does not justify authorship should be mentioned in this section, if required.

Author contributions: Authors are required to include a statement to specify the contributions of each author. The statement describes the tasks of individual authors referred to by their initials. Listed below is an example of author contributions statement:
Conceived and designed the experiments: HD, SS. Performed the experiments: SS. Analyzed the data: HD, SS, MMM, ARB. Research space and equipment: HD, MMM, ARB. Contributed reagents/materials/analysis tools: HD. wrote the paper: SS, HD.

Conflict of interest: All authors must disclose any financial and personal relationships with other people or organizations that could inappropriately influence (bias) their work. Examples of potential conflicts of interest include employment, consultancies, stock ownership, honoraria, paid expert testimony, patent applications/registrations, and grants or other funding. If there are no conflicts of interest then please state 'The authors declare that there is no conflict of interest'. This form can be downloaded from the IJVST website.

Abstract

Abstract (in English and Persian) no more than 250 words should contain the purpose of the study, findings and the conclusion made on the basis of the findings. Authors who are not native Persian speakers may submit their manuscript with an abstract in English only. Abbreviations and reference citations may not be used in the abstracts.

Keywords

For indexing purposes, each submitted manuscript should include three to seven keywords, following the abstract and preferably chosen from the Medical Subject Headings (MESH). Keywords should express the precise content of the manuscript.

Introduction

Introduction should be as concise as possible, and clearly explain the main objective and hypothesis of the investigation.

Results

Results indicate the results of an original research in a clear and logical sequence. Do not repeat data that are already covered in tables and illustrations. In manuscripts describing more than one animal, all animals should be assigned a case number.

Discussion

Discussion should include the answer to the question proposed in the introduction and empha-

size the new and important aspects of the study and the conclusions that follow from them. It could include the implication, application, or speculation of the findings and their limitations, relate the observations to other relevant studies, and links the conclusions with the goals of the study. Recommendations, when appropriate, may be included.

Materials and methods

Materials and methods should be described in sufficient details to allow other researchers to reproduce the results. Specify any statistical computer programs used .The methods of data collection and use of statistical analysis will be checked by the referees and if necessary, a statistician. Drugs and therapeutic agents, reagents, softwares and equipments should be given in the format: name (trade name, manufacturer name, city, country), e.g. Statview 5 (SAS Institute, Inc., Cary, NC, USA).

Animals: All animal experiments should comply with the ARRIVE (https://arriveguidelines.org/) guidelines and the authors should clearly indicate in the manuscript the ethical code of the study.

Gene names: The standard gene names, as provided by HGNC (HUGO Gene Nomenclature Committee) should be used. Gene names must be italicized. If the case of mammalian species and if gene names refer to rodent species, they must be upper case; if they refer to non-rodent species they must be written in capitals. If they refer to other species, they must written lower case. Protein names are written in capitals and are not italicized. As an example:

Mouse beta actin gene: *Actb*
Bovine beta actin gene: *ACTB*
Chicken beta actin gene: *actb*
Beta actin protein: ACTB

Quantitative PCR: If the quantitative PCR method has been used, the related section in Materials and Methods must be written following the reference:

Bustin SA, Benes V, Garson JA, Hellemans J, Huggett J, Kubista M, Mueller R, Nolan T, Pfaffl MW, Shipley GL, Vandesompele J, Wittwer CT. The MIQE guidelines: minimum information for publication of quantitative real-time PCR experiments. Clin Chem. 2009 Apr;55(4):611-22.

The following information must be provided in the section:

Protocol for DNA/RNA extraction, including quantification and determination of purity;

Reverse transcription (if used): amount of RNA, concentration of all reagents: primers concentration (either random primers or oligonucleotides), reverse transcriptase and master mix components;

qPCR: sequence of forward and reverse primers, probes, amplicon size, accession number of Genebank; thermocycler parameters (i.e. denaturation, annealing and extension steps, number of cycles, melting curves); validation of PCR products; non-template controls for reverse transcription and qPCR should be included in all reactions; and

Data analysis: details for the quantitative or relative analysis.

Use of antibodies: Authors must show that the antibodies are validated and their specificity sis con-

firmed.

References

Must be up-to-dated and limited to those that are necessary. Lists of references should be given in numerical order in the text, and in the reference list. Please use Vancouver style. To download the Vancouver Style follow the link in the IJVST website which could be used in the Endnote software.

Example piece of text and reference list :

An unhealthy diet, obesity and physical inactivity play a role in the onset of type 2 diabetes, but it has been shown that increased physical activity substantially reduces the risk [1], and participation in regular physical activity is one of the major recommendation of the evidence based guidelines for the primary prevention of diseases [2]. According to the 2004-05 National Health Survey, more than half a million Australians (3.5% of the population) have diabetes mellitus which had been medically diagnosed and most of these people have the Type 2 condition [3]. Gestational diabetes is also on the increase, rising steadily between 2000-01 and 2005-06 [4]. Approximately two thirds of those with diabetes have been prescribed medication [3], but it is of concern that a recent review of the literature found that many people do not take their medication as prescribed [5]. Many patients also self monitor the disease by measuring their blood glucose levels with a glucose meter but Song and Lipman [6] have concerns about how well this is managed.

References for the above example:

1. Hull J, Forton J, Thompson A. Paediatric respiratory medicine. Oxford: Oxford University Press; 2015.

2. Eckerman AK, Dowd T, Chong E, Nixon L, Gray R, Johnson S. Binan Goonj: bridging cultures in Aboriginal health. 3rd ed. Chatswood, NSW: Elsevier Australia; 2010.

3. Johnson C, Anderson SR, Dallimore J, Winser S, Warrell D, Imray C, et al. Oxford handbook of expedition and wilderness medicine. Oxford: Oxford University Press; 2015.

4. McLatchie GR, Borley NR, Chikwe J, editors. Oxford handbook of clinical surgery. Oxford: Oxford University Press; 2013.

5. Petitti DB, Crooks VC, Buckwalter JG, Chiu V. Blood pressure levels before dementia. Arch Neurol. 2005; 62(1):112-6.

6. Liaw S, Hasan I, Wade, V, Canalese R, Kelaher M, Lau P, et al. Improving cultural respect to improve Aboriginal health in general practice: a multi-perspective pragmatic study. Aust Fam Physician. 2015; 44(6):387-92.

Tables

Please submit tables as individual files and editable text and not as images. Place all table notes below the table body. Each table should have a title which is followed by explanation of results shown in the table. Use of vertical rules must be avoided. Tables should be self-explanatory, and clearly arranged. Tables should provide easier understanding and not duplicate information already included in the text or figures. Each table should be typewritten with double spacing on a separate file and numbered in order of citation in the text with Arabic numerals. Each table should have a concise heading that makes it comprehensible without reference to the text of the article. Explain any non-standard abbreviations in a footnote to the table.

Figures

Figures must be submitted in individual files (format: TIFF, Dimensions: Width: 789 – 2250 pixels

at 300 dpi Height maximum: 2625 pixels at 300 dpi, Resolution: 300 – 600 dpi, file size: less than 10 MB, Text within figures: Arial or Symbol font only in 8-12 point). The text and other labels should be placed in the figure as un-compressed layers. Each figure should have a title which is followed by explanation of results shown in the figure. Figures should be numbered in order of citation in the text with Arabic numerals.

For the use of bar diagrams the following publication should be consulted:

Weissgerber TL, Milic NM, Winham SJ, Garovic VD. Beyond bar and line graphs: time for a new data presentation paradigm. PLoS Biol. 2015; 13(4):e1002128.

The bar diagrams should be provided in color and in a well-designed and professional format. Please do not use different shades of gray. The axes of diagrams should have titles and units. Also, the source file of the image (Excel etc.) should be provided for typesetting.

Illustrations should be numbered as cited in the sequential order in the text, with a legend at the end of the manuscript. Color photographs are accepted at no extra charge. The editors and publisher reserve the right to reject illustrations or figures based upon poor quality of submitted materials.

If a published figure is used, the publisher's permission needs to be presented to the office, and the figure should be referenced in its legend.

Use of Italics

Gene symbols, Latin terms (i.e. *in vivo, in vitro, ex vivo, in utero, in situ*, and etc.) and species scientific names (using the binomial nomenclature), should be typed in italics, while the first letter of the genus name must be capitalized (i.e. *Homo sapiens*).

PUBLICATION ETHICS

Iranian Journal of Veterinary Science and Technology is aligned with COPE's (Committee on Publication Ethics) best practice guidelines for dealing with ethical issues in journal publishing and adopts the COPE guidelines. The journal members (editor, editorial board and the journal manager) have agreed to meet the purposes and objectives of the Journal.

Ethical guidelines for authors:

Authorship Criteria

IJVST requires authors to confirm that they and their co-authors meet all four criteria for authorship based on the guidelines of The International Committee of Medical Journal Editors (ICMJE) (verbatim as follows):

1. Substantial contributions to the conception or design of the work; or the acquisition, analysis, or interpretation of data for the work; AND
2. Drafting the work or revising it critically for important intellectual content; AND
3. Final approval of the version to be published; AND
4. Agreement to be accountable for all aspects of the work in ensuring that questions related to the accuracy or integrity of any part of the work are appropriately investigated and resolved.

The section "Author Contributions" in the manuscript should illustrate and clarify who contributed to the work and how. If a contributor does not meet all four above criteria should be acknowledged in the "Acknowledgements" section of the article.

Author agreements and conflict of interest

Written authorization from all authors for publication of the article is mandatory for IJVST to start the review process. This form entitled "Conflict of interest declaration and author agreement form" must be signed and completed by all authors. This statement and signatures certifies that all authors have seen and approved the manuscript being submitted. Also, the authors by signing this form warrant that the article is the Authors' original work, that the article has not received prior publication and is not under consideration for publication elsewhere, and that the corresponding author shall bear full responsibility for the submission.

Editors and members of editorial board as authors

Editor and members of editorial board are excluded from publication decisions when they are authors or have contributed to a manuscript.

Publication Ethics

Ethical guidelines for Peer reviewers

Iranian Journal of Veterinary Science and Technology (IJVST) follows and adheres to COPE Ethical Guidelines for Peer Reviewers. IJVST peer reviews all submitted manuscripts with contents in the scope of the journal. The process has been explained in the section "Peer Review Process".

Ethical guidelines for Editor

Iranian Journal of Veterinary Science and Technology regarding the responsibilities of the editors follows and adheres to COPE Ethical Guidelines for editors. The main guidelines are summarized in the guide to ethical editing from COPE.

PEER REVIEW PROCESS

Iranian Journal of Veterinary Science and Technology peer reviews all submitted manuscripts with contents within the scope of the journal.

Initial assessment

The submitted manuscript will be subjected to a primary review by the editor or a member of the editorial board for suitability and relevance of the findings to the scope of the journal and quality of the science presented in the paper (sufficient originality, having a message that is important to the general field of Veterinary Medicine, quality of data, novelty, English language, and overall manuscript quality) within two weeks. If the paper is evaluated to be relevant to the scope of the journal and having enough scientific rigor and novelty, it will be sent for the next stage. Otherwise, those manuscripts which are evaluated as not-appropriate in the initial review will be rejected at this stage.

Initial screen

The initial screen will be performed by the editorial office for the structure and format of the manuscript.

Peer review (double-blind)

The manuscripts which are found to be appropriate after the initial screen will be sent for external review by experts in the related field. We have prepared a checklist for reviewers that summarizes their evaluation of the manuscript. The items in this checklist are:

1. TITLE is clear and adequate
2. ABSTRACT clearly presents objects, methods, and results.
3. INTRODUCTION well-structured and provides a rationale for the experiments described.
4. MATERIALS AND METHODS are sufficiently explained and is detailed enough to be reproduced.
5. RESULTS are clearly presented and supported by figures and tables.
6. DISCUSSION properly interprets the results and places the results into a larger research context, and contains all important references.
7. Conclusions are logically derived from the data presented.
8. English Language/style/grammar is clear, correct, and unambiguous.
9. Figures and tables are of good quality and well-designed and clearly illustrate the results of the study.
10. References are appropriate.
11. Regarding this article are you concerned about any issues relating to author misconduct such as plagiarism and unethical behavior.
12. Comments on the importance of the article.

Final Decision

Based on the reviewers' recommendations a final decision is made by the editor and if needed the help of a member of the editorial board (depending on the field of study). Decisions will include accept, minor revision, major revision with and without re-review, and reject. We aim to reach a final decision on each manuscript as soon as their review results are available.

Iranian Journal of Veterinary Science and Technology

Faculty of Veterinary Medicine, Ferdowsi University of Mashhad, Azadi Square, Mashhad, IRAN
P.O. Box: 1793; Postal Code: 9177948974

Tel: 0098 51 3880 3742
Fax: 0098 51 3876 3852

Web: ijvst.um.ac.ir
Email: ijvst@um.ac.ir